



α -Ketoglutarate, amino acid homeostasis and lifespan in a yeast model of Niemann-Pick type C1

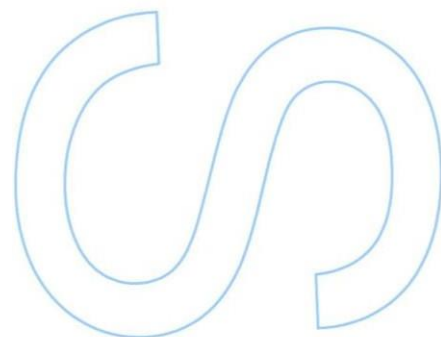
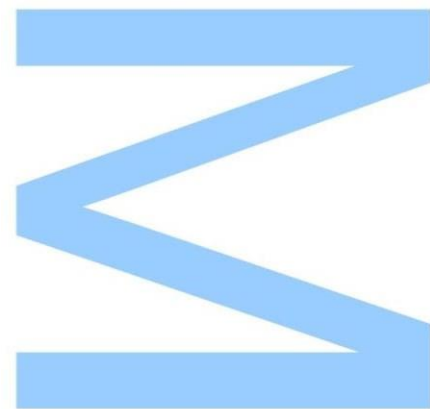
Rafaela Silva Costa

Mestrado em Bioquímica

Yeast Signalling Networks, i3S - Instituto de Investigação e Inovação em Saúde, Universidade do Porto
2021

Orientador

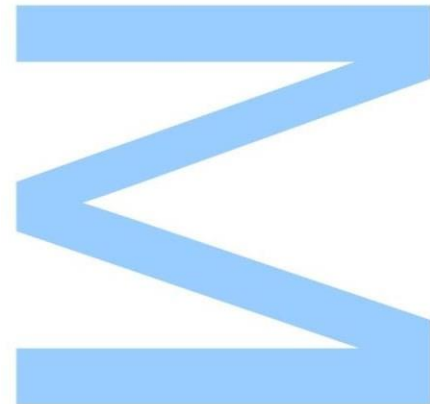
Vítor Manuel Vieira da Costa, Professor Associado, Instituto de Ciências Biomédicas Abel Salazar; Investigador Principal, IBMC/i3S, Universidade do Porto



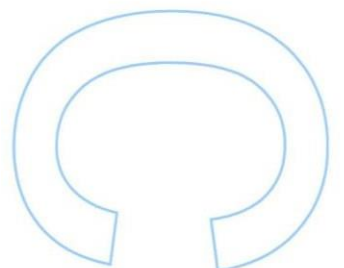
Todas as correções determinadas
pelo júri, e só essas, foram efetuadas.

O Presidente do Júri,

Porto, _____ / _____







Agradecimentos

Em primeiro lugar, dirijo os meus sinceros agradecimentos ao Prof. Vítor Costa pela oportunidade de realizar a minha dissertação de mestrado no grupo Yeast Signalling Networks e por me supervisionar, no papel de orientador. Estou muito grata pelo acompanhamento e pela análise crítica do trabalho, que foram constantes ao longo deste ano e fundamentais para chegar a este produto final. Para além de um excelente profissional, o Professor é uma pessoa muito acessível e isso reflete-se no seu método de ensino e na ótima relação que tem com os alunos. Tornou-me numa entusiasta da Bioquímica, de que me orgulho.

Em segundo lugar, agradeço aos restantes membros do grupo – Clara Pereira, Cláudia Leite, Pedro Moradas Ferreira, Telma Martins e Vítor Teixeira –, pelas sugestões para o trabalho, por todas as dúvidas esclarecidas e pela forma amigável como me receberam. Em particular, quero realçar o meu agradecimento à Telma, que me acompanhou na aprendizagem das técnicas laboratoriais, na análise dos resultados e na escrita da dissertação. Obrigada por me ofereceres diferentes perspetivas do trabalho e pelo rigor instruído. Aprendi muito contigo e vou recordar com carinho a tua companhia. Aproveito para mencionar as colegas de trabalho Verónica Nogueira e Maria Tavares e o grupo Phenotypic Evolution, que também me acompanharam e apoiaram neste percurso.

De seguida, gostaria de agradecer à Doutora Belém Sampaio-Marques e à Prof.^a Paula Ludovico, da Universidade do Minho, pela colaboração na análise dos níveis de aminoácidos. Do mesmo modo, agradeço à Doutora Paula Soares e ao Doutor Marcelo Correia, do grupo Cancer Signalling & Metabolism (i3S), pela cedência dos anticorpos para detetar a histona H3.

Por fim, deixo um agradecimento especial aos meus pais pelo esforço diário investido na minha educação, saúde e bem-estar. Obrigada pela vossa paciência, compreensão e por me fazerem genuinamente feliz. Ao meu irmão e aos meus amigos, quer da faculdade quer de Vila do Conde, estou grata pelos momentos de distração e animação, mas também por estarem sempre lá para mim. Serão sempre o meu porto de abrigo.

Esta foi uma viagem muito enriquecedora, tanto a nível profissional como pessoal, constituindo um marco importante na minha vida. A todos vós, por fazerem parte dela, um eterno “obrigada”.

Resumo

A Niemann-Pick tipo C1 (NPC1) é uma doença autossómica recessiva de armazenamento lisossomal (LSD) causada por mutações na proteína NPC1, que medeia o transporte de colesterol de endossomas tardios e lisossomas (LE/Lys). Assim, a principal consequência desta doença é a acumulação de colesterol nos LE/Lys, sendo também caracterizada por armazenamento involuntário de esfingolípidos (ex., ceramida) e morte prematura. O modelo de *Saccharomyces cerevisiae* da NPC1 resulta da deleção da proteína Ncr1 (ortólogo da proteína NPC1). Tal como células de mamífero sem NPC1, células de levedura sem Ncr1 (*ncr1* Δ) possuem tempo de vida cronológico (CLS) diminuído e disfunção mitocondrial, que resultam da acumulação de fitoceramida e consequente hiperativação da fosfatase Sit4. O Gln3 é um ativador transcricional da via Repressão Catabólica por Azoto (NCR) e está hiperativado em células *ncr1* Δ de modo dependente da Sit4. Como o Gln3 promove a síntese de glutamato (Glu) e glutamina (Gln) a partir de α -cetoglutarato (α -KG), foi colocada a hipótese de que células *ncr1* Δ podem ter níveis aumentados desses aminoácidos, ativando a via do TORC1 (*Target of Rapamycin Complex 1*), que é um inibidor da função mitocondrial e autofagia, importantes para a longevidade. Assim, este estudo teve como objetivo caracterizar um potencial papel do Gln3 nos fenótipos já descritos de CLS diminuído e disfunção mitocondrial nas células *ncr1* Δ , mas também nas vias do TORC1 e autofagia. Os resultados sugerem que tanto a sinalização pelo TORC1 como a autofagia estão diminuídos nestas células, de modo independente do Gln3, e que este tem um papel minoritário na morte prematura deste organismo modelo, não contribuindo para a disfunção mitocondrial. Como o Gln3 regula a síntese e transporte de aminoácidos, e defeitos na autofagia podem comprometer a reciclagem destas moléculas, procurámos caracterizar a homeostasia de aminoácidos nas células *ncr1* Δ . Os resultados indicam que células *ncr1* Δ possuem níveis superiores de Glu, mas não de Gln, enquanto os níveis de α -KG estão diminuídos, o que sugere que a aminação de α -KG a Glu está aumentada. A análise revelou ainda uma tendência geral de acumulação de aminoácidos a nível intracelular e vacuolar, em células *ncr1* Δ . Curiosamente, observámos que a suplementação com α -KG, Glu ou Gln (em menor extensão) aumenta a longevidade destas células. O efeito benéfico do α -KG é acompanhado por uma diminuição da ativação do TORC1, enquanto o Glu aumenta a ativação do complexo. Apesar de os suplementos modularem a via do TORC1, o fluxo autofágico nas células *ncr1* Δ não é recuperado. Em geral, estes resultados mostram que a sinalização pelo TORC1, a autofagia e homeostasia de aminoácidos estão alterados neste modelo de levedura da NPC1, de acordo com observações em células ou tecidos NPC1 de mamífero. Mais estudos serão necessários para caracterizar os efeitos protetores da suplementação com α -KG, Glu e Gln.

Palavras-chave

Niemann-Pick tipo C1, *Saccharomyces cerevisiae*, Ncr1, tempo de vida cronológico, TORC1, autofagia, homeostasia de aminoácidos, α -cetogluturato.

Abstract

Niemann-Pick type C1 (NPC1) is an autosomal recessive lysosomal storage disease caused by mutations in the NPC1 protein, which is involved in cholesterol export from late endosomes/lysosomes (LE/Lys). Hence, cholesterol accumulation in LE/Lys is the primary hallmark of disease, also characterized by abnormal storage of sphingolipids (e.g., ceramide) and premature death. The *Saccharomyces cerevisiae* model of NPC1 originates from deletion of the Ncr1 protein (NPC1 protein orthologue). Like NPC1 mammalian cells, yeast lacking Ncr1 (*ncr1Δ* cells) exhibit a shortened chronological lifespan (CLS) and mitochondrial dysfunction, which result from phytoceramide accumulation and consequent hyperactivation of the Sit4 phosphatase. Gln3 is a transcriptional activator of the Nitrogen Catabolite Repression (NCR) pathway and is upregulated in *ncr1Δ* cells, in a Sit4-dependent manner. Since Gln3 is known to promote glutamate (Glu) and glutamine (Gln) synthesis from α-ketoglutarate (α-KG), we hypothesized that the levels of these amino acids could be increased in *ncr1Δ* cells, activating the Target of Rapamycin Complex 1 (TORC1), which is an inhibitor of mitochondrial function and autophagy, important for longevity. Hence, this study aimed to characterize the potential role of Gln3 in the previously described shortened CLS and mitochondrial dysfunction phenotypes of *ncr1Δ* cells, but also in the TORC1 and autophagy pathways. The results suggest that TORC1 signalling and autophagic flux are decreased in *ncr1Δ* cells, in a Gln3-independent manner, and that Gln3 seems to play a minor role in the premature death of this model organism, with no impact on mitochondrial dysfunction. Since Gln3 regulates amino acid synthesis and uptake, and autophagy impairment may compromise amino acid recycling, we sought to characterize amino acid homeostasis in *ncr1Δ* cells. Our results indicate that *ncr1Δ* cells have increased levels of Glu, but not Gln, while α-KG levels are reduced, suggesting that α-KG amination to Glu is upregulated. The analysis further revealed a general tendency for intracellular and vacuolar amino acid accumulation in *ncr1Δ* cultures. Interestingly, we observed that supplementation of α-KG, Glu or Gln (in less extent) extends the CLS of *ncr1Δ* cells. The beneficial effect of α-KG is accompanied by TORC1 downregulation, whereas Glu increases its activation. Although the supplements modulate TORC1 activity, the autophagic flux of *ncr1Δ* is not restored. Overall, these results show that TORC1 signalling, autophagy and amino acid homeostasis are altered in this yeast model of NPC1, in agreement with reports on mammalian NPC1 cells or tissues. Further studies are necessary to fully comprehend the protective effects of α-KG, Glu and Gln supplementation.

Keywords

Niemann-Pick type C1, *Saccharomyces cerevisiae*, Ncr1, chronological lifespan, TORC1, autophagy, amino acid homeostasis, α -ketoglutarate.

Table of contents

Agradecimentos	i
Resumo	iii
Abstract	v
Table of contents	vii
List of tables	ix
List of figures	x
List of abbreviations	xi
CHAPTER 1. Introduction	1
1.1. Niemann-Pick type C	2
1.1.1. Introduction to Niemann-Pick disorders	2
1.1.2. General aspects and clinical description	2
1.1.3. Genetic aetiology and cellular pathology	3
1.1.4. Treatment of Niemann-Pick type C	5
1.1.5. The <i>Saccharomyces cerevisiae</i> model of Niemann-Pick type C1	6
1.2. TOR signalling	7
1.2.1. Structure and function of TORC1 and TORC2	7
1.2.2. TORC1 activation by amino acids	8
1.2.3. TORC1-mediated regulation of longevity and mitochondrial function	9
1.2.4. Regulation of Nitrogen Catabolite Repression by TORC1 and Sit4	10
1.3. Autophagy and amino acid homeostasis	12
1.3.1. General aspects of autophagy	12
1.3.2. Autophagy machinery and regulation	13
1.3.3. Autophagy and amino acid homeostasis impact longevity	15
1.4. α -Ketoglutarate as an anti-aging metabolite	16
CHAPTER 2. Aim of the study	19
CHAPTER 3. Materials and methods	21

3.1. Yeast strains and growth conditions.....	22
3.2. Gene disruption.....	22
3.3. Plasmid construction and amplification	24
3.4. Yeast transformation.....	24
3.5. Chronological lifespan.....	25
3.6. Oxygen consumption and growth in glycerol plates.....	25
3.7. α-Ketoglutarate levels	26
3.8. Western blotting.....	26
3.8.1. TORC1 activity	26
3.8.2. Autophagic flux.....	27
3.8.3. Histone H3 levels.....	27
3.9. Isolation of intact vacuoles	28
3.10. Amino acid levels.....	29
3.11. Mutation frequency.....	29
3.12. Statistical analysis.....	30
CHAPTER 4. Results and discussion.....	31
4.1. TORC1 signalling is decreased in yeast lacking Ncr1	32
4.2. Autophagic flux is impaired in yeast lacking Ncr1, in a Gln3-independent manner	33
4.3. The shortened chronological lifespan and mitochondrial dysfunction of yeast lacking Ncr1 are not caused by Gln3 hyperactivation.....	36
4.4. Yeast lacking Ncr1 have decreased levels of α-ketoglutarate	38
4.5. α-Ketoglutarate, glutamate and glutamine extend the chronological lifespan and modulate TORC1 activity in yeast lacking Ncr1.....	39
4.6. Amino acid homeostasis is altered in yeast lacking Ncr1	44
4.7. Yeast lacking Ncr1 have decreased levels of histone H3	50
CHAPTER 5. Conclusions and future perspectives	53
CHAPTER 6. References.....	59

List of tables

Table 1 – Strains, genotypes and sources of <i>S. cerevisiae</i> used in this study.....	22
Table 2 – Polymerase chain reaction (PCR) programs and primers used in this study.	23
Table 3 – pH values of <i>S. cerevisiae</i> BY4741 and <i>ncr1</i> Δ cultures at day 2 of the chronological lifespan assay.....	41

List of figures

Figure 1 – Topological representation of human NPC1 protein.....	4
Figure 2 – Mammalian and <i>S. cerevisiae</i> TORC1 signalling at the lysosomal/vacuolar surface..	8
Figure 3 – TORC1 and Sit4 regulate Gln3 activation in the Nitrogen Catabolite Repression (NCR) pathway of <i>S. cerevisiae</i> (simplified representation of the mechanism)..	11
Figure 4 – Glutamate and glutamine synthesis in <i>S. cerevisiae</i>	12
Figure 5 – The vacuole is an important regulator of amino acid homeostasis in <i>S. cerevisiae</i>	14
Figure 6 – Autophagy regulation by TORC1, PKA and Sch9 in <i>S. cerevisiae</i>	15
Figure 7 – TORC1 signalling is altered in yeast lacking Ncr1, in a Gln3-independent manner..	33
Figure 8 – Autophagic flux of yeast lacking Ncr1 is impaired in stationary phase, in a Gln3- independent manner.....	35
Figure 9 – Yeast lacking Ncr1 exhibit a Gln3-independent short chronological lifespan.....	37
Figure 10 – Increased activity of Gln3 in yeast lacking Ncr1 does not cause mitochondrial dysfunction.....	38
Figure 11 – α-Ketoglutarate levels are decreased in yeast lacking Ncr1.....	39
Figure 12 – Supplementation of growth medium with α-ketoglutarate, glutamate or glutamine increases the chronological lifespan of wild type and Ncr1-deficient yeast cells.....	40
Figure 13 – Supplementation of growth medium with α-ketoglutarate, glutamate or glutamine modulates TORC1 activity in yeast lacking Ncr1.....	43
Figure 14 – Supplementation of growth medium with α-ketoglutarate, glutamate or glutamine increases autophagic flux in the wild type strain, but not in yeast lacking Ncr1.....	44
Figure 15 – Yeast lacking Ncr1 have increased levels of glutamate and phenylalanine in late exponential phase and accumulate various amino acids during post-diauxic shift phase.....	46
Figure 16 – Supplementation of growth medium with α-KG decreases phenylalanine accumulation in yeast lacking Ncr1 grown to late exponential phase.....	48
Figure 17 – Supplementation of growth medium with α-KG does not significantly impact the amino acid content of yeast lacking Ncr1 grown to post-diauxic shift phase.....	49
Figure 18 – Vacuoles of yeast lacking Ncr1 exhibit significant threonine accumulation.....	50
Figure 19 – Yeast lacking Ncr1 have decreased levels of histone H3.....	51

List of abbreviations

AMPK	AMP-activated protein kinase
Atg	Autophagy-related
CAPP	Ceramide-activated protein phosphatase
CFUs	Colony-forming units
CLS	Chronological lifespan
CNS	Central nervous system
CRD	Cysteine-rich domain
Gdh1/2/3	Glutamate dehydrogenase 1/2/3
Gln	Glutamine
Glu	Glutamate
GS	Glutamine synthetase
JmjC	Jumonji C
LB	Lysogeny broth
LDL	Low-density lipoprotein
LE/Lys	Late endosomes/lysosomes
LSDs	Lysosomal storage diseases
MLD	Middle luminal domain
NCR	Nitrogen catabolite repression
Ncr1	Niemann-Pick type C-related protein 1
NPC	Niemann-Pick type C
NPC1/2	Niemann-Pick type C1/2
NTD	N-terminal domain
PCR	Polymerase chain reaction
PDS	Post-diauxic shift
PE	Phosphatidylethanolamine
PKA	Protein kinase A
PP2A	Protein phosphatase 2A

Rps6	Ribosomal protein S6
S6K	S6 kinase
SC	Synthetic complete
SSD	Sterol-sensing domain
TBS	Tris-buffered saline
TBST	Tris-buffered saline containing Tween 20
TOR	Target of rapamycin
TORC1/2	Target of rapamycin complex 1/2
V-ATPase	Vacuolar H ⁺ -ATPase
YPD	Yeast extract peptone dextrose
α-KG	α-Ketoglutarate

CHAPTER 1. Introduction

Lysosomes were first acknowledged in the 1950s by Christian de Duve (1) and since then have emerged as highly dynamic organelles involved in processes like autophagy, nutrient sensing, metabolic signalling, cell growth and death. Due to their crucial role in cellular homeostasis and fitness, investigation on these organelles and associated disorders has escalated over the years. Lysosomal storage diseases (LSDs), comprehending 70 rare inherited disorders, are characterized by progressive accumulation of biological molecules (lipids, proteins, oligosaccharides, among others) in the lysosome, as a result of mutations in proteins important for lysosomal function (2). Loss or decreased function of these proteins induce morphological alterations and malfunction of the organelle, ultimately causing cell damage. In this study, we focus on Niemann-Pick type C (NPC), an LSD with neurovisceral involvement.

1.1. Niemann-Pick type C

1.1.1. Introduction to Niemann-Pick disorders

Niemann-Pick refers to a heterogeneous group of LSDs that cause hepatosplenomegaly and, in some cases, central nervous system (CNS) damage, due to abnormal storage of unesterified cholesterol and/or sphingomyelin in lysosomes (3). Lipid accumulation results from mutations in genes encoding lysosomal-residing proteins. Therefore, depending on the affected gene and symptoms, these disorders can be subcategorized into the main types A, B or C. Both types A and B originate from mutations in acid sphingomyelinase-coding *SMPD1*, which impair sphingomyelin degradation. However, type A typically manifests in infancy, with severe CNS injury causing premature death, whereas type B mostly develops in childhood/adolescence and CNS is usually unaffected (4). Type C can be caused by mutations in *NPC1* or *NPC2*, thus being further classified into Niemann-Pick type C1 (NPC1) or Niemann-Pick type C2 (NPC2), respectively. Niemann-Pick diseases are inherited in an autosomal recessive manner, so mutations must affect both alleles of the gene for disease manifestation (3, 5).

1.1.2. General aspects and clinical description

NPC is a rare disorder, with a predicted incidence of approximately 1 in 89000 conceptions, with variations between ethnic groups (6). It is mainly characterized by accumulation of unesterified cholesterol in late endosomes/lysosomes (LE/Lys), as a result of impaired intracellular lipid trafficking. Abnormal storage of sphingosine and sphingolipids including glucosylceramide, sphingomyelin and gangliosides, is also observed, with tissue-dependent profiles. Although lipid build-up is detectable in most tissues, the brain and visceral organs

such as the liver, spleen and, occasionally, the lungs, are the most severely damaged organs (7, 8). Due to severe neurodegeneration, which affects about 90% of patients, and visceral organ failure, premature death occurs, making NPC a fatal neurovisceral sphingolipidosis (3, 7).

The clinical profile of NPC is remarkably diverse, especially due to the varying onset age of neurological symptoms, which highly determine the course of disease and patient life expectancy. Hence, NPC is categorized into the early-infantile (<2 years), late-infantile (2-6 years), juvenile (6-15 years) and adult (>15 years) forms. The infantile forms are essentially characterized by visceral defects, including hepatomegaly, splenomegaly and cholestatic jaundice; in late infancy, neurological symptoms such as hypotonia and motor developmental delay may manifest. The juvenile onset age is mostly of neurological nature, comprising cerebellar ataxia, vertical supranuclear gaze palsy, dysphagia and dysarthria. These symptoms are also observed in the adult form, which is further associated with dementia and, often, psychiatric disturbances. In summary, defects in systemic organs commonly arise at a young age, while neurological symptoms can manifest years later, gradually developing over time. Although some patients reach 60-70 years of age, most die prematurely at 10-25 [reviewed in (3, 9)].

1.1.3. Genetic aetiology and cellular pathology

As mentioned before, NPC is caused by loss-of-function point mutations in *NPC1*, in 95% of cases, or *NPC2*, in 5% of cases (3, 10). These genes encode the NPC1 and NPC2 proteins, respectively, which are co-ordinately involved in intracellular lipid trafficking through the endocytic pathway, namely cholesterol insertion in the membrane of LE/Lys and egress from this compartment (11). Hence, despite being structural and functionally distinct, dysfunction of either NPC1 or NPC2 promote similar cellular defects, making the biochemical phenotypes and symptoms of NPC1 and NPC2 patients indistinguishable (12).

NPC2 is a small 132-amino acid globular glycoprotein, found in the lumen of LE/Lys. Structurally, it is composed of seven β -strands, which arrange into two β -sheets that create a loosely packed and expandable hydrophobic pocket with high affinity for cholesterol. Consistently, NPC2 has been proposed to bind low density lipoprotein (LDL)-derived cholesterol within LE/Lys and transfer it to NPC1, among other proteins that mediate lipid export from this subcellular compartment (13, 14). NPC1 is a large 1278-amino acid integral membrane protein of LE/Lys, with 13 transmembrane segments and 3 luminal domains (Figure 1). The luminal N-terminal domain (NTD) of NPC1 receives the cholesterol molecule from NPC2, specifically interacting with the lipid's 3 β -hydroxyl moiety, opposite from the aliphatic

isooctyl tail that is buried in the hydrophobic pocket of NPC2 (15). The middle luminal domain (MLD) of NPC1 is predicted to serve as a platform for interaction with NPC2, facilitating cholesterol transfer from NPC2 to the NTD of NPC1 (16). Regarding the sterol-sensing domain (SSD), formed by the transmembrane segments 3-8, studies have indicated it harbours an additional cholesterol-binding site (11). In this model, the NTD delivers the cholesterol molecule to the SSD, specifically to a cavity that is open to both the lumen and the luminal leaflet of LE/Lys membrane. Cholesterol is likely integrated in the luminal leaflet, which would require it to flip to the cytoplasmic leaflet to exit LE/Lys, but how flipping occurs is not known (11). Hence, the mechanism of NPC1-mediated cholesterol export from LE/Lys is not fully understood.

Up to date, over 250 mutations in *NPC1* have been reported to cause NPC1 disease and they can affect most domains of the NPC1 protein. Mutations in the cysteine-rich domain (CRD), whose function is not completely clear, account for the largest percentage of cases (17, 18). In particular, the CRD I1061T (Figure 1) affects about 20% of patients of western European ancestry and is associated with the severe juvenile onset age (3). I1061T prevents correct folding of NPC1, leading to its retention and subsequent proteasome-mediated degradation in the endoplasmic reticulum (19), where the protein is synthesized. Consequently, NPC1 levels become significantly reduced (19). Disease-causing mutations in *NPC1* can also delay the transport of NPC1 through the secretory pathway or simply impair its activity in LE/Lys (for example, mutations in the NTD can impair cholesterol binding) (15, 19, 20). Consistently, delivery of cholesterol to the endoplasmic reticulum and the cell membrane is compromised, with abnormal build-up in LE/Lys (21, 22).

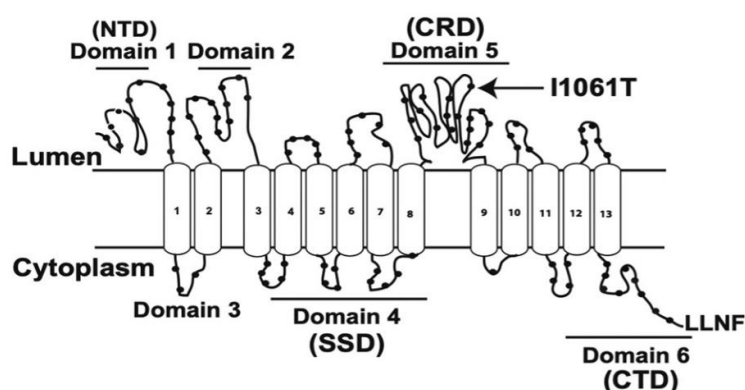


Figure 1 – Topological representation of human NPC1 protein. NPC1 localizes to the late endosomal/lysosomal system and is composed of 13 transmembrane segments, 3 large luminal domains – the N-terminal domain (NTD), the middle luminal domain (domain 2) and the cysteine-rich domain (CRD) –, the membrane-embedded sterol sensing domain (SSD) and a cytoplasmic C-terminal domain (CTD). The I1061T mutation on the CRD is indicated with an arrow (23).

It is worth noting that the brain does not obtain cholesterol from plasma LDL, as these particles do not cross the blood-brain barrier. Instead, cholesterol is mostly synthesized by *de novo* synthesis in the endoplasmic reticulum, which does not require the function of NPC1. This could explain why brains of NPC1 patients do not have increased cholesterol mass (7). However, as previously mentioned, disease-causing mutations in *NPC1* induce severe neurodegeneration, associated with death of Purkinje neurons in the cerebellum (24). Furthermore, Karten *et al.* (25) have shown that, although cholesterol content of NPC1-deficient mice sympathetic neurons is unaltered, there is preferential cholesterol build-up in LE/Lys. This contributes to uncertainty regarding how NPC1 dysfunction affects cholesterol trafficking in the brain and has such deleterious effects in this organ. On the other hand, the livers of NPC1 patients display massive cholesterol accumulation, which is explained by the fact that plasma LDL are endocytosed by hepatocytes for lipid catabolism (8). The lipid profiles of the brain and visceral organs also include increased levels of GM2 and GM3 gangliosides in the former and of glucosylceramide and sphingosine in the latter (7). Hence, lipid trafficking and metabolism are severely altered in NPC1 disease (7).

How lipid accumulation contributes to lysosomal dysfunction is still not fully clear, but various studies have reported autophagic defects in NPC1-deficient cells (26-29). Mitochondrial dysfunction is also documented. Intriguingly, mitochondrial cholesterol levels are significantly increased in NPC1 mouse brains (correlating with decreased activity of ATP synthase and ATP levels) and patient fibroblasts (30, 31). Moreover, *NPC1* knockdown in human neurons leads to fragmentation of the mitochondrial network, which seems to derive from impaired mitophagy (26). Of note, neurons largely rely on mitochondrial respiration for energy supply and, consequently, adequate excitability and neurotransmission in the CNS (32).

1.1.4. Treatment of Niemann-Pick type C

Up to date, no curative therapy has been developed for NPC, so only symptomatic treatment can be provided to retard disease progression. Since lipid accumulation in LE/Lys is the primary hallmark of NPC (7), investigation on therapies that revert this defect has been pursued. Miglustat (Zavesca®, Actelion Pharmaceuticals Ltd.) is the only disease-modifying therapy ever approved for NPC treatment and provides a substrate reduction approach. It crosses the blood-brain barrier and blocks the first step in glycosphingolipids biosynthesis by reversibly inhibiting glucosylceramide synthase, thus ameliorating cellular glycosphingolipid storage (33, 34). A recent study showed that about 70% of patients under continuous Miglustat treatment have stabilized or improved neurological symptoms over time, so this therapy

attenuates disease progression even though cholesterol metabolism is not directly addressed (35).

1.1.5. The *Saccharomyces cerevisiae* model of Niemann-Pick type C1

The budding yeast *Saccharomyces cerevisiae*, a simple unicellular eukaryote, is widely used to study signalling pathways and molecular mechanisms involved in human diseases, as many of these processes are evolutionary conserved. In fact, about 25% of disease-related human genes have an orthologue in yeast (36). The yeast orthologue of human NPC1 is the Niemann-Pick type C-related protein 1 (Ncr1). It localizes to the membrane of the vacuole, which is the lysosome equivalent in yeast, and 32% of its amino acid sequence is identical to NPC1's (37). Moreover, the NTD, MLD, SSD and CRD of NPC1 are conserved, as are multiple amino acid residues affected by disease-causing mutations (37, 38).

NPC1 and Ncr1 were predicted to have similar functions, as expression of lysosomal membrane-tagged Ncr1 in NPC1-deficient mammalian cells rescued disease phenotypes such as lysosomal accumulation of cholesterol and gangliosides (39). Function equivalence was recently confirmed by Winkler *et al.* (38), who revealed that the yeast Ncr1 and the NPC2 orthologue (also named NPC2) work together to deliver sterols to the vacuolar membrane. According to their model, yeast NPC2 binds a sterol in the vacuole, docks to the MLD of Ncr1 and transfers the lipid to the NTD. Then, the NTD delivers it to a hydrophobic tunnel of Ncr1, which leads to the membrane-embedded SSD. Lastly, the sterol is predicted to diffuse from the SSD into the cytoplasmic leaflet of the LE/Lys membrane for integration or subcellular redistribution. Thus, this sterol transport mechanism seems to be conserved in yeast and mammals (38).

The *S. cerevisiae* model of NPC1 results from disruption of the *NCR1* open reading frame, which generates yeast lacking Ncr1 (*ncr1Δ* cells). Importantly, Ncr1 absence in yeast recapitulates multiple phenotypes observed in NPC1 mammalian cells. For instance, *ncr1Δ* cells display increased levels of ergosterol (the most abundant membrane sterol in yeast, with similar functions to mammalian cholesterol) in the endosomal system, whose acidification is reduced (40, 41). In analogy to sphingosine and ceramide accumulation in LE/Lys of NPC1-deficient cells (42, 43), *ncr1Δ* cells have increased levels of phytosphingosine and dihydrosphingosine in post-diauxic shift phase (PDS, respiratory phase) and of phytoceramide in both exponential (fermentative) and PDS phases (41, 44). Moreover, the mutant displays mitochondrial network fragmentation and mitochondrial membrane depolarization (41). Mitochondrial respiration is also impaired, as oxygen consumption is decreased and the cells are not capable of growing on agar plates with glycerol – an exclusively respiratory substrate

– as sole carbon source (41). Notably, these mitochondrial defects are associated with decreased oxidative stress resistance and shortened lifespan (41). The similarity between the phenotypes of NPC1-deficient mammalian cells and Ncr1-deficient yeast, together with the structural and functional conservation of the NPC1/NPC2 system, validate this yeast model of NPC1 to study the molecular basis of the disease.

Recently, Vilaça *et al.* (44) showed that mitochondrial dysfunction and premature death of *ncr1Δ* cells result from phytoceramide accumulation and consequent increase in the activation of the Ser/Thr phosphatase Sit4, as *SIT4* deletion restores mitochondrial respiration and longevity. Also, *ncr1Δ* cells have increased activation of Gln3, mediated by Sit4 (44). The functions of Sit4 and Gln3 are explored in section 1.2.4.

1.2. TOR signalling

1.2.1. Structure and function of TORC1 and TORC2

Target of Rapamycin (TOR) is a phosphoinositide 3-kinase (PI3K)-related Ser/Thr kinase with a central role in eukaryotic signalling pathways that regulate cell growth and proliferation (45). TOR was first identified in *S. cerevisiae* as a target of rapamycin, through an analysis of mutations that induced resistance to the growth-inhibitory effect of this macrolide (46). Later, it was identified in mammalian cells, being highly conserved throughout evolution (47, 48).

In mammals, TOR is solely encoded by the *TOR* gene and it can be the catalytic subunit of two different complexes – TOR Complex 1 (TORC1) and TOR Complex 2 (TORC2) –, by interacting with different partner proteins (Figure 2) (45). Contrarily, *S. cerevisiae* possesses two TOR genes, *TOR1* and *TOR2*, which encode the paralogs Tor1 and Tor2, respectively. Nonetheless, the structures and functions of TORC1 and TORC2 are conserved (48, 49).

Yeast TORC1 is composed of either Tor1 or Tor2, Kog1, Lst8 and Tco89 (Figure 2), whereas TORC2 can only have Tor2 as the catalytic core, with Avo1, Avo2, Avo3, Lst8 and Bit61 as the remaining subunits (48, 50). In addition to being structurally distinct, the two complexes respond to different stimuli and regulate different processes in the cell to ultimately promote cell growth. TORC1 senses nutrient availability, cell energy status, stress and growth factors to stimulate nutrient mobilization, transcription, protein and lipid synthesis and ribosome biogenesis, whereas catabolic processes (e.g., autophagy) are inhibited (Figure 2). On the other hand, TORC2 mostly responds to growth factors and regulates cytoskeletal remodelling and cell cycle progression [reviewed in (45, 49)]. Studies with rapamycin have facilitated the separate characterization of these two TOR signalling branches, as rapamycin interacts with Fpr1 (equivalent to mammalian FKBP12) to allosterically inhibit TORC1 but not TORC2. TORC2 cannot bind to rapamycin-Fpr1 and, thus, is considered insensitive to the antibiotic

(47, 48). Rapamycin treatment mimics nutrient starvation, promoting exit from the cell cycle and entrance into the quiescent G0 stage (51).

In humans, TORC1 signalling dysregulation has been increasingly implicated in various diseases, including cancer, neurodegenerative disorders and LSDs (52). In the case of NPC1, there are divergent observations regarding the degree of TORC1 activation in NPC1 cells, but some studies have suggested that dysregulation of TORC1 signalling is implicated in the pathogenesis of the disease (53, 54).

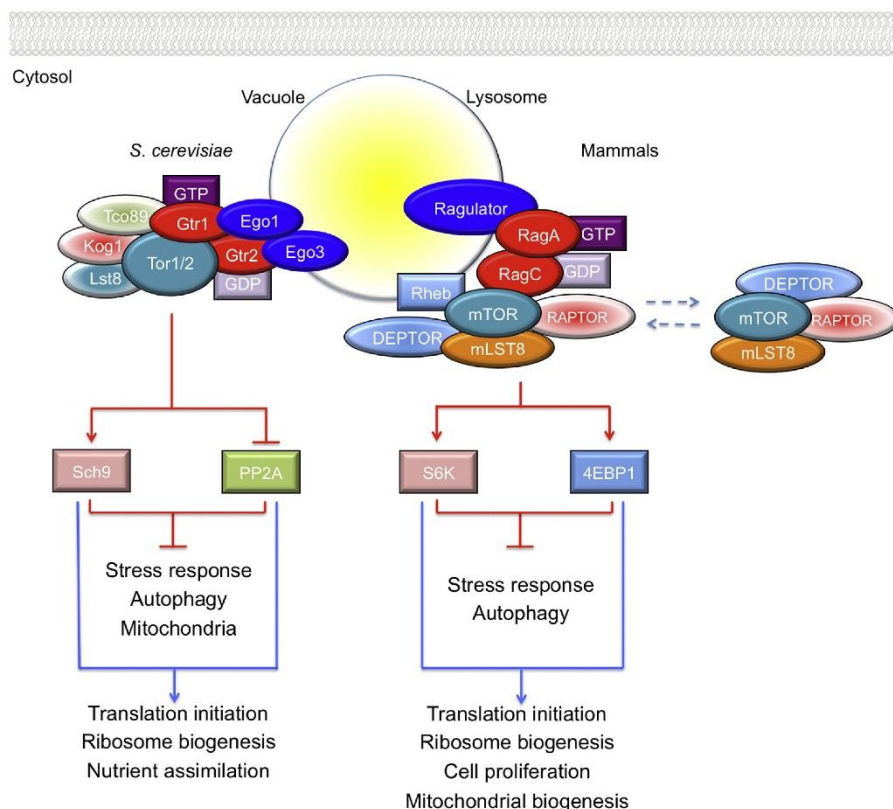


Figure 2 – Mammalian and *S. cerevisiae* TORC1 signalling at the lysosomal/vacuolar surface. Yeast TORC1 is composed of Tor1 or 2, Lst8, Kog1– orthologues of mammalian mTOR, mLST8 and RAPTOR, respectively – and the yeast-specific Tco89. Mammalian TORC1 is recruited to the lysosomal surface by Rag GTPases, in response to amino acids, where it is activated by GTP-bound Rheb. Ribosomal protein S6 kinase (S6K) and 4EBP1 are downstream targets of mammalian TORC1. Yeast TORC1 constitutively localizes to the vacuolar membrane and is activated by amino acids and other nitrogen sources via the Gtr1-Gtr2 complex, directly phosphorylating and activating Sch9 (S6K homologue) or inhibiting protein phosphatase 2A (PP2A) via Tap42 phosphorylation (55).

1.2.2. TORC1 activation by amino acids

In addition to being the building blocks of proteins – the most diverse and abundant macromolecules in the cell –, amino acids are involved in metabolic signalling, the synthesis of nucleotides and neurotransmitters, and constitute an energy source for multiple cell types (56). Hence, amino acid homeostasis, which according to Aris *et al.* (57) comprises the import,

synthesis, use, catabolism and recycling of amino acids, has an important role in cellular fitness and longevity (57-59). Lysosomes/vacuoles are crucial mediators of amino acid homeostasis and provide a platform for amino acid sensing and TORC1 activation.

In both mammals and yeast, amino acids (among other nutrients) activate TORC1 to stimulate cell growth. In mammalian cells, amino acid availability is perceived by the Rag GTPases, which locate to the lysosomal surface and recruit mTORC1 for GTP-bound Rheb-mediated activation (Figure 2). In yeast, TORC1 locates to the rim of the vacuole, independently of amino acid levels (60). The Gtr1-Gtr2 (Rag GTPases orthologues) heterodimer is anchored to the vacuolar membrane by the Ego1-Ego2-Ego3 complex and senses nitrogen sources, including amino acids. When these are available, Gtr1 and Gtr2 bind GTP and GDP, respectively, associating with and activating TORC1 (Figure 2). Thus, although yeast possesses a Rheb orthologue (Rhb1), it does not mediate TORC1 activation (60). In both mammals and yeast, the vacuolar H⁺-ATPase (V-ATPase) – a protein complex that pumps protons into lysosomes/vacuoles, coupled with ATP hydrolysis – is also involved in amino acid-mediated TORC1 activation, detecting luminal amino acid levels (61, 62). Importantly, distinct amino acids seem to activate TORC1 via different mechanisms and with different efficiency. For example, leucine activates TORC1 through Rag GTPases/Gtr1-Gtr2, whereas glutamine (Gln) can stimulate TORC1 independently of these complexes (63-65). Moreover, Gln-mediated TORC1 activation in yeast is more sustained in time than that promoted by leucine or glutamate (Glu) (63). Interestingly, not only do amino acid availability and quality impact TORC1 signalling, TORC1 inhibition was shown to alter the amino acid profile of yeast cells (66).

1.2.3. TORC1-mediated regulation of longevity and mitochondrial function

For years now, yeast has been a useful model organism to study longevity and aging-related diseases, because multiple pathways contributing to these phenomena are conserved (36). The yeast chronological lifespan (CLS) consists in the period that non-dividing cells in stationary phase remain viable (67). Hence, yeast CLS is a model for the aging process of post-mitotic cells in multicellular organisms (e.g., neurons) (68).

TORC1 is an important regulator of longevity in both yeast and higher eukaryotes (69). In yeast, *TOR1* deletion or rapamycin treatment significantly extend CLS. This is associated with increased mitochondrial respiration and electrochemical potential and a beneficial production of superoxide throughout growth, thus indicating that TORC1 inhibits mitochondrial function and that this is disadvantageous for longevity (70, 71). Importantly, the effects of TORC1 on mitochondrial function are mostly mediated by its downstream effector Sch9 [homologue of mammalian ribosomal protein S6 kinase (S6K)], a positive regulator of translation initiation and

ribosome biogenesis, whose deficiency also increases CLS and mitochondrial fitness (72). In fact, the beneficial effect of caloric restriction on yeast longevity partially derives from attenuation of the TORC1/Sch9 pathway (73, 74). TORC1 downregulation also contributes to increased CLS through activation of the stress resistance transcription factors Gis1 and Msn2/4 (activated by Rim15), which promote proteostasis, the activity of antioxidant enzymes and accumulation of glycerol and glycogen under nutrient starvation (74, 75). Lastly, TORC1 downregulation promotes autophagy induction (see section 1.3.2.), which enhances yeast CLS, too (76).

1.2.4. Regulation of Nitrogen Catabolite Repression by TORC1 and Sit4

Yeast Sit4 is a protein phosphatase 2A (PP2A)-related Ser/Thr phosphatase and functional homologue of mammalian protein phosphatase 6 (77). It controls cell cycle progression and is a negative regulator of mitochondrial function, as disruption of *SIT4* in yeast lacking mitochondrial DNA restores mitochondrial electrochemical potential and cell proliferation (78, 79). Consistently, downregulation of Sit4 increases CLS (80). Importantly, this phosphatase is capable of forming distinct complexes in the cell: it is the catalytic subunit of the ceramide-activated protein phosphatase (CAPP) complex, by interacting with the regulatory subunits Tpd3 and Cdc55, but it can also interact with Sit4-associated proteins (SAPs), such as Tap42 (79, 81, 82). Sit4 functions downstream of TORC1 and is also involved in nutrient signalling, regulating the yeast Nitrogen Catabolite Repression (NCR) pathway (83).

The NCR pathway is responsive to nitrogen availability, modulating gene transcription to repress the mobilization and utilization of poor nitrogen sources when preferred ones are available. Among these genes are amino acid permeases, transaminases and enzymes involved in amino acid synthesis and degradation (84). Preferred nitrogen sources include Gln, asparagine, Glu and ammonium, as they can easily be converted into (other) amino acids and/or support cell growth, whereas proline, urea and γ -aminobutyrate are poor, less preferred, nitrogen sources (63, 84). Indeed, Gln is the nitrogen source of election for yeast and a major activator of TORC1, also involved in the regulation of the NCR (63, 84, 85).

Among the downstream targets of TORC1 and Sit4 is the GATA-binding transcription factor Gln3, one of the two positive regulators of NCR-sensitive genes (Figure 3) (86). When preferred nitrogen sources are available, namely Gln, TORC1 is activated and phosphorylates Gln3. Consequently, Ure2, a negative regulator of transcription, binds to the phosphorylated form of Gln3, sequestering it in the cytoplasm and thus repressing NCR-sensitive gene expression (83, 86). TORC1 is also predicted to bind and phosphorylate the Tap42-Sit4 complex, inactivating the Sit4 phosphatase, which has been proposed to regulate Gln3 activity

by dephosphorylating it and promoting its migration to the nucleus (81, 83, 87). Contrastingly, under poor nitrogen conditions or rapamycin treatment, TORC1 is downregulated, so Gln3 is not phosphorylated by this complex and migrates to the nucleus to derepress NCR-sensitive transcription (88, 89). Moreover, the Tap42-Sit4 complex dissociates from TORC1 and Sit4 dephosphorylates Gln3, abolishing the interaction with Ure2 and promoting Gln3 translocation to the nucleus (Figure 3) (81, 83, 87, 90).

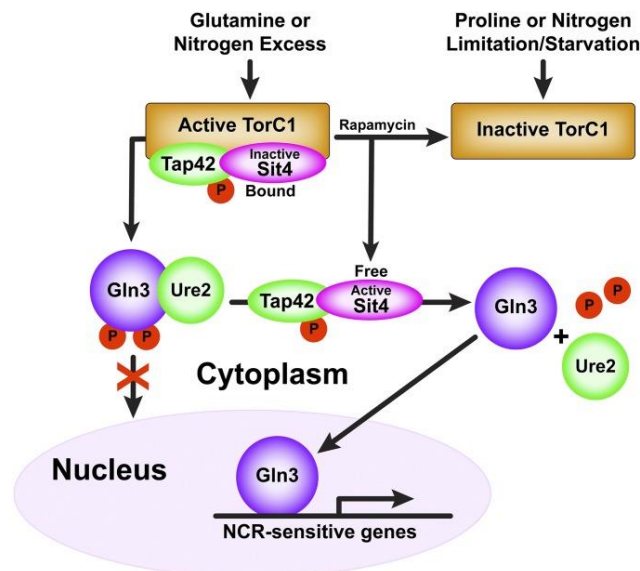


Figure 3 – TORC1 and Sit4 regulate Gln3 activation in the Nitrogen Catabolite Repression (NCR) pathway of *S. cerevisiae* (simplified representation of the mechanism). Glutamine or nitrogen abundance induce TORC1 activation, which mediates the cytoplasmic sequestering of Gln3 and repression of NCR-sensitive gene transcription. Poor nitrogen sources (proline), nitrogen starvation or rapamycin inactivate TORC1, thus freeing Sit4 to dephosphorylate Gln3. Gln3 dissociates from Ure2 and promotes NCR-sensitive gene expression in the nucleus (91).

Among the genes regulated by Gln3 are *GDH1* and *GLN1*, whose transcription is derepressed upon Gln3 activation (84). *GDH1* and *GLN1* encode the NADPH-dependent glutamate dehydrogenase 1 (Gdh1) and glutamine synthetase (GS) enzymes, respectively. Gdh1 catalyses Glu synthesis from α -ketoglutarate (α -KG) and ammonium, whereas GS catalyses ATP-dependent condensation of Glu and ammonium to yield Gln – the only pathway for Gln synthesis in yeast (Figure 4) (84, 92). Glu can also be produced through the activity of the Gdh1 paralog, Gdh3, which catalyses the same reaction except α -KG is used at a lower rate (93). Moreover, Gdh1 seems to have an important role in Glu synthesis during exponential growth, whereas Gdh3 is mostly expressed in stationary phase for resistance to stress-induced apoptosis (94). Another pathway for Glu synthesis, although less contributory (92), involves the oligomeric NADH-dependent glutamate synthase (Glt1/GOGAT), which transfers the amide group of Gln to α -KG, generating Glu (Figure 4) (84). Furthermore, transaminases

(aminotransferases) can use amino acids such as branched-chain amino acids, aromatic amino acids and methionine for reversible amination of α-KG to Glu (92).

Notably, the amino and amide groups of Glu and Gln, respectively, provide all the nitrogen necessary for cellular biosynthetic processes, including the synthesis of purines and pyrimidines and other amino acids (95). Disruption of *GDH1* and consequent decrease in Glu and Gln synthesis was shown to reduce the amino acid pool of exponentially growing cells by 38% (96). This shows that maintenance of adequate levels of Glu, Gln and their precursor, α-KG, is important for amino acid homeostasis.

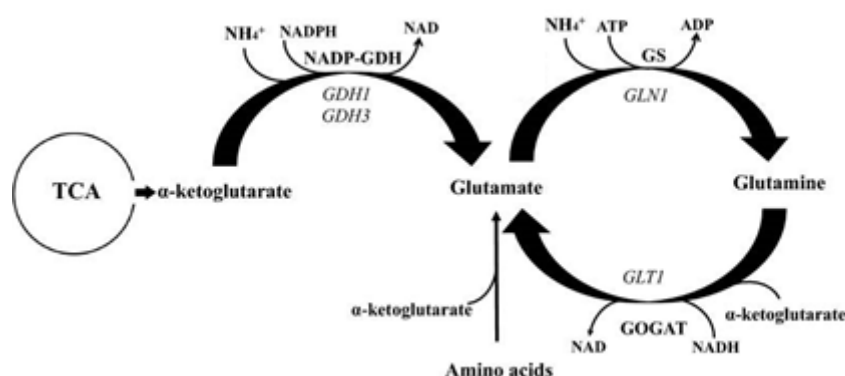


Figure 4 – Glutamate and glutamine synthesis in *S. cerevisiae*. Gdh1 (encoded by *GDH1*) catalyses glutamate synthesis from α-ketoglutarate – a Krebs cycle intermediate –, and ammonium, whereas GS (encoded by *GLN1*) synthesizes glutamine from glutamate and ammonium. The enzymes encoded by *GDH3* and *GLT1* also contribute to glutamate synthesis, through different mechanisms (see text). Adapted from (92).

1.3. Autophagy and amino acid homeostasis

1.3.1. General aspects of autophagy

In addition to being platforms for nutrient sensing and intracellular signalling, lysosomes and yeast vacuoles have a long-recognized role in autophagy – an intracellular pathway that promotes enzymatic degradation of cytoplasmic components (biomolecules and organelles) and subsequent recycling of their building blocks. In yeast, autophagy can be subclassified into macroautophagy or microautophagy, both culminating in substrate delivery to the vacuole, where hydrolytic enzymes reside. However, macroautophagy requires *de novo* assembly of a cytoplasmic isolation membrane (phagophore), which expands to entrap the substrate and, when sealed, forms the autophagosome – a double membrane vesicle that fuses with the lysosome/vacuole for substrate breakdown (97). Contrarily, microautophagy involves invagination of the vacuolar membrane and formation of luminal vesicles that contain the cytoplasmic substrate (98). Both macroautophagy and microautophagy are evolutionarily conserved from yeast to mammals, but the cytoplasm-to-vacuole targeting (Cvt) pathway is

solely found in yeast, consisting in a constitutive biosynthetic process that uses autophagic machinery to transport hydrolases to the vacuole (99).

Macroautophagy (hereinafter referred to as “autophagy”) commonly refers to a non-selective process, in which cytoplasmic material is engulfed in bulk (100), but cytoplasmic components can also be selectively targeted for degradation. For example, mitophagy promotes selective degradation of superfluous and defective mitochondria, preventing their accumulation and damage of biomolecules by reactive oxygen species (101). In addition to defective organelles, oxidized molecules, misfolded proteins and aggregates can undergo degradation. Thus, autophagy plays a fundamental role in quality control and protection from cell death, requiring tight regulation. Indeed, its dysregulation can contribute to severe pathology, including neurodegeneration (100). As post-mitotic cells, neurons do not have the capacity to disseminate damaged organelles or molecules to daughter cells, so autophagy is crucial for their efficient degradation and homeostasis maintenance (68).

1.3.2. Autophagy machinery and regulation

Most of the molecular machinery required for non-selective autophagy was first identified in yeast, including the conserved core of autophagy-related (Atg) proteins (102, 103). Up to date, over 30 Atg proteins have been discovered through studies in yeast and mammals and at least 17 are fundamental for induction, nucleation, expansion and maturation of autophagosomes, as well as for fusion with lysosomes (55, 104). According to the stage in which they are involved, Atg proteins can be subcategorized into different groups. Among these is the Atg1 kinase complex, crucial for autophagy initiation and formed by the Ser/Thr kinase Atg1 (homologue of mammalian ULK1), Atg13 and the Atg17-Atg31-Atg29 subcomplex (100, 104). Assembly of this complex is required for activation of Atg1, which dimerizes and auto-phosphorylates to promote biogenesis of the phagophore (105, 106). Also worthy of mention is the Atg8 conjugation system, involved in phagophore expansion and sealing (107). Atg8 (LC3 homologue) is a ubiquitin-like protein that, upon autophagy initiation, is conjugated to phosphatidylethanolamine (PE) in the inner and outer sides of the phagophore membrane, by ubiquitin-like Atg machinery (108, 109). Reaching full assembly of autophagosomes, the interaction between Atg8 and PE in the outer membrane is abolished by Atg4, playing an important role in Atg8 recycling (110). In contrast, Atg8 molecules in the inner membrane of the autophagosome remain associated to PE. Only when autophagosomes and vacuoles merge do they deconjugate and Atg8 is degraded by vacuolar hydrolases. Therefore, Atg8 is a signature characteristic of autophagic vesicles (104, 111). Of note, both selective and non-selective types of autophagy require the core Atg machinery (100).

As a housekeeping mechanism that maintains general homeostasis, autophagy is executed at basal levels under normal growing conditions. However, under adverse circumstances, such as nitrogen or amino acid starvation, it is strongly upregulated (112). Hence, yeast vacuoles (and mammalian lysosomes) are important for maintenance of adequate amino acid levels in the cytoplasm, delivering autophagy-derived amino acids to this compartment when reserves are limiting (56, 113). Consistently, yeast lacking essential Atg proteins are not capable of restoring amino acid pool levels following nitrogen starvation, so protein synthesis and cellular viability are compromised (113). Importantly, the yeast vacuole also functions as an amino acid storage compartment. Vacuolar membrane transporters mediate flux of amino acids in and out of this organelle, the majority relying on the H^+ gradient established by V-ATPase for H^+ /amino acid antiport or symport (114-116). Amino acid transport across the vacuolar membrane is a balanced and adaptable process, responding to the metabolic status of the cell and environmental conditions (Figure 5) (114, 117).

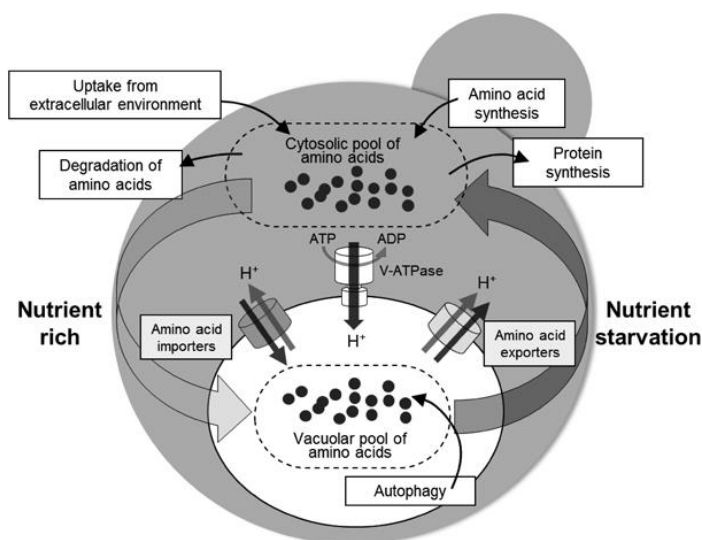


Figure 5 – The vacuole is an important regulator of amino acid homeostasis in *S. cerevisiae*. Yeast vacuoles are amino acid storage organelles and display multiple transmembrane amino acid transporters that assist amino acid flow to and from the cytosol. Under amino acid starvation, stored amino acids or amino acids resulting from autophagy upregulation are delivered to the cytosol to replenish the free amino acid pool. Moreover, amino acid synthesis is increased. In contrast, when cytosolic amino acids are abundant, they can be stored in the vacuole, used for protein synthesis or degraded, so adequate cytosolic levels are maintained. Notably, V-ATPase activity promotes vacuolar acidification, which in turn is essential for efficient proteolysis in the vacuole and amino acid transport (117).

As a sensor of nutrient availability and stress, TORC1 is a central element in autophagy regulation and was first acknowledged as an autophagy inhibitor by Noda *et al.* (118), who observed that rapamycin treatment induced autophagy in yeast. TORC1 is most activated throughout exponential growth, when amino acid uptake and *de novo* synthesis are increased (66), so autophagy is maintained at constitutive levels (119). When amino acids become scarce, especially during stationary phase, TORC1 is inactive and autophagy is upregulated

for increased protein turnover and replenishment of the free amino acid pool (112, 119). Modulation of autophagy by TORC1 involves its kinase activity. Active TORC1 hyperphosphorylates Atg13, which decreases its affinity for Atg1 and, consequently, the Atg17-Atg31-Atg29 subcomplex. This prevents Atg1 activation, compromising autophagy initiation. In contrast, inactivation of TORC1 allows Atg13 dephosphorylation, so the Atg1 kinase complex is assembled, Atg1 is activated and phagophore biogenesis takes place (120). PP2A has been proposed to counteract TORC1 activity, dephosphorylating Atg13 and inducing autophagy under nutrient starvation (121). Like TORC1, protein kinase A (PKA) can phosphorylate Atg13 (and Atg1) and inhibit autophagy (105). Other downstream targets of PKA are Rim15 and the Msn2/4 transcription factors, also inhibited by Sch9 for autophagy downregulation (Figure 6) (75).

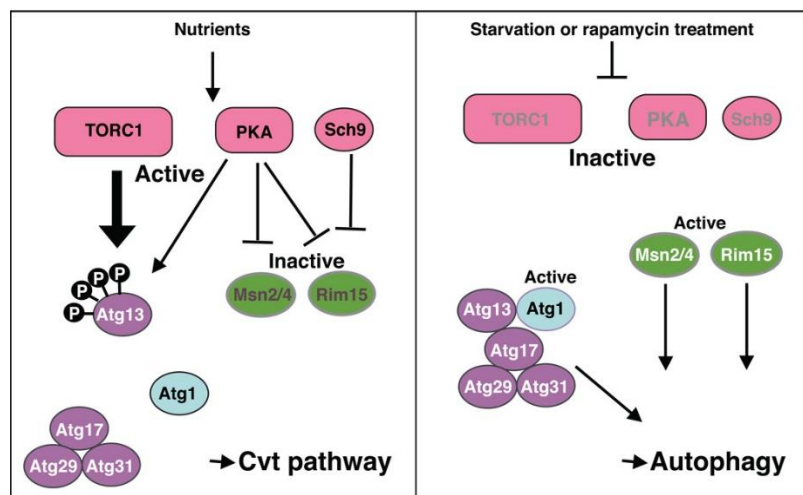


Figure 6 – Autophagy regulation by TORC1, PKA and Sch9 in *S. cerevisiae*. Under nutrient abundance, Atg13 can be phosphorylated by TORC1 and PKA, preventing its association with Atg1 and the Atg17-Atg31-Atg29 subcomplex. Therefore, Atg1 is not activated and autophagy initiation does not occur. Under nutrient limitation or rapamycin treatment, TORC1 is downregulated, so autophagy is promoted through assembly of the Atg1 kinase complex, driving biogenesis of the phagosome assembly site. PKA and Sch9 are negative regulators of Rim15 and Msn2/4, which stimulate autophagy when activated (122).

1.3.3. Autophagy and amino acid homeostasis impact longevity

In mammals, autophagy was shown to decline with aging, alongside decreased expression of proteins involved in the process, including Atg proteins (123, 124). In yeast, studies have shown that deletion of autophagy-essential *ATG* genes decreases CLS, both under normal growth conditions and nitrogen limitation (58, 125). Hence, autophagy is crucial for normal lifespan. Indeed, it is a common mechanism of various longevity-enhancing pathways (75). Consistent with its role in cellular homeostasis and fitness, autophagy upregulation extends the lifespan of multiple organisms, from yeast to mammals, also delaying aging-related

phenotypes (58, 126). Like TORC1 downregulation, autophagy seems to be required for CLS extension by caloric restriction in yeast, promoting respiration proficiency (57, 58). As previously discussed, TORC1 inhibition enhances yeast longevity and this is partially caused by autophagy stimulation, as the lifespan-extending effect of rapamycin requires autophagy upregulation (76). Of note, the cytoprotective effect of autophagy against aging is well established, but this mechanism can be detrimental when excessively and persistently executed (e.g., under proteotoxic stress), causing cell death (127).

In agreement with the role of autophagy in maintaining amino acid homeostasis and promoting longevity, amino acid composition of yeast growth media was shown to significantly impact the CLS of autophagy-deficient cells (58). While autophagy is required for normal longevity in synthetic media, it is not in yeast extract peptone dextrose (YPD, rich media), which is consistent with the fact that autophagy is induced under amino acid limitation and that growth in YPD requires lower amino acid recycling (58, 118, 128). Moreover, individual amino acid supplementation can increase the CLS of autophagy-deficient yeast (58).

Limiting the levels of some essential amino acids was shown to negatively affect yeast CLS, whereas increased supply can extend CLS, in association with augmented cell biomass and resistance to oxidative and thermal stresses (58, 129). Supplementation of growth media with non-essential amino acids can impact longevity, too. For instance, the branched-chain amino acids isoleucine and valine were shown to enhance yeast CLS, partially repressing the general amino acid control pathway, which is responsive to starvation for one or more amino acids, and potentially upregulating protein synthesis (129). In contrast, other amino acids seem to have a deleterious effect on lifespan and restriction can enhance longevity. For example, methionine limitation increases rat and yeast lifespan, mimicking effects of caloric restriction at least in the former (130-132). In yeast, methionine restriction was shown to upregulate *ATG* genes and increase CLS in a mitophagy-dependent manner (131). These studies, among others, indicate that amino acid availability impacts both mammalian and yeast aging (59). Notably, recent reports show that amino acid metabolism is altered in the liver and brain of NPC1 mice models, with potential implication in disease pathogenesis (133, 134).

1.4. α-Ketoglutarate as an anti-aging metabolite

α-KG, also known as 2-oxoglutarate, is an endogenous metabolite with several biological functions. As an intermediate of the Krebs cycle, α-KG plays a role in the production of the reducing agent NADH, required for ATP synthesis through mitochondrial oxidative phosphorylation (135). Also, it participates in nitrogen and amino acid metabolism, being a direct or indirect precursor of several amino acids, including Glu and Gln, proline, arginine and

lysine (136). Additionally, α-KG is a cofactor of α-KG-dependent dioxygenases. These include prolyl hydroxylases, which are important for collagen biosynthesis (in mammals), but also the DNA-demethylating Tet enzymes and histone demethylases, involved in epigenetic regulation (135, 137).

Recent studies have focused on the physiological role of α-KG as a metabolite that delays the aging of various organisms. An α-KG-supplemented diet increases both lifespan and healthspan of mice, in association with reduced levels of inflammatory cytokines (138). In *Drosophila melanogaster* and *Caenorhabditis elegans*, α-KG also extends longevity, which is associated with TOR signalling inhibition (139, 140). In *C. elegans*, α-KG was shown to bind and inhibit the β subunit of ATP synthase, decreasing ATP production and, consequently, the cellular ATP/AMP ratio (139). This resulted in AMP-activated protein kinase (AMPK) upregulation, promoting inhibition of TORC1 and induction of autophagy – two factors that mediate longevity extension in various organisms. Hence, α-KG increased the lifespan of this organism by approximately 50% (140). Likewise, AMPK and TOR are up- and downregulated, respectively, in *D. melanogaster* treated with α-KG, contributing to increased expression of *ATG* genes and phagosome formation (139). In mammals, contrasting observations regarding TORC1 and autophagy regulation by α-KG have been made (140-143).

The main pathways for α-KG synthesis in *S. cerevisiae* include oxidative decarboxylation of isocitrate by isocitrate dehydrogenase (a reaction of the Krebs cycle), oxidative deamination of Glu by NADH-dependent glutamate dehydrogenase 2 (Gdh2) and deamination of Glu by transaminases, also yielding other amino acids (92, 144). Importantly, supplementation of growth medium with α-KG also increases yeast CLS, which is associated with augmented mitochondrial respiration and low-level production of reactive oxygen species, promoting the activation of antioxidant defences and ultimately increasing oxidative stress resistance in stationary phase (145). α-KG-mediated longevity extension is also accompanied by augmented cell biomass, total protein and amino acid levels, and storage of glycogen and glucose (145, 146). Increased activity of Gdh1 and GS by approximately 50% was also observed and likely contributes to the increased amino acid pool (146). In contrast to other organisms, modulation of TORC1 and autophagy by α-KG in yeast has not been described.

As a cofactor of enzymes that catalyse epigenetic modifications, α-KG also regulates chromatin structure and gene transcription, which in turn affect aging and longevity (135). Eukaryotes have four broadly conserved core histone proteins – H2A, H2B, H3 and H4 – that form an octamer by combination of an H2A-H2B dimer and a H3-H4 tetramer (147). In yeast, there are two copies of each core histone gene, arranged in opposite orientation to the gene encoding its partner in the nucleosome: the pair *HHT1-HHF1* encodes histones H3 and H4, whereas *HHT2-HHF2* encodes H2A and H2B (148, 149). Deletion of *HHT1-HHF1* and

decreased expression of H3 and H4 negatively impact CLS, whereas increased levels of histone proteins extend both replicative lifespan and CLS (150, 151). Consistently, histone levels decrease throughout aging (151). CLS is also influenced by the methylation state of specific histone lysine residues, which can be reversibly mono-, di- or trimethylated. For instance, trimethylation of lysine 4 in histone H3 (H3K4me3) of yeast is required for normal CLS, preventing premature aging by promotion of histone gene expression, and trimethylation of lysine 36 (H3K36me3) is important for replicative lifespan, enhancing transcription fidelity (150, 152). α -KG is a cofactor of Jumonji C (JmjC) domain-containing demethylases, which mediate demethylation of histone lysine residues. Thus, yeast JmjC proteins, such as Jhd2 (H3K4 demethylase), Jhd1 and Rph1 (H3K36 demethylases), play an important role in lifespan regulation (150, 152).

CHAPTER 2. Aim of the study

Recently, Vilaça *et al.* (44) showed that phytoceramide-mediated hyperactivation of the Ser/Thr phosphatase Sit4 in *ncr1* Δ yeast cells contributes to mitochondrial dysfunction and a shortened CLS. Moreover, Gln3 activity is increased in these cells, in a Sit4-dependent manner (44). As previously discussed, Gln3 is a transcription factor that, under the regulation of TORC1 and Sit4, promotes the expression of NCR-sensitive genes, such as *GDH1* and *GLN1* (84). These genes are involved in the synthesis of the amino acids Glu and Gln, respectively, which can activate TORC1 in yeast (the former to a lesser extent) (85). Thus, we hypothesized that Glu and Gln levels of *ncr1* Δ cells may be augmented, in a Gln3-dependent manner, stimulating TORC1 activity. Since TORC1 is a known inhibitor of mitochondrial function, its hyperactivation could contribute to the mitochondrial dysfunction phenotype of these cells. TORC1 also inhibits autophagy and impaired autophagic flux in NPC1-deficient cells is heavily documented, so we further hypothesized that *ncr1* Δ cells display autophagic defects, causing accumulation of defective mitochondria and premature death. Of note, Gln3 hyperactivation and autophagy impairment may affect amino acid homeostasis, which impacts yeast CLS (57). Increased activity of Gln3 could also decrease α -KG levels of *ncr1* Δ cells, as α -KG is used for Glu and Gln synthesis (84). Besides being an intermediate of the Krebs cycle, α -KG has emerged as a key metabolite in longevity extension. Therefore, a potential decrease in α -KG levels of *ncr1* Δ cells could negatively impact their lifespan.

This study aimed to: 1) evaluate TORC1 activation and the autophagic flux in *ncr1* Δ cells; 2) determine the role of Gln3 in those phenotypes and in the previously reported shortened CLS and mitochondrial dysfunction of *ncr1* Δ cells, and 3) characterize amino acid and α -KG homeostasis in *ncr1* Δ cells, and their role in the CLS of this model of NPC1.

CHAPTER 3. Materials and methods

3.1. Yeast strains and growth conditions

S. cerevisiae strains used in this study are depicted in Table 1.

Yeast cells were grown aerobically to early exponential ($OD_{600} = 0.6$), late exponential ($OD_{600} = 2$), PDS ($OD_{600} = 5-6$) or stationary phases ($OD_{600} = 8-12$; 2 days after early exponential phase) in Erlenmeyer flasks placed on an orbital shaker (140 rpm), at 26 °C. Growth media were used with a 1:5 ratio of medium volume to flask volume and comprised: YPD [2% (w/v) bacteriological peptone, 1% (w/v) yeast extract and 2% (w/v) glucose] and synthetic complete drop-out medium containing either glucose [SC – 2% (w/v) glucose, drop-out, 0.67% (w/v) yeast nitrogen base without amino acids and, when appropriate, 0.008% (w/v) histidine, 0.04% (w/v) leucine, 0.008% (w/v) tryptophan and 0.008% (w/v) uracil] or glycerol [SC-glycerol – with 3% (v/v) glycerol instead of glucose]. When indicated, SC or SC-glycerol media were supplemented with α-ketoglutaric acid (Sigma-Aldrich), L-glutamic acid (Merck), L-glutamine (Sigma), or L-arginine monohydrochloride (Roth) for a 10 mM final concentration. Media pH was adjusted to that of non-supplemented media before autoclaving, using 5 M NaOH and a pH electrode (WTW inoLab pH 720). Solid media were prepared by adding 1.5% (w/v) agar.

Table 1 – Strains, genotypes and sources of *S. cerevisiae* used in this study.

Yeast strain	Genotype	Source
BY4741	MATa, <i>his3Δ1</i> , <i>leu2Δ0</i> , <i>met15Δ0</i> , <i>ura3Δ0</i>	EUROSCARF
<i>ncr1Δ</i>	BY4741 <i>ncr1Δ::KanMX4</i>	Vilaça <i>et al.</i> (44)
<i>ncr1Δ</i>	BY4741 <i>ncr1Δ::MXURA3</i>	This study
<i>gln3Δ</i>	BY4741 <i>gln3Δ::KanMX4</i>	This study
<i>ncr1Δgln3Δ</i>	BY4741 <i>ncr1Δ::MXURA3 gln3Δ::KanMX4</i>	This study

3.2. Gene disruption

Yeast null mutants were generated by replacement of target genes with deletion cassettes, i.e., linear DNA fragments containing a selectable marker gene that allows artificial selection of transformants. When flanked by homologous regions of the target gene, these cassettes disrupt the latter by homologous recombination.

Gene deletion cassettes were amplified by polymerase chain reaction (PCR) prior to yeast transformation, using T100 Thermal Cycler (Bio-Rad). For cassette amplification from plasmid DNA, reaction mixtures consisted of: 5 ng of plasmid, forward and reverse primers (0.25 μM), 20 μL of Supreme NZYtaq II 2x Green Master Mix (NZYTech) and ultrapure water for a final volume of 40 μL. For colony PCR, yeast cells were firstly resuspended in 9 μL of ultrapure

water and heated in the microwave for 30 seconds at 750 W, for cell lysis. Then, the primers (0.25 μM) and 10 μL of Supreme NZYtaq II 2x Green Master Mix were added. PCR programs and primers used are listed in Table 2.

Table 2 – Polymerase chain reaction (PCR) programs and primers used in this study.

Gene or disruption cassette	Primer name, application and nucleotide sequence	PCR program		
		Annealing temperature / °C	Elongation time / s	Cycles
<i>MXURA3</i>	p82_FW (amplification): 5' TCCTTGACAGTCTTGACG 3'	47	45	36
	p83_RV (amplification): 5' GTATAGCGACCAGCATTC 3'			
<i>ncr1::MXURA3</i>	CaURA_FW (confirmation): 5' AGAGAGCAGAACTCATGC 3'	49	60	34
	Ncr1_ext_RV (confirmation): 5' TTACGAGTGAAGCGTTCTGG 3'			
<i>gln3::KanMX4</i>	GLN3_FW (amplification): 5' TCTATTACCCGGCGGACAG 3'	60	60	34
	GLN3_RV (amplification): 5' GCTCAGGATTGTGGTCAGAG 3'			
	GLN3_CONF (confirmation): 5' CTCTATCTCTACCTGGCC 3'	48	45	34
	p83_RV (confirmation): 5' GTATAGCGACCAGCATTC 3'			

PCR products were analysed by nucleic acid electrophoresis using a 1% (w/v) agarose gel prepared in Tris-acetate-EDTA (TAE) with addition of 0.005% (v/v) GreenSafe Premium (NZYTech). The purification and quantification of amplified DNA were performed using NZYMiniprep (NZYTech) and NanoDrop 1000 Spectrophotometer (Thermo Fisher Scientific), respectively.

For construction of *ncr1Δ::MXURA3* mutants, the *MXURA3* cassette was firstly amplified from pAG61 plasmid. *Escherichia coli* carrying pAG61 were grown overnight in liquid lysogeny broth medium [LB – 1% (w/v) tryptone, 1% (w/v) NaCl, 0.5% (w/v) yeast extract] supplemented with 0.01% (w/v) ampicillin (LB + amp), at 37 °C. After its extraction, purification and quantification, pAG61 was used for amplification of *MXURA3* by PCR as described in Table 2. Lastly, *ncr1Δ::KanMX4* cells were transformed with the cassette, generating *ncr1Δ::MXURA3* mutants by *KanMX4* replacement. Cassette substitution was confirmed by PCR.

To create *gln3Δ::KanMX4* and the double mutant *ncr1Δ::MXURA3 gln3Δ::KanMX4*, the *KanMX4* cassette with flanking regions of *GLN3* was amplified by colony PCR using the *gln3Δ::KanMX4* mutant from EUROSCARF. The amplified fragment was purified and used to transform BY4741 and *ncr1Δ::MXURA3*, generating *gln3Δ* cells and the double mutant, respectively. *GLN3* disruption was confirmed by PCR.

3.3. Plasmid construction and amplification

To analyse autophagic flux levels, yeast cells were firstly transformed with plasmid pRS413-GFP-ATG8 (*HIS3* marker), which was created in this study from pRS416-GFP-ATG8 (*URA3* marker, lab collection). For that purpose, pRS413 and pRS416-GFP-ATG8, previously isolated from *E. coli*, were doubly digested with restriction enzymes *SacI* and *SalI* in *Bam*HI buffer (Thermo Fisher Scientific), at 37 °C, for 2 hours. The products of each reaction mixture were analysed by nucleic acid electrophoresis; then, the pRS413 backbone and the promotor-GFP-ATG8 fragment (hereinafter referred to as “insert”) from pRS416 were purified using NZYGelpure Kit (NZYTech) and quantified. Introduction of the insert into pRS413 was conducted using Rapid DNA Ligation Kit (Thermo Fisher Scientific): 50 ng of vector were incubated with the insert (1:3 molar ratio) and DNA ligase in ligation buffer at room temperature for 2 hours (a negative control was performed without insert). An aliquot of DH5α *E. coli* (100 μL) was transformed with the ligation reaction mixture (10 μL) by incubating 30 min on ice, followed by 90 seconds at 42 °C and 2 min on ice. LB was then added for a final volume of 1 mL. Cells were incubated at 37 °C for 1 hour and plated in solid LB + amp for overnight growth at 37 °C. Lastly, pRS413-GFP-ATG8 was amplified by inoculation of a transformed colony in liquid LB + amp, at 37 °C. After purification and quantification, the plasmid was used for yeast transformation.

3.4. Yeast transformation

Yeast were transformed using the lithium acetate/single-stranded carrier DNA/PEG method described by Gietz *et al.* (153). Briefly, cells (20-mL culture) were grown to early exponential phase in YPD and collected by centrifugation at 4000 rpm for 5 min. The pellet was resuspended in 2 mL of water and equally distributed between two microcentrifuge tubes – one to harbour the transformants and the other non-transformed cells (negative control). After washing, cells were resuspended in 240 μL of 50% (w/v) PEG 3350, 36 μL of 1 M lithium acetate, 25 μL of single-stranded carrier DNA (5 mg/mL), the appropriate volume of plasmid DNA or gene disruption cassette solution (replaced with water for the control) and water for a

final volume of 360 μ L. For transformations with pRS413-GFP-ATG8, the mixtures were incubated at 42 °C for 30 minutes and, after washing with sterile water, cells were plated in solid SC medium lacking histidine. For transformation with deletion cassette, the incubation at 42 °C was preceded by 30 min incubation at 26 °C. Importantly, in case of deletion with *KanMX4*, cells were then transferred to YPD media and allowed to recover with incubation at 26 °C, for 4 hours, before plating in solid YPD supplemented with 0.02% (w/v) geneticin. For transformation with *MXURA3*, cells were plated in SC lacking uracil immediately after incubation at 42 °C.

3.5. Chronological lifespan

Yeast CLS was assessed as described in (154). Overnight cultures were diluted to $OD_{600} = 0.2$ in SC, non-supplemented or supplemented with 10 mM α -KG, Glu, Gln or arginine, grown to PDS (24 h; day 0 of the CLS assay) and maintained in growth medium over time. At indicated timepoints, a standard dilution of the cultures was plated on solid YPD and the number of colony-forming units (CFUs) was counted after 3-day incubation at 26 °C. Viability was expressed as the percentage of CFUs counted for each day in relation to day 0. The area under each lifespan curve was computed using GraphPad Prism 8. Culture pH was monitored throughout the assay using a pH electrode (WTW inoLab pH 720).

3.6. Oxygen consumption and growth in glycerol plates

Oxygen consumption rate was measured using an oxygen electrode system (Oxygraph+, Hansatech). Cells (3×10^8) grown to PDS in SC medium were harvested and washed with water. Next, cells were resuspended in 1 mL of phosphate-buffered saline (137 mM NaCl, 2.7 mM KCl, 8 mM Na_2HPO_4 , 2 mM KH_2PO_4). This suspension was loaded into the oxygen chamber and oxygen levels were measured for 1 min, with constant magnetic stirring, at room temperature. Data was analysed with Oxyg32 software (version 2.25).

For analysis of respiratory growth capacity, cells grown to PDS in SC, with and without 10 mM α -KG, were diluted to $OD_{600} = 0.1$ in sterile water and three 10-fold serial dilutions were made. Each dilution prepared from non-supplemented SC cultures was pipetted (10 μ L) onto SC and SC-glycerol plates, while dilutions of SC cultures supplemented with α -KG were pipetted onto SC-glycerol plates containing 10 mM α -KG. The plates were incubated at 26 °C for 4 days.

3.7. α-Ketoglutarate levels

Intracellular levels of α-KG were assessed using the α-ketoglutarate assay kit from Sigma-Aldrich (product number: MAK054), which is based on a coupled enzyme reaction. Briefly, yeast cells grown to late exponential phase in SC medium (30 mL) were harvested and washed with water. Next, the cells were mechanically lysed in 120 μL of assay buffer by vigorous vortexing with 0.5 mm zirconia beads (Biospec). Following centrifugation, the supernatant was collected and protein levels were measured using Pierce BCA Protein Assay Kit (Thermo Fisher Scientific). Protein concentration was normalized to 5 mg/mL and samples were deproteinized with 3 kDa molecular weight cut-off centrifugal filters (VWR) at 13000 g for 25 min. Lastly, 50 μL of sample incubated with the appropriate reaction mixture at 37 °C for 30 min and fluorometric detection of the product (proportional to α-KG) was conducted at $\lambda_{ex} = 535 \text{ nm}/\lambda_{em} = 587 \text{ nm}$ using Synergy Mx microplate reader (BioTek) and Gen5 software.

3.8. Western blotting

3.8.1. TORC1 activity

Cells grown to early exponential and PDS phases in SC, non-supplemented or containing 10 mM α-KG, Glu or Gln, were harvested and washed with water. Post-alkaline protein extraction was subsequently performed as described in (155): cells were treated with 0.1 M NaOH for 5 minutes at room temperature, pelleted and resuspended in sample buffer [2% (w/v) SDS, 10% (v/v) glycerol, 0.002% (w/v) blue bromophenol, 0.125 M Tris-HCl pH 6.8]. After boiling for 5 minutes at 95 °C, samples were centrifuged at 13000 rpm for 3 min, and the supernatant collected. Total protein levels of the supernatant were determined using Pierce BCA Protein Assay Kit (Thermo Fisher Scientific).

For sample preparation, protein extracts (20 μg) were diluted in sample buffer and 5% (v/v) β-mercaptoethanol was added for a final volume of 10 μL. After 5-min incubation at 95 °C, proteins were separated by SDS-polyacrylamide gel electrophoresis (SDS-PAGE) in a 10% polyacrylamide gel, at 85-110 V. Then, proteins were transferred to a nitrocellulose membrane (GE Healthcare Lifesciences) at 40 mA/cm², for 1 hour, using Tris-glycine transfer buffer (59.9 mM Tris, 48.8 mM glycine, 1.62 mM SDS) with 20% (v/v) methanol for semi-dry transfer. Next, the membrane was stained with Ponceau S [0.5% (w/v) Ponceau S, 5% (v/v) acetic acid] to confirm protein electrotransfer, and destained with Tris-buffered saline (TBS – 19.8 mM Tris, 150.6 mM NaCl, pH 7.6).

For immunodetection of phospho-Rps6 (Ser232/233) and Pgc1 (loading control), membranes were blocked with 5% (w/v) non-fat dry milk prepared in TBS containing 0.05% (v/v) Tween 20

(TBST 0.05%), for 1 hour (room temperature). Membranes were then probed with the following primary antibodies, prepared in blocking buffer: rabbit anti-phospho-Rps6 (S235/236) (Cell Signaling) at 1:6000, overnight (4 °C), and mouse anti-Pgk1 (Thermo Fisher Scientific) at 1:20000, for 1 hour (room temperature). Following three 5-min washes with TBST 0.05%, membranes were probed with the appropriate peroxidase-linked secondary antibody – goat anti-rabbit IgG (Sigma-Aldrich) or goat anti-mouse IgG (Invitrogen) –, at 1:10000, for 1 hour (room temperature). Lastly, membranes were washed three times for 5 min with TBST 0.05% and one time with TBS. Immunodetection was conducted using WesternBright ECL kit and LucentBlue x-ray films (Advansta). Film scanning and densitometric quantification were performed using GS-800 Calibrated Densitometer and Quantity One 1-D analysis software (Bio-Rad).

3.8.2. Autophagic flux

To evaluate autophagic flux levels, cells carrying pRS413-GFP-ATG8 were grown to early exponential and/or stationary phase in SC lacking histidine, supplemented or not with 10 mM α-KG, Glu or Gln. As a positive control, exponentially growing BY4741 cells were treated with rapamycin (200 ng/mL) for 4 hours. Samples were prepared as described for measurement of TORC1 activity, except 15 µg of protein extract were loaded in a 12% polyacrylamide gel. Protein transfer was performed at 40 mA/cm² for 1 hour, followed by membrane blocking with TBST 0.05% containing 5% (w/v) non-fat dry milk, for 1 hour (room temperature). Membranes were firstly probed with mouse anti-GFP primary antibody (Roche), prepared at 1:3000 in blocking buffer, overnight (4 °C), and later with goat anti-mouse IgG (Invitrogen), at 1:10000, for 1 hour (room temperature). For detection of Pgk1, membranes were stripped by incubation at 50 °C for 30 minutes in stripping buffer (62.5 mM Tris-HCl pH 6.8, 2% SDS, 100 mM β-mercaptoethanol). After washing with deionised water and TBST 0.05% for β-mercaptoethanol removal, membranes were blocked again and probed with anti-Pgk1 (Thermo Fisher Scientific).

3.8.3. Histone H3 levels

Yeast cells grown in SC with and without 10 mM α-KG were harvested at early exponential and stationary phase growth phases. Histones were then extracted according to Zhang *et al.* (156): cell pellets were sequentially treated with 2 M lithium acetate and 0.4 M NaOH for 5 min, on ice; after centrifugation, cells were resuspended in sample buffer, incubated at 95 °C for 5 min and centrifuged at 13000 rpm for 3 min. The supernatant was collected and protein

concentration was determined using Pierce BCA Protein Assay Kit (Thermo Fisher Scientific). SDS-PAGE was performed as described before, except 25 µg of protein were loaded in a 15% polyacrylamide gel. Protein transfer was conducted at 20 mA/cm² for 1 hour.

For detection of histone H3, membranes were firstly blocked with 5% (w/v) non-fat dry milk prepared in TBS containing 0.1% (v/v) Tween 20 (TBST 0.1%), for 1 hour (room temperature), and then probed with rabbit anti-histone H3 antibody (Cell Signaling), prepared at 1:2000 in blocking buffer, overnight (4 °C). Goat anti-rabbit IgG (Sigma) prepared at 1:5000 in blocking buffer was used as secondary antibody, with incubation for 1 hour (room temperature). Immunodetection of Pgk1 was carried out as described above.

3.9. Isolation of intact vacuoles

The protocol for vacuole isolation was based on (157) and (158). Yeast cells (2 L culture) grown to late exponential phase in SC medium were harvested by centrifugation at 4000 rpm for 10 min (High Speed Centrifuge Beckman Avanti J-26 XP, rotor JLA-8 1000) and washed with 1 M Tris-HCl (pH 8.9). After measuring the wet weight of cells, the pellet was resuspended in 25 mL of Tris-HCl, to which 250 µL of 1 M dithiothreitol were added. This mixture incubated at 30 °C for 10 min, with gentle agitation. Cells were then harvested and resuspended in spheroplasting buffer, containing: 2.5 mL of 1.1 M sorbitol per g of cells, 1 mM PMSF, and 1.3 mg or 1.5 mg of zymolyase (20T, Amsbio) per g of wild type or *ncr1Δ::KanMX4* cells, respectively. Formation of spheroplasts was conducted at 30 °C for 40-80 minutes, with light agitation. This process was monitored under the microscope and by OD₆₀₀ measurement over time. For the latter, the suspension was diluted 100-fold in water. Ideally, a decrease in 90% and 75% of the initial OD was obtained for the wild type and *ncr1Δ* strains, respectively.

All steps following spheroplast formation were performed on ice or at 4 °C. Spheroplasts were harvested by centrifugation, washed with 1.1 M sorbitol and resuspended in 30 mL of ice-cold lysis buffer (10 mM Tris-MES, 12% Ficoll, 0.1 mM MgCl₂, pH 6.9) containing protease inhibitor cocktail (PIC – Roche). The suspension was firstly homogenized using a P1000 pipette (with cut tips for a hole diameter of 4 mm) and then a 40-mL Dounce homogenizer (Wheaton), using the loose pestle for 15 up and down strokes. The spheroplast lysate was evenly distributed between two centrifuge tubes (38.5 mL Open-Top Thinwall Ultra-Clear Tube, Beckman Coulter) and equal volumes of 8% Ficoll (10 mM Tris-MES, 8% Ficoll, 0.5 mM MgCl₂, pH 6.9 with PIC) and 4% Ficoll (10 mM Tris-MES, 4% Ficoll, 0.5 mM MgCl₂, pH 6.9 with PIC) solutions were sequentially added for a final volume of 38 mL. Vacuoles were isolated by gradient centrifugation at 30 000 rpm for 2 hours, 4 °C (SW 32 Ti Swinging-Bucket Rotor, Beckman Coulter). The white coat on top of the 4% Ficoll layer was pipetted (using cut tips) to 2-mL

microcentrifuge tubes, diluted to half with 10 mM Tris-MES, 0.5 mM MgCl₂, pH 6.9 (containing PIC) and centrifugated at 5 200 g for 20 min, 4 °C, to concentrate the organelles. Finally, vacuolar protein concentration was measured using Pierce BCA Protein Assay Kit (Thermo Fisher Scientific).

3.10. Amino acid levels

For analysis of amino acid levels, BY4741 and *ncr1Δ::KanMX4* cells grown to late exponential and PDS phases in SC, supplemented or not with 10 mM α-KG, were harvested by centrifugation and washed with water. The amino acid content of vacuoles isolated from BY4741 and *ncr1Δ::KanMX4* cells (see section 2.10.) was also determined. Analyses were performed at the University of Minho, Portugal.

Amino acids of whole cells or vacuoles were extracted using a modified version of the protocol described by McCombie *et al.* (159). Firstly, samples were resuspended in 300 μL of chloroform:methanol (1:2) and transferred to a 2-mL bead beater vial, to which 0.5 mm acid-washed beads were added. Bead beating was executed for 1 min at 4°C, four times, using a homogenization setting for membrane disruption. Then, the lysate was transferred to a new Eppendorf and the beads were rinsed with 300 μL of chloroform:methanol (1:2). The wash was added to the lysate, as well as 200 μL of chloroform:methanol (1:2) and 200 μL of water. This mixture was vortexed and centrifuged at 14000 rpm for 10 min, at 4°C. The resulting aqueous layer was isolated, transferred to a new Eppendorf and analysed by high performance liquid chromatography. Precolumn derivatization using ortho-phthalaldehyde (OPA with methanol ≥ 99.9%, potassium borate 1 M pH 9.5 and mercaptoethanol ≥ 99.0%) 1:5 (Sigma Aldrich) was performed and the Gilson UV/VIS-155 detector (338 nm) was used. The mobile phases for elution were degasified for 30 min and comprised: inorganic mobile phase A, pH 7.8 [350 mM Na₂HPO₄•2H₂O:250mM sodium phosphate dibasic (1:1) (Merck) with acetonitrile in water (10:2:13)] and organic mobile phase B [acetonitrile:methanol:water (3:3:4) (HPLC grade, HiPerSolv Chromanorm, VWR Chemicals)]. Standard solutions were prepared in Milli-Q water (Millipore). A Gilson bomb system was used, with a 40 °C Hi-Chrom C18 (model HI5C18-250A) 5-μm particle column. Data was analysed with Gilson Uniprot Software (version 5.11).

3.11. Mutation frequency

L-canavanine is a toxic analogue of L-arginine that interferes with the activity of enzymes that use the latter as a substrate. Mutations in the *CAN1* gene, which encodes for a plasma membrane arginine permease, confer resistance to L-canavanine and increase gradually

throughout yeast aging, being associated with decreased genomic stability and CLS (160, 161). Consistently, evaluation of cell growth capacity in canavanine selective medium is useful to determine the rate of *CAN1* spontaneous mutations and, hence, genomic instability (161). Determination of spontaneous mutation frequency was conducted according to Weinberger *et al.* (161). BY4741 and *ncr1* Δ cells were grown to PDS and stationary phases in SC medium and a standard dilution of the cultures was plated on solid SC and SC lacking arginine but supplemented with L-canavanine sulphate (60 mg/L) (Sigma Aldrich). The plates were incubated at 26 °C for 3 days and the number of CFUs per plate was counted. Mutation frequency was calculated as the ratio between the number of CFUs grown in canavanine selective plates and CFUs grown in SC plates.

3.12. Statistical analysis

The results are presented as the mean and standard deviation (SD) or mean and standard error of the mean (SEM) of at least two independent experiments. The statistical analysis of results was performed with GraphPad Prism software (version 9.2.0). Values were compared using the two-tailed *t*-test ($p < 0.05$). For the intracellular and vacuolar amino acid analyses, unpaired *t*-tests were performed with multiple comparisons, using the Holm-Šídák method ($p < 0.05$).

CHAPTER 4. Results and discussion

4.1. TORC1 signalling is decreased in yeast lacking Ncr1

In a recent study, Vilaça *et al.* (44) suggested a link between phytoceramide accumulation in *ncr1Δ* yeast cells and Sit4-mediated activation of the GATA transcription factor Gln3 – a positive regulator of NCR-sensitive gene transcription, known to upregulate *GDH1* and *GLN1* expression (84). TORC1 is also involved in Gln3 regulation, and it senses nutrient availability to ultimately promote cell growth, being activated by Gln and other amino acids (48). Importantly, TORC1 hyperactivation decreases lifespan whereas its downregulation extends the lifespan of multiple organisms (128). Thus, we hypothesized that TORC1 could be dysregulated in the yeast model of NPC1 (*ncr1Δ*), contributing to the decreased CLS and mitochondrial dysfunction of this mutant. To test this, we characterized TORC1 activity in BY4741 (wild type), *ncr1Δ*, *gln3Δ* and *ncr1Δgln3Δ* cells grown to early exponential and PDS phases, by assessing TORC1-mediated phosphorylation of ribosomal protein S6 (Rps6 in yeast) at S232/233 (S235/236 in human S6) (162).

Cells lacking Ncr1 showed significantly lower levels of phospho-Rps6 than the wild type strain, at both growth phases tested (Figure 7). This suggests TORC1 signalling is downregulated in this yeast model of NPC1. Consistently with having decreased levels of Gln due to *GLN1* downregulation (63, 163), the *gln3Δ* mutant also had decreased TORC1 activity, similar to that observed in *ncr1Δ* cells. Similar results were obtained for the double mutant *ncr1Δgln3Δ*, indicating that hyperactivation of Gln3 does not contribute to TORC1 signalling dysregulation in Ncr1-deficient yeast cells.

The decreased TORC1 activity in *ncr1Δ* cells may contribute to their slower growth rate in comparison to the wild type strain (not shown), as TORC1 is a major promotor of cell growth. Moreover, since TORC1 is a negative regulator of Gln3, its reduced activity, together with the previously reported hyperactivation of Sit4 (44), is likely to contribute to the hyperactivation of Gln3. As previously mentioned, *TOR1* deletion or rapamycin-mediated TORC1 inhibition increase yeast CLS (70, 71), so it is intriguing that TORC1 is downregulated in the short-lived *ncr1Δ* mutant. Nonetheless, this observation indicates that the premature death and mitochondrial dysfunction of yeast lacking Ncr1 do not derive from TORC1 upregulation.

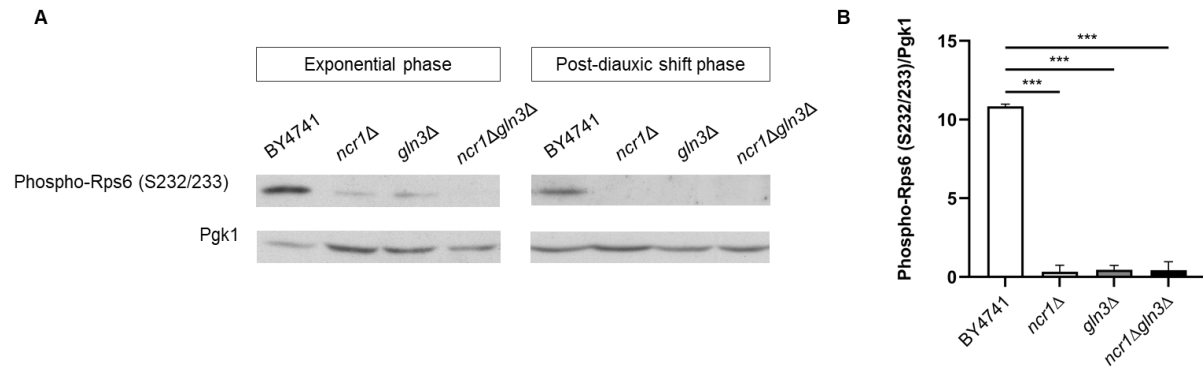


Figure 7 – TORC1 signalling is altered in yeast lacking Ncr1, in a Gln3-independent manner. **A)** *S. cerevisiae* BY4741, *ncr1Δ*, *gln3Δ* and *ncr1Δgln3Δ* cells were grown in SC medium to early exponential and post-diauxic shift phases. The levels of phospho-Rps6 (S232/233), used as read-out of TORC1 activity, were evaluated by western blotting. Pgk1 was used as loading control. **B)** Phospho-Rps6 (S232/233)/Pgk1 ratio in BY4741, *ncr1Δ*, *gln3Δ* and *ncr1Δgln3Δ* cells grown to early exponential phase. Values shown are the mean \pm SD of three independent experiments. *** $p < 0.001$.

Consistent with our results, Xu *et al.* (53) reported that siRNA-mediated knockdown of *NPC1* in human endothelial cells inhibited TORC1. However, Davis *et al.* (54) observed that lysosomal cholesterol build-up in *NPC1*-defective engineered neurons induced TORC1 hyperactivation. In *NPC1*-deficient mice embryonic fibroblasts and *NPC1* patient fibroblasts no alterations were reported (28). Overall, these diverging results suggest that disruption of *NPC1* function can have different effects on TORC1 activity, depending on the cells or tissues analysed. Interestingly, both upregulation and downregulation of TORC1 have been shown to rescue phenotypes of *NPC1* disease (27, 54, 164).

A recent study showed that mammalian TORC1 is activated by lysosomal cholesterol through a mechanism that involves the lysosomal SLC38A9 amino acid transporter, whereas *NPC1* inactivates TORC1 by removing cholesterol from the lysosome (165). Indeed, loss of function of *NPC1* and consequent lysosomal cholesterol accumulation are the cause for TORC1 hyperactivation in the *NPC1* model of Davis *et al.* (54). Up to date, ergosterol-promoted TORC1 activation in yeast has not been described.

4.2. Autophagic flux is impaired in yeast lacking Ncr1, in a Gln3-independent manner

Autophagy is a conserved and tightly regulated catabolic process with a fundamental role in development, survival and aging (100). Under normal growth conditions, it is executed at basal levels for general maintenance of homeostasis. However, if nutrients are scarce, it is upregulated for increased turnover of macromolecules and utilization of their building blocks (112). Damaged molecules and organelles can also be targeted for degradation, increasing

the threshold for apoptosis. Hence, defects in autophagy can contribute to neurodegeneration and accelerated aging, being highly common in LSDs (2, 68).

We hypothesized that autophagy could be impaired in *ncr1Δ* cells, although in a TORC1-independent manner, since TORC1 signalling was decreased in these cells. Defects in autophagy may arise from dysregulation of other molecular pathways. Indeed, Gln3 has been proposed to transcriptionally regulate *ATG* genes (166, 167). Bernard *et al.* (167) showed that Gln3 is required for *ATG8* expression under nitrogen starvation, but its absence does not impact autophagic flux under these conditions. On the other hand, Gln3 decreases Atg8 levels in normal growing conditions and this negatively affects autophagy in the short term after nitrogen starvation induction. Hence, Gln3 is predicted to directly or indirectly repress *ATG8* (167). Atg8 is essential for autophagy execution, as *ATG8* disruption abolishes autophagosome formation under nutrient starvation (168).

Throughout autophagosome formation, Atg8 remains associated to its inner membrane by conjugation to PE. Only when the autophagosome and vacuole fuse does it suffer proteolysis (110, 111). Hence, the autophagic flux of yeast cells is commonly monitored by assessing Atg8 delivery to the vacuole. For that, cells are transformed with a plasmid that expresses N-terminal GFP-tagged Atg8, under control of the endogenous promoter. When delivered to the vacuole, GFP-Atg8 is cleaved and, while Atg8 is rapidly degraded, GFP is resistant to hydrolysis. Thus, the levels of free GFP are indicative of autophagy flux levels (111). To assess if the autophagic flux of *ncr1Δ* cells was impaired and if this could derive from Gln3 hyperactivation, we transformed BY4741, *ncr1Δ*, *gln3Δ* and *ncr1Δgln3Δ* cells with pRS413-GFP-ATG8. These cells were grown to early exponential and stationary phases in SC medium lacking histidine and processing of GFP-Atg8 was monitored by western blotting, using an anti-GFP antibody. In exponentially growing cells, autophagy was not detected, probably due to the low levels at which it operates under growing conditions (Figure 8 – A). However, reaching stationary phase, when nutrients become scarce, autophagy was induced in the wild type strain with a flux of 12%, but not in *ncr1Δ* cells (Figure 8 – A, B). This confirms our hypothesis that autophagy is blocked in the yeast model of NPC1. Consistent with decreased TORC1 activity, the *gln3Δ* mutant displayed a 3-fold increase in autophagic flux, in relation to the wild type. However, the double mutant *ncr1Δgln3Δ*, like *ncr1Δ* cells, was not capable of inducing autophagy (Figure 8 – A, B). Thus, autophagic flux impairment in *ncr1Δ* cells is not caused by Gln3 hyperactivation. Atg8 quantification (sum of GFP-Atg8 and free GFP levels; Figure 8 – C) showed that Atg8 expression was also significantly reduced in *ncr1Δ* cells (7.5-fold), in relation to the wild type. So, decreased levels of Atg8 may contribute to the defective autophagic flux of *ncr1Δ* cells, through reduced autophagosome formation. Atg8 levels were not significantly increased in the *gln3Δ* mutant and deletion of *GLN3* in *ncr1Δ* cells did not restore Atg8 to normal levels,

indicating that decreased Atg8 expression in the *ncr1* Δ mutant did not result from Gln3 hyperactivation.

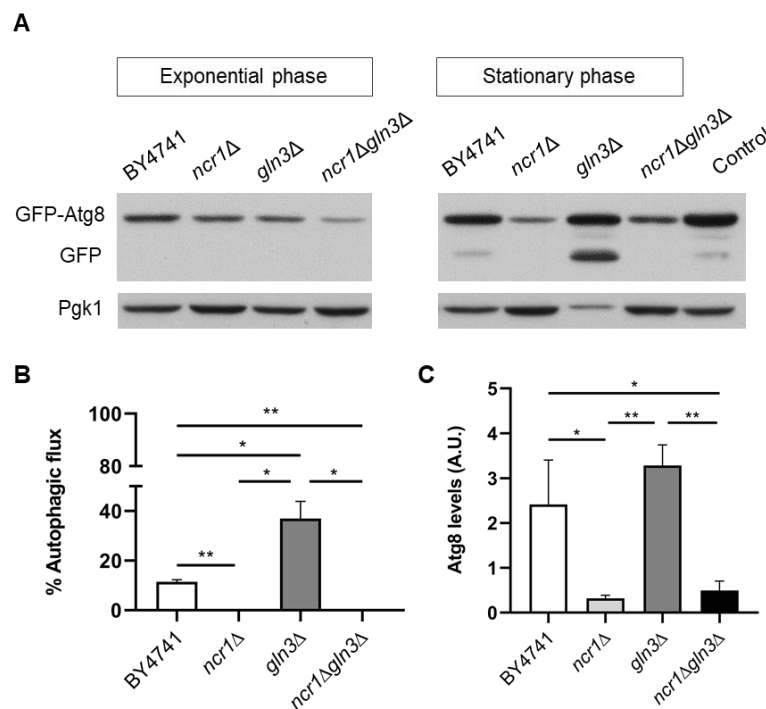


Figure 8 – Autophagic flux of yeast lacking Ncr1 is impaired in stationary phase, in a Gln3-independent manner. A) *S. cerevisiae* BY4741, *ncr1* Δ , *gln3* Δ and *ncr1* Δ *gln3* Δ cells carrying pRS413-GFP-ATG8 were grown to early exponential and stationary phases. Exponentially growing BY4741 cells were treated with rapamycin for positive control. GFP-Atg8 and free GFP levels were analysed by western blotting. Pgk1 was used as loading control. **B)** Percentage of autophagic flux [(GFP)/(GFP+GFP-Atg8)×100] of BY4741, *ncr1* Δ , *gln3* Δ and *ncr1* Δ *gln3* Δ cells in stationary phase. **C)** Atg8 levels [(GFP+GFP-Atg8)/Pgk1 ratio, in arbitrary units (A.U.)] of BY4741, *ncr1* Δ , *gln3* Δ and *ncr1* Δ *gln3* Δ cells in stationary phase. Values shown are the mean \pm SD of at least three independent experiments. * $p < 0.05$; ** $p < 0.01$.

Since autophagy is important for the maintenance of a healthy mitochondrial network and organismal longevity (125), its impairment is likely to contribute to the mitochondrial defects and premature death of the *ncr1* Δ mutant. Additionally, we hypothesized that autophagy blockage could compromise amino acid homeostasis in *ncr1* Δ cells, because this catabolic pathway helps to maintain the cytosolic amino acid pool at adequate levels, especially under nutrient starvation (114, 117). Defects in amino acid homeostasis may also contribute to decreased TORC1 activity, as TORC1 is activated by amino acids, namely Gln and leucine, in yeast (63). Of note, the previously reported reduced acidification of *ncr1* Δ vacuoles may be related with the defective autophagic flux, as a low pH is required for activity of hydrolytic enzymes (40, 114). Vacuolar acidification, mediated by V-ATPase, is also important for maintenance of the cytosolic pH, mitochondrial function and amino acid transport across the vacuolar membrane (114).

Consistent with our results, studies have shown that the autophagic flux is impaired in NPC1-deficient mammalian cells, as autophagosome turnover is decreased (the levels of p62, a cargo receptor, are increased), leading to their accumulation in the cell (higher levels of lipidated LC3) (27-29). Notably, cholesterol build-up could derive from autophagic flux blockage but has also been suggested to cause it (29). Sarkar *et al.* (28) suggested that autophagosome accumulation results from impaired recruitment of SNARE machinery to endosomes, compromising their fusion with autophagosomes. In their study, autophagy stimulation restored autophagic flux, increasing cell viability, although without ameliorating cholesterol storage (29). Hence, combination of autophagy-inducing and cholesterol-depleting drugs could benefit NPC1 patients (27). In line with our hypothesis that autophagy blockage may contribute to mitochondrial dysfunction in *ncr1Δ* cells, autophagic flux impairment in NPC1-knockdown human neurons promotes accumulation of fragmented mitochondria, which is particularly deleterious to neurons (169). In NPC1-defective engineered neurons, TORC1 inhibition and consequent increased mitophagy were shown to ameliorate mitochondrial dysfunction (54).

4.3. The shortened chronological lifespan and mitochondrial dysfunction of yeast lacking Ncr1 are not caused by Gln3 hyperactivation

As mentioned before, yeast lacking Ncr1 have decreased CLS in relation to the wild type strain, which is caused by Sit4 upregulation (41). To uncover a potential role of the Sit4-mediated hyperactivation of Gln3 in the aging of these cells, we assessed the CLS of BY4741, *ncr1Δ*, *gln3Δ* and *ncr1Δgln3Δ* cells grown in SC medium (Figure 9, A). For quantitative evaluation of CLS, the area under each lifespan curve was calculated (Figure 9, B).

Consistent with previous reports (41, 44), the *ncr1Δ* mutant presented a shortened CLS and *gln3Δ* cells had increased longevity in relation to the wild type, which likely correlates with the increased autophagic flux in stationary phase that we described earlier and increased resistance to oxidative stress reported elsewhere (128). *GLN3* deletion in *ncr1Δ* cells promoted a slight increase in their CLS (1.6-fold), suggesting that hyperactivation of Gln3 mildly impacts the chronological aging of the *ncr1Δ* mutant. Since the short CLS was not significantly reverted, we conclude that other targets downstream of Sit4, or Sit4 itself, are more deleterious to *ncr1Δ* cells than Gln3.

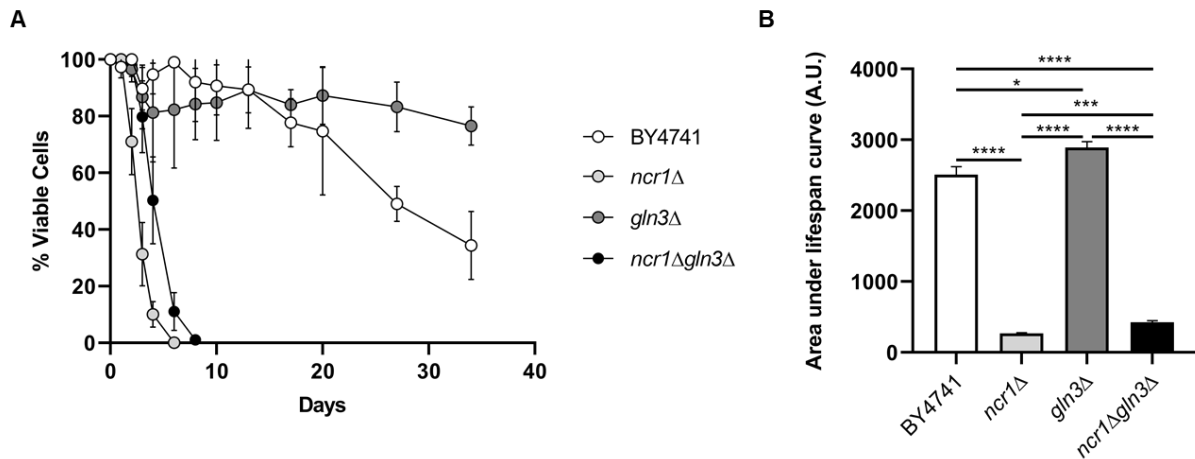


Figure 9 – Yeast lacking Ncr1 exhibit a Gln3-independent short chronological lifespan. **A)** *S. cerevisiae* BY4741, *ncr1Δ*, *gln3Δ* and *ncr1Δgln3Δ* cells were grown to post-diauxic shift phase and maintained in growth medium. The curves of cell viability over time (chronological lifespan curves) are shown. Values are the mean \pm SD of at least three independent experiments. **B)** Area under the lifespan curves, in arbitrary units (A.U.). Values presented are the mean \pm SEM of at least three independent experiments. * $p < 0.05$; *** $p < 0.001$; **** $p < 0.0001$.

Since mitochondrial function is fundamental for longevity (70, 71) and *GLN3* disruption promoted a modest increase in the CLS of *ncr1Δ* cells, the role of Gln3 in the mitochondrial respiration of these cells was also assessed. For that, we tested BY4741, *ncr1Δ*, *gln3Δ* and *ncr1Δgln3Δ* cells for their capacity to grow in agar plates containing glycerol – a non-fermentative substrate – as sole carbon source (Figure 10, A). Moreover, the oxygen consumption rate of each strain was measured (Figure 10, B).

In agreement with former reports, *ncr1Δ* cells were capable of growing in plates containing glucose – a fermentative substrate – as sole carbon source, but not in glycerol plates. Consistently, their oxygen consumption rate was significantly reduced (10-fold). Hence, mitochondrial respiration is impaired in this yeast model of NPC1 (41). Contrastingly, *gln3Δ* cells were able to use glycerol as a carbon source and had oxygen consumption similar to the wild type, indicating that mitochondrial respiration is intact in these cells. Nonetheless, disruption of *GLN3* in *ncr1Δ* cells did not revert their inability to use glycerol nor their low oxygen consumption. Therefore, we conclude that hyperactivation of Gln3 in *ncr1Δ* cells does not contribute to mitochondrial dysfunction.

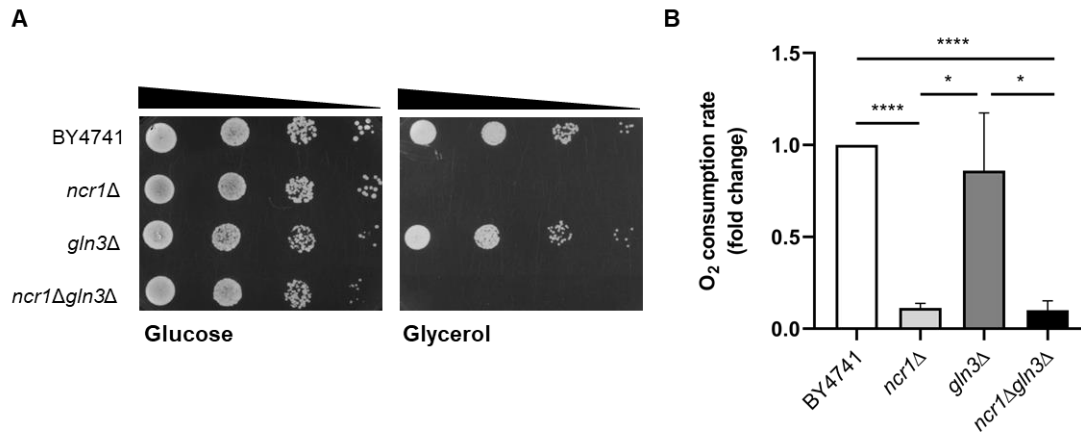


Figure 10 – Increased activity of Gln3 in yeast lacking Ncr1 does not cause mitochondrial dysfunction. A) *S. cerevisiae* BY4741, *ncr1Δ*, *gln3Δ* and *ncr1Δgln3Δ* cultures grown to post-diauxic shift phase were diluted to an OD₆₀₀ = 0.1, which was further used to perform three ten-fold serial dilutions. For each strain, the four dilutions were sequentially pipetted onto agar plates containing either glucose or glycerol as sole carbon source. Cell growth capacity was evaluated after 3-day incubation at 26 °C. **B)** The oxygen consumption rate of BY4741, *ncr1Δ*, *gln3Δ* and *ncr1Δgln3Δ* cells grown to post-diauxic shift phase was assessed and the fold change in relation to the wild type strain was calculated. Values shown are the mean ± SD of three independent experiments. * p < 0.05; **** p < 0.0001.

4.4. Yeast lacking Ncr1 have decreased levels of α-ketoglutarate

As a promoter of NCR-sensitive gene transcription, Gln3 positively regulates the expression of the Gdh1 and GS enzymes, which use α-KG to produce Glu and Gln, respectively (84). Gln3 is hyperactivated in *ncr1Δ* cells, so we hypothesized that α-KG consumption was increased, causing depletion of its intracellular levels. α-KG is an important intermediate of the Krebs cycle and supplementation of this metabolite increases mitochondrial respiration in yeast cells (145), so we further hypothesized that α-KG limitation could contribute to the mitochondrial dysfunction phenotype of the *ncr1Δ* mutant. To test this, we analysed the concentration of α-KG in BY4741 and *ncr1Δ* cells grown to late exponential phase (Figure 11). Additionally, we evaluated the respiration capacity of BY4741 and *ncr1Δ* cells grown in SC medium supplemented with 10 mM α-KG, by plating them in glycerol agar plates also containing 10 mM α-KG.

In agreement with our hypothesis, *ncr1Δ* cells displayed significantly lower α-KG levels (0.013 ng/μg of protein) than the wild type strain (0.2 ng/μg of protein). However, supplementation of liquid growth medium and glycerol agar plates with 10 mM α-KG was not sufficient for *ncr1Δ* cells to use glycerol as a carbon source, suggesting that increased α-KG supply does not ameliorate defects in mitochondrial respiration (results not shown). Therefore, α-KG deficiency does not seem to contribute to mitochondrial dysfunction in *ncr1Δ* cells. Since this metabolite has multiple functions in the cell, α-KG limitation could contribute to the premature aging of *ncr1Δ* cells due to impairment of other processes.

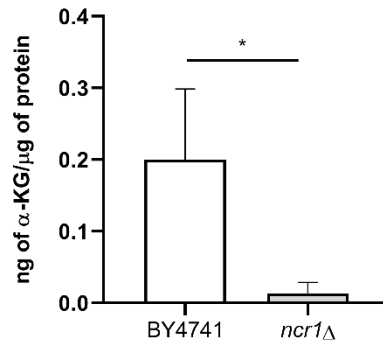


Figure 11 – α-Ketoglutarate levels are decreased in yeast lacking Ncr1. *S. cerevisiae* BY4741 and *ncr1*Δ cells were grown to late exponential phase and intracellular α-ketoglutarate levels were measured. Values shown are the mean ± SD of three independent experiments. * $p < 0.05$.

4.5. α-Ketoglutarate, glutamate and glutamine extend the chronological lifespan and modulate TORC1 activity in yeast lacking Ncr1

Recent reports demonstrate that α-KG delays the aging of several organisms through modulation of metabolic pathways (139, 140). Indeed, supplementation of growth medium with α-KG extends yeast CLS, which is not only associated with augmented levels of mitochondrial function and oxidative stress resistance, but also of protein synthesis (146, 170). The latter is likely due to the fact that α-KG is a precursor of multiple amino acids, playing an important role in amino acid metabolism (84, 136).

We observed that the intracellular α-KG levels of the *ncr1*Δ mutant are significantly reduced. Moreover, Gln3, TORC1 and autophagy are dysregulated, which may affect amino acid homeostasis. Since Gln3 is hyperactivated in *ncr1*Δ cells, the levels of Glu and Gln could be altered in these cells, as are the levels of their precursor, α-KG. Hence, we sought to characterize the effect of α-KG, Glu or Gln supplementation on the CLS of the *ncr1*Δ mutant. For that, BY4741 and *ncr1*Δ cells were grown in SC medium supplemented or not with 10 mM α-KG, Glu or Gln and CLS was assessed (Figure 12).

Supplementation of growth medium with α-KG, Glu or Gln increased the CLS of the wild type strain in similar extent, with a fold change varying from 1.4-1.6 (in relation to the CLS of the same strain grown in non-supplemented SC). Likewise, supplementation of *ncr1*Δ cells with these compounds had a significant impact on their CLS, but with different degree of effect. Similar to the effect on wild type cells, Gln induced a 1.5-fold increase in the CLS of *ncr1*Δ cells. However, α-KG and Glu promoted a larger increase of 2.4-fold and 3-fold, respectively. We also supplemented growth medium with 10 mM arginine, which increased the CLS of the

wild type strain, but not of *ncr1 Δ cells (not shown). This suggests that the protective effect of these supplements does not simply derive from increased nitrogen supply. Hence, nitrogen starvation per se does not seem to be the cause for the premature death of *ncr1 Δ cells.**

Like α -KG, Glu supplementation of growth medium had been reported to extend the CLS of wild type yeast cells (132). We did not find studies on the effect of Gln supplementation on *S. cerevisiae* longevity. However, in contrast with our results, GS inhibition by methionine sulphoximine and consequent decrease in Gln synthesis was shown to increase yeast CLS, due to TORC1 downregulation (85, 128).

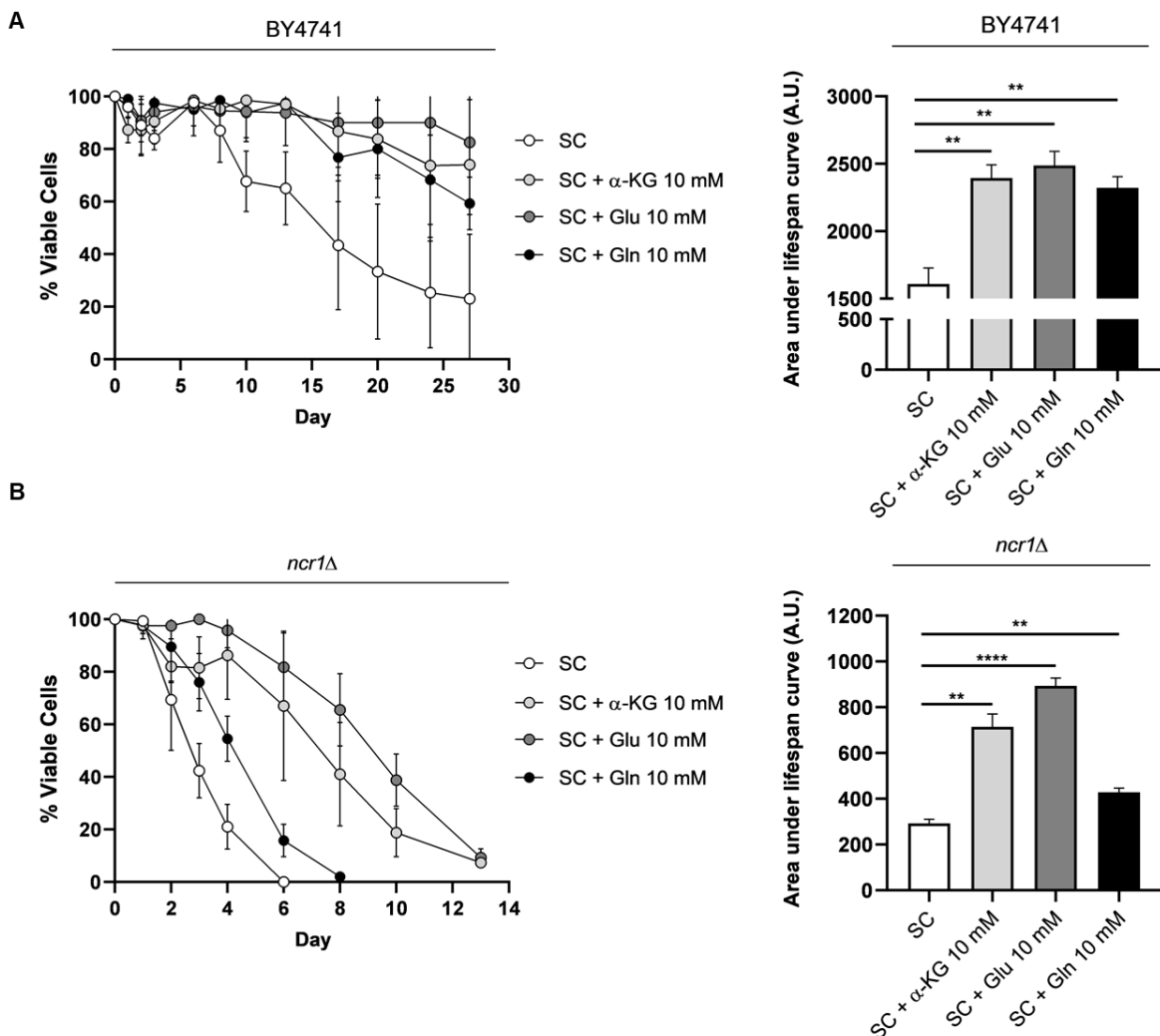


Figure 12 – Supplementation of growth medium with α -ketoglutarate, glutamate or glutamine increases the chronological lifespan of wild type and *Ncr1*-deficient yeast cells. *S. cerevisiae* BY4741 (A) and *ncr1 Δ cells (B) were grown to post-diauxic shift phase in SC medium supplemented or not with 10 mM α -ketoglutarate (α -KG), glutamate (Glu) or glutamine (Gln). The chronological lifespan curves (left; mean \pm SD of at least three independent experiments) and the area under each curve, in arbitrary units (A.U.) (right; mean \pm SEM of at least three independent experiments) are shown. ** $p < 0.01$; **** $p < 0.0001$.*

To have more insight on the effects of α -KG, Glu and Gln supplementation, the pH of the BY4741 and *ncr1 Δ yeast cultures was monitored during the CLS assay (Table 3). Importantly,*

the pH of supplemented media was adjusted to that of non-supplemented medium (approximately 5.2), so all cultures started with similar pH values. In cultures aged for 2 days, growth medium suffered an increase in acidification (Table 3), which remained stabilized thereafter (not shown). Interestingly, acidification was more accentuated in non-supplemented cultures, in comparison to supplemented ones, and pH decay was similar for wild type and *ncr1Δ* strains. Studies indicate that medium acidification results from secretion and extracellular accumulation of acetic acid (among other organic acids) during fermentative growth, which has been proposed to negatively impact the aging of yeast cells by inducing programmed cell death (171, 172). Consistently, buffering growth medium alleviates the effects of acetic acid and extends CLS (171). The beneficial effect of caloric restriction on yeast CLS is also associated with attenuated medium acidification, in addition to TORC1 inhibition and increased autophagic flux (73, 125, 171). Taking this into consideration, the decreased acidification of wild type and *ncr1Δ* cultures supplemented with 10 mM α-KG, Glu or Gln (to a lesser extent) may be related with the CLS-extending effect of these compounds. Notably, α-KG has been proposed to mediate CLS extension through caloric restriction, which is consistent with the facts that it does not further increase the longevity of calorie-restricted organisms and that α-KG levels increase in organisms ranging from yeast to mammals under nutrient limitation (140, 173, 174).

Although α-KG and Glu supplementation promoted a similar pH decrease in wild type and *ncr1Δ* cultures, the protective effect of these compounds was greater in the latter (Figure 12). Since we observed that *ncr1Δ* cells have decreased α-KG levels, a larger positive effect of α-KG supplementation in these cells in relation to the wild type was expected and raises the hypothesis that α-KG supplementation could increase CLS by replenishment of intracellular α-KG levels. The also greater effect of additional Glu supply suggests that Glu levels may be altered in *ncr1Δ* cells.

Table 3 – pH values of *S. cerevisiae* BY4741 and *ncr1Δ* cultures at day 2 of the chronological lifespan assay. Values are the mean ± SD of at least two independent experiments.

Medium	Culture pH	
	BY4741	<i>ncr1Δ</i>
SC	2.9 ± 0.1	3.0 ± 0.1
SC + α-KG 10 mM	4.2 ± 0.3	4.0 ± 0.1
SC + Glu 10 mM	4.2 ± 0.5	3.9 ± 0.1
SC + Gln 10 mM	3.4 ± 0.1	3.5 ± 0.1

In *C. elegans*, α-KG mediates lifespan extension through downregulation of the TORC1 pathway, by inhibiting ATP synthase, decreasing ATP production and consequently increasing

the AMP/ATP ratio, which promotes TORC1 inhibition by AMPK (140). In yeast, it is unknown whether modulation of TOR signalling contributes to the CLS-extending effect of this metabolite. The mechanism of Glu-mediated increase of yeast CLS is also not clear, but it is associated with increased cell biomass and oxidative stress resistance (132). As a nitrogen source, Glu was shown to stimulate TORC1 activation in yeast, but its effect is less sustained than that of Gln (63).

We observed that TORC1 activity is reduced in the *ncr1Δ* mutant, which could result from alterations in amino acid homeostasis, since activation of this complex is regulated by amino acids. To investigate if modulation of the TORC1 pathway contributes to the protective effect of α-KG, Glu or Gln, we assessed the levels of phospho-Rps6 (S232/233) in BY4741 and *ncr1Δ* cells grown in SC medium supplemented or not with these compounds (Figure 13, A). The levels in supplemented cultures were normalized to the levels in the respective strain grown in non-supplemented medium (Figure 13 – B, C).

We did not detect alterations in wild type cells supplemented with α-KG, Glu or Gln (Figure 13 – A, B). Although Glu and Gln have been reported to stimulate TORC1 activation in yeast (63), in our studies cells were treated with the supplements for a longer period (about 15 hours), so TORC1 activity may have returned to basal levels. On the other hand, we observed significant alterations in TORC1 activity of supplemented *ncr1Δ* cells (Figure 13 – A, C): α-KG reduced TORC1 activity by 2-fold, whereas Glu increased it by 2.3-fold. Gln supplementation showed a tendency to increase TORC1 activity, but its effect was not statistically significant.

Since supplementation with α-KG, Glu or Gln increased the CLS of *ncr1Δ* cells (although to different extent) but have distinct impact on TORC1 activity in these cells, it is unclear if or how modulation of this pathway contributes to the CLS-extending effect of these compounds. Nonetheless, wild type and *ncr1Δ* cells responded differently to supplementation of growth medium with all three compounds – an amido acid precursor and two amino acids with important functions in amino metabolism –, which further suggests that amino acid homeostasis may be altered in *ncr1Δ* cells.

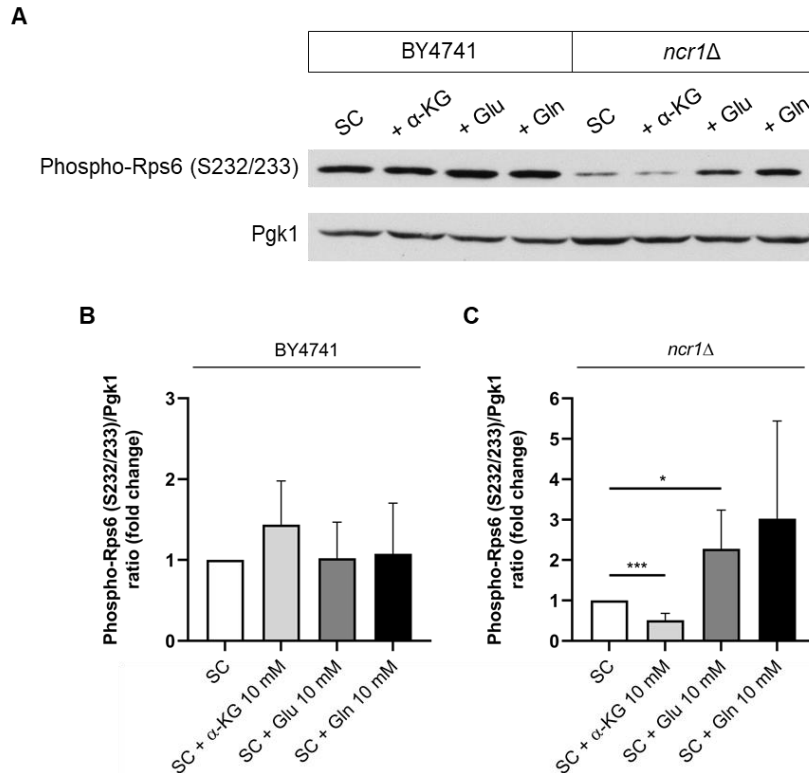


Figure 13 – Supplementation of growth medium with α -ketoglutarate, glutamate or glutamine modulates TORC1 activity in yeast lacking Ncr1. **A)** *S. cerevisiae* BY4741 and *ncr1* Δ cells were grown to exponential phase in SC medium supplemented or not with 10 mM α -ketoglutarate (α -KG), glutamate (Glu) or glutamine (Gln). The levels of phospho-Rps6 (S232/233) were evaluated by western blotting. Pgk1 was used as loading control. **B, C)** The fold change in the phospho-Rps6 (S232/233)/Pgk1 ratio in BY4741 and *ncr1* Δ cells grown in supplemented media was calculated in relation to the ratio in the same strain grown in non-supplemented media. Values shown are the mean \pm SD of at least four independent experiments. * $p < 0.05$; *** $p < 0.001$.

As previously mentioned, impairment of autophagic flux can contribute to defects in amino acid homeostasis, since autophagy is an important pathway for protein breakdown into amino acids, especially during stationary phase and nutrient limitation (113). The resulting amino acids exit the lysosome/vacuole through permeases and can be reutilized for *de novo* protein synthesis, among other processes (113, 175). In this work, we found that the autophagic flux of *ncr1* Δ cells is blocked in stationary phase, which may compromise amino acid homeostasis by reducing amino acid recycling. Since TORC1 is a major regulator of autophagy and the supplementation of *ncr1* Δ cells with α -KG, Glu and Gln induced alterations in TORC1 activity, we also assessed the effects of these compounds on their autophagic flux. For that, BY4741 and *ncr1* Δ cells expressing pRS413-GFP-ATG8 were grown to stationary phase in SC lacking histidine, supplemented or not with 10 mM α -KG, Glu or Gln. GFP-Atg8 hydrolysis was analysed by western blotting (Figure 14).

Intriguingly, although we did not detect alterations in TORC1 activity in supplemented wild type cells, α -KG, Glu and Gln increased autophagic flux in these cells. These results suggest that the compounds may promote autophagy independently of TORC1 modulation. The increased

autophagic flux in wild type yeast cells supplemented with α-KG is consistent with previous reports of augmented autophagy in *D. melanogaster* and *C. elegans* treated with α-KG (139, 140). In contrast, α-KG, Glu or Gln supplementation did not restore the autophagic flux of *ncr1Δ* cells, even though changes in TORC1 activity were registered. Again, this suggests that autophagic dysfunction in *ncr1Δ* cells arises from dysregulation of other pathways other than TORC1. Indeed, we observed that Atg8 expression is reduced in *ncr1Δ* cells, so autophagosome formation may be compromised. We conclude that α-KG, Glu and Gln-mediated extension of CLS in *ncr1Δ* cells, in contrast with wild type cells, is not associated with increased autophagic flux.

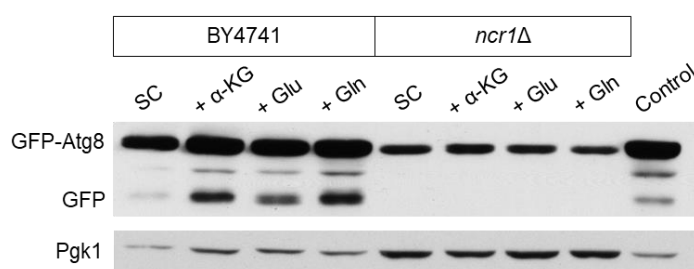


Figure 14 – Supplementation of growth medium with α-ketoglutarate, glutamate or glutamine increases autophagic flux in the wild type strain, but not in yeast lacking Ncr1. *S. cerevisiae* BY4741 and *ncr1Δ* cells carrying pRS413-GFP-ATG8 were grown to stationary phase in SC medium lacking histidine, supplemented or not with 10 mM α-ketoglutarate (α-KG), glutamate (Glu) or glutamine (Gln). Exponentially growing BY4741 cells were treated with rapamycin for positive control. GFP-Atg8 and free GFP levels were analysed by western blotting and Pgk1 was used as loading control. A representative figure of four independent experiments with similar results is shown.

4.6. Amino acid homeostasis is altered in yeast lacking Ncr1

In line with our findings, we sought to characterize amino acid homeostasis in *ncr1Δ* cells and potential effects of α-KG supplementation on amino acid levels. For that, we assessed the amino acid content of BY4741 and *ncr1Δ* cells grown to late exponential and PDS phases in SC supplemented or not with 10 mM α-KG (Figures 15-17).

In relation to the wild type, exponentially growing *ncr1Δ* cells exhibited significant increases in Glu (2-fold) and phenylalanine (1.6-fold) levels. Moreover, a tendency for accumulation of tyrosine (3.2-fold), asparagine (2.1-fold), histidine (3.1-fold), threonine (4-fold) and alanine (2.3-fold) was observed, while the lysine content tended to be reduced in approximately 2-fold (Figure 15 – A). A recent study showed that ergosterol is fundamental for the function of the lysine permease Lyp1 (176). Hence, this raises the hypothesis that potential ergosterol limitation in *ncr1Δ* yeast membranes, in analogy to what is observed in NPC1-deficient cells (21), could affect Lyp1-mediated uptake of lysine from extracellular medium during exponential

growth. Plus, the decrease of α -KG levels in *ncr1* Δ cells may compromise lysine biosynthesis since this amino acid is synthesized from α -KG (136).

In PDS phase, Glu levels of *ncr1* Δ cells remained significantly increased, with a 9-fold change in relation to the wild type. Additionally, significant increases in the levels of asparagine (7.8-fold), histidine (6.1-fold), aspartate (8.3-fold), isoleucine (5.3-fold) and methionine/valine (5.1-fold) were registered. In fact, *ncr1* Δ cells grown to PDS phase exhibited a tendency to accumulate most amino acids analysed, except for tyrosine (Figure 15 – B).

Of note, Gln levels were not altered during exponential growth and exhibited only a slight tendency for increase in PDS phase (1.6-fold change in relation to the wild type), comparing to other amino acids. Hence, unlike initially hypothesized, the results suggest that Gln levels of *ncr1* Δ cells are not significantly increased, in agreement with the observation that TORC1 activity is not upregulated in this yeast model of NPC1. Consistently, leucine levels were also not increased. In contrast, Glu levels were significantly augmented at both growth stages evaluated. These observations, together with the fact that α -KG levels are decreased, suggest that Gln3 hyperactivation in yeast lacking Ncr1 may upregulate Glu synthesis from α -KG, potentially through increased transcription of *GDH1*. As previously mentioned, Glu can be deaminated to α -KG by Gdh2 or transaminases, so the beneficial effect of Glu supplementation on the CLS of *ncr1* Δ cells could derive from increased α -KG production, preventing its limitation. Since Glu is used for the synthesis of various amino acids, providing 85% of the nitrogen necessary for yeast biosynthetic pathways (92, 95), the increased amino acid content of *ncr1* Δ cells may result from augmented amino acid synthesis from α -KG and Glu. Moreover, increased amino acid levels may result from reduced TORC1 activity and consequent decrease in amino acid utilization for protein synthesis. Further studies are required to confirm these hypotheses.

Interestingly, glutamatergic neurotransmission is increased in the brain of NPC1 mice (177). However, Glu levels in cerebellar neurons are not altered, at least in presymptomatic stages of disease (133). Contrastingly, but in agreement with our results, livers of NPC1 mice were shown to have increased Glu levels at postsymptomatic stages of disease (134). Additional alterations in NPC1 mice cerebellum comprise increased levels of branched chain amino acids, asparagine, threonine, serine and glycine (133). Valine, threonine, phenylalanine and tyrosine are increased in the liver at a later stage of disease (134).

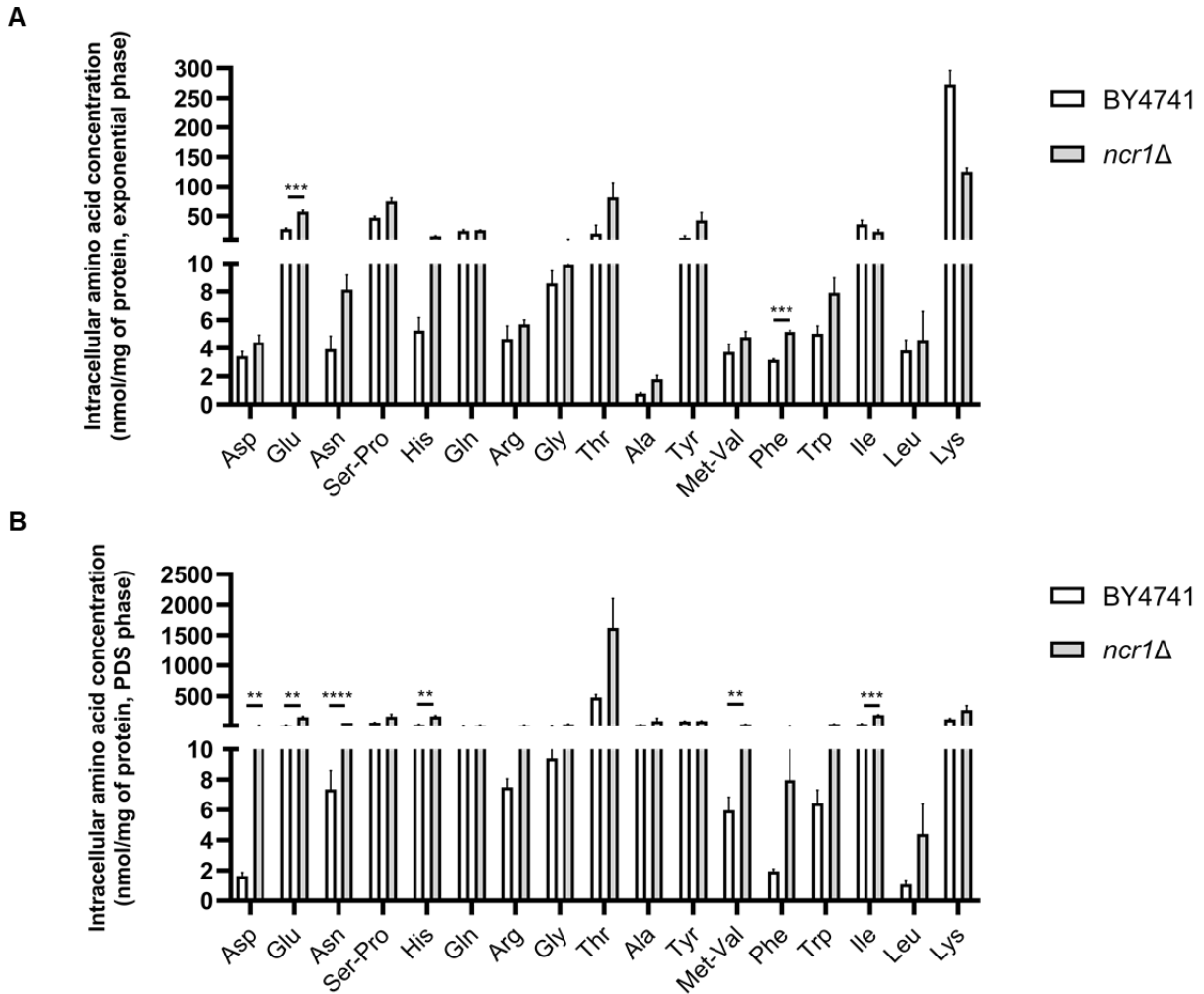


Figure 15 – Yeast lacking Ncr1 have increased levels of glutamate and phenylalanine in late exponential phase and accumulate various amino acids during post-diauxic shift phase. Intracellular amino acid content of *S. cerevisiae* BY4741 and *ncr1Δ* cells grown to late exponential (A) and post-diauxic shift (PDS) (B) phases in SC medium. Values are the mean \pm SEM of at least two independent experiments. ** $p < 0.01$, *** $p < 0.001$, **** $p < 0.0001$.

In wild type cells grown to late exponential phase, α-KG supplementation induced a statistically significant 2-fold increase in Glu levels (Figure 16 – A). In fact, a tendency for increase of most amino acids (e.g., tyrosine, histidine, threonine, alanine and leucine, in over 2-fold) was observed. Indeed, α-KG supplementation had been reported to increase free amino acid levels in exponentially growing yeast (146). In PDS phase, the α-KG-mediated increase in amino acid content seemed lower, but the tendency for accumulation of Glu was maintained, in line with the fact that α-KG is a direct precursor of Glu (Figure 17 – A) (92). Interestingly, Ncr1 absence suppressed the tendency for amino acid increase mediated by α-KG supplementation, at both growth stages tested. In late exponential phase, α-KG supplementation even promoted a statistically significant 1.6-fold decrease in phenylalanine levels (Figure 16 – A), which were increased during growth in non-supplemented media (Figure 15). Of note, phenylalanine levels

are increased in NPC1 mice liver, as mentioned before (134). In aged *D. melanogaster*, phenylalanine levels are also increased (178) and phenylalanine supplementation was shown to decrease the lifespan of *C. elegans* (179). Moreover, rats submitted to dietary restriction exhibit decreased phenylalanine levels in the liver and enhanced longevity (59). In yeast, phenylalanine supplementation showed a tendency to decrease CLS, but so did its restriction (132). Therefore, it is not clear if α-KG-mediated suppression of phenylalanine accumulation in *ncr1Δ* cells could be related with its CLS-extending effect.

The only amino acid that showed a slight tendency to increase in *ncr1Δ* cells grown to late exponential phase under α-KG supplementation was lysine (1.7-fold) (Figure 16 – B), which is synthesized from α-KG (136) and whose levels were downregulated in late exponential phase (Figure 15 – A). Another interesting observation is that the accumulation of aspartate in *ncr1Δ* cells grown to PDS (Figure 15 – B) tended to decrease in approximately 4-fold when α-KG was supplemented (Figure 17 – B). A study showed that, besides methionine restriction, limitation of aspartate showed the most significant increase in yeast CLS (out of 15 amino acids), whereas increased supply tended to decrease CLS (132). Thus, increased α-KG supply may promote longevity at least partially by limiting aspartate availability.

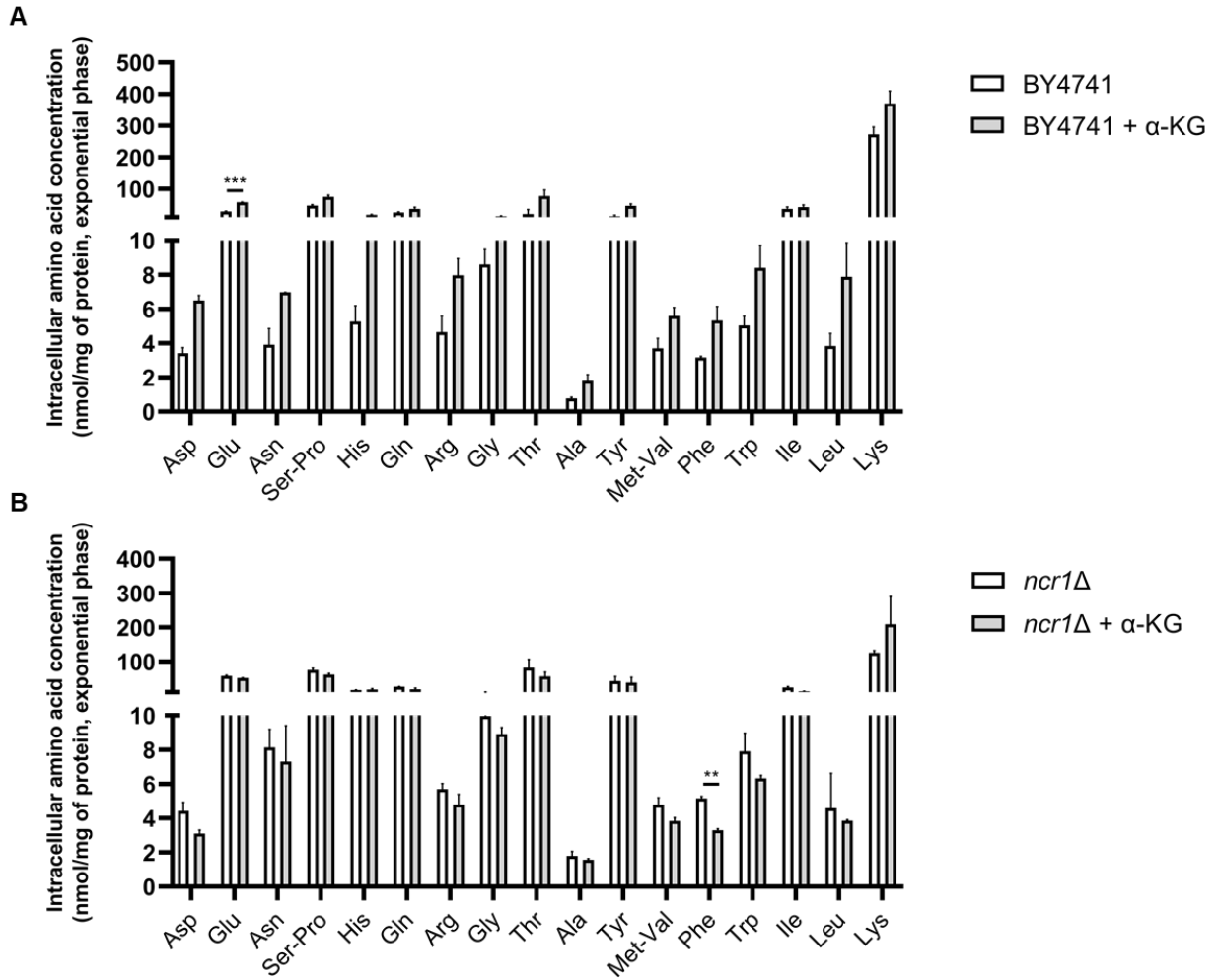
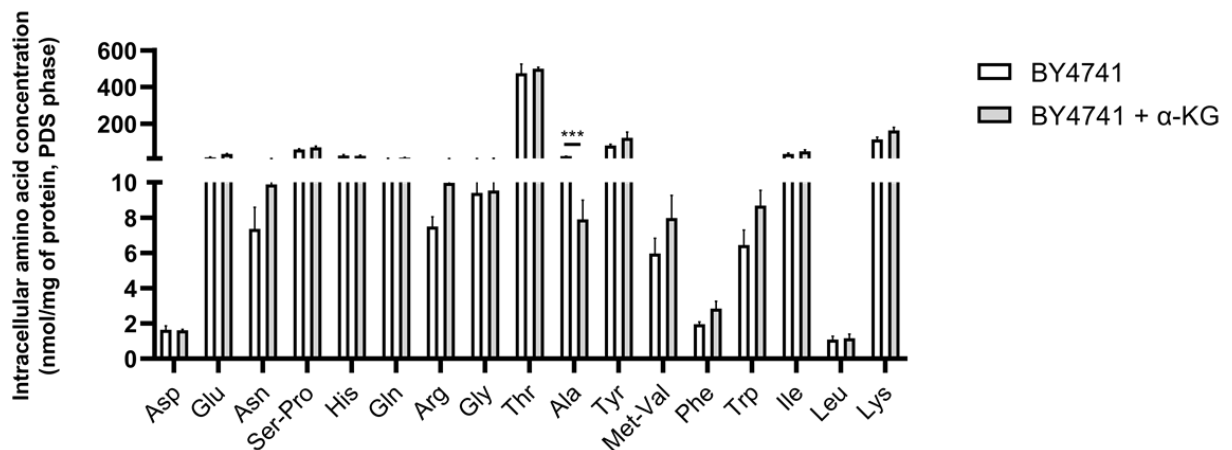


Figure 16 – Supplementation of growth medium with α-KG decreases phenylalanine accumulation in yeast lacking Ncr1 grown to late exponential phase. Intracellular amino acid content of *S. cerevisiae* BY4741 (A) and *ncr1Δ* cells (B) grown to late exponential phases in SC medium supplemented or not with 10 mM α-KG. Values are the mean ± SEM of at least two independent experiments. ** p < 0.01, *** p < 0.001.

A



B

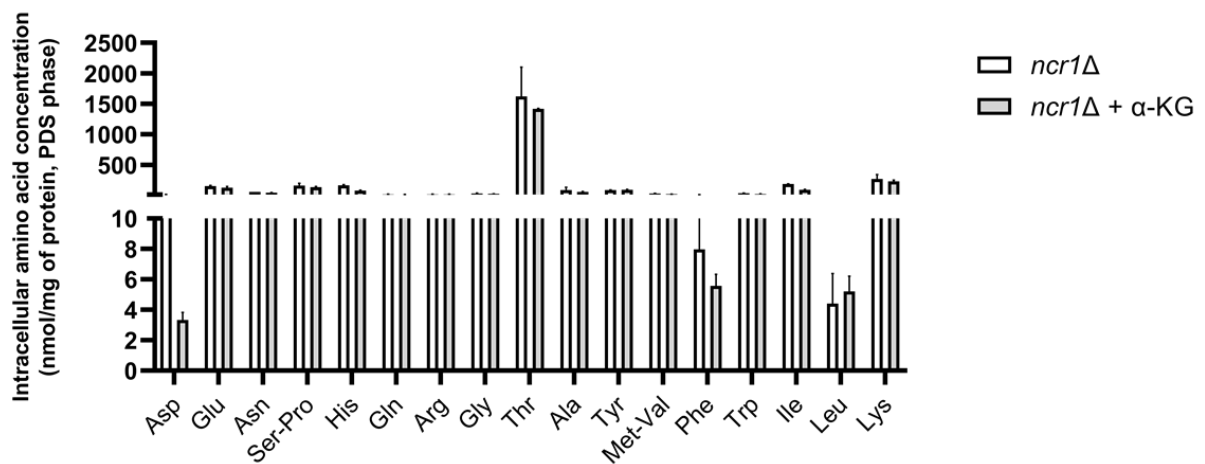


Figure 17 – Supplementation of growth medium with α-KG does not significantly impact the amino acid content of yeast lacking Ncr1 grown to post-diauxic shift phase. Intracellular amino acid content of *S. cerevisiae* BY4741 and *ncr1Δ* cells grown to late exponential (A) and post-diauxic shift (PDS) (B) phases in SC medium supplemented or not with 10 mM α-KG. Values are the mean ± SEM of at least two independent experiments. *** p < 0.001.

In addition to the intracellular amino acid analysis, we assessed the amino acid profile of vacuoles isolated from BY4741 and *ncr1Δ* cells in late exponential phase (Figure 18). Our results reveal abnormal storage of threonine in vacuoles of *ncr1Δ* cells and a general trend for amino acid accumulation. Specifically, Glu, aspartate, serine, Gln, arginine, glycine, methionine/valine and lysine levels showed a tendency to increase 1.4-1.6 fold in *ncr1Δ* vacuoles. Since phenylalanine, asparagine, histidine and alanine were not detected in vacuolar fractions of *ncr1Δ* cells, the accumulation of these amino acids in late exponential phase (Figure 15 – A) probably occurs in the cytosol or another organelle. Regarding lysine, the tendency for a decrease in intracellular levels, along with vacuolar accumulation in *ncr1Δ* cells, suggests that its cytosolic availability may be decreased in these cells.

Vacuolar membranes possess various amino acid transporters, most of which mediate coupled transport of specific amino acids with H⁺ (antiport or symport) (114, 117). Thus, alterations in

transporters that regulate amino acid flux to and from the cytosol may contribute to changes of amino acid homeostasis in *ncr1Δ* cells. Indeed, studies of our group showed that the phosphorylation state of some vacuolar amino acid transporters, including Avt6 [Glu and aspartate exporter (117)] and Vsb1 [arginine importer (180)], is altered in these cells (Telma Martins *et al.*, unpublished). Further analyses regarding intracellular and vacuolar amino acid levels will be performed for accurate characterization of the effect of Ncr1 absence on amino acid homeostasis.

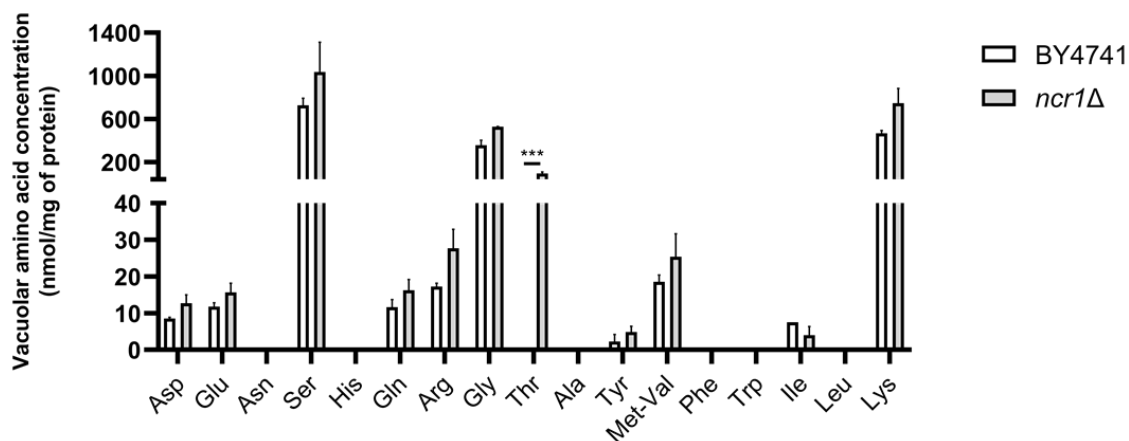


Figure 18 – Vacuoles of yeast lacking Ncr1 exhibit significant threonine accumulation. Amino acid content of vacuolar fractions isolated from *S. cerevisiae* BY4741 and *ncr1Δ* cells grown to late exponential phase in SC medium. Values are the mean ± SEM of at least two independent experiments. *** $p < 0.001$.

4.7. Yeast lacking Ncr1 have decreased levels of histone H3

Histone levels and epigenetic modifications of histone proteins, including methylation of lysine residues, severely impact organismal lifespan. In fact, epigenetic alterations and genomic instability are hallmarks of aging (135, 151). In yeast, histone levels decline during aging and increasing histone expression extends yeast longevity (150, 151). Importantly, H3K4me3 extends CLS by increasing histone expression. Hence, the landscape of histone lysine methylations also impacts histone levels (150). As a cofactor of JmjC-containing histone demethylases, α-KG was shown to regulate histone methylation and, consequently, the aging of eukaryotic cells (181).

Thus far, we reported that *ncr1Δ* cells have decreased intracellular α-KG levels and supplementation of growth medium with this metabolite extends its shortened CLS, also decreasing TORC1 activity but with no impact on autophagy. The link between α-KG and histone modulation led us to investigate if *ncr1Δ* cells had decreased expression of histone H3 and if α-KG supplementation affected H3 levels. To test this, BY4741 and *ncr1Δ* cells were

grown to early exponential and stationary phases (T0 of aging) in SC medium, supplemented or not with 10 mM α-KG, and histone H3 levels were evaluated by western blotting (Figure 19, A). For a quantitative analysis, the fold change in relation to non-supplemented wild type cells in exponential phase was calculated (Figure 19, B).

During growth from exponential to stationary phase, histone H3 levels of wild type cells increased 6-fold, which was abrogated under α-KG supplementation. It should be noted that, at the timepoint analysed (T0 of aging), viability of wild type cells is close to 100%, so it was expectable that the decrease in histone H3 levels reported in the literature for aged cells was not detected at this phase. Since other studies suggested a correlation between lifespan extension and the increase of histone levels (150), more studies are required to assess if α-KG supplementation of wild type cells increases histone levels in aged cells or at least prevents its decline during ageing. Non-supplemented *ncr1Δ* cells presented decreased levels of histone H3 in relation to the wild type at both exponential (5-fold) and stationary phases (9-fold). Therefore, the shortened CLS of the *ncr1Δ* mutant may be related with decreased histone H3 levels, in agreement with reports that show decreased H3 expression in aged yeast cells (150, 151). We did not assess H3 levels at later timepoints as the viability of *ncr1Δ* cells decreases rapidly. The supplementation of *ncr1Δ* cells with α-KG had little to no effect on histone H3 expression, suggesting that α-KG does not seem to increase longevity of *ncr1Δ* cells through regulation of H3 levels. Since α-KG was shown to regulate histone demethylases rather than histone levels directly, its protective effect in both wild type and *ncr1Δ* cells may be associated with the modulation of H3 methylation rather than its levels per se. More studies are required to test this hypothesis.

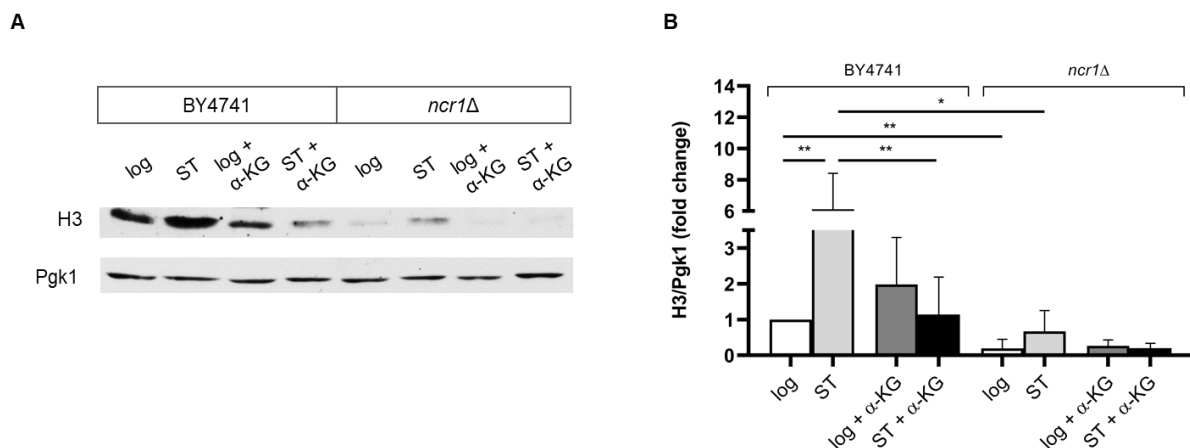


Figure 19 – Yeast lacking Ncr1 have decreased levels of histone H3. A) *S. cerevisiae* BY4741 and *ncr1Δ* cells were grown to early exponential (log) and stationary (ST) phases in SC medium supplemented or not with 10 mM α-ketoglutarate (α-KG). Histone H3 levels were analysed by western blotting. Pgk1 was used as loading control. **B)** The fold change in histone H3 levels (H3/Pgk1 ratio) in relation to the levels of exponentially growing BY4741 (in non-supplemented medium) was calculated. Values shown are the mean ± SD of four independent experiments. * p < 0.05; ** p < 0.01.

To test if decreased levels of histone H3 could compromise genome stability in *ncr1* Δ cells, the frequency of spontaneous mutations in BY4741 and *ncr1* Δ cells, grown to PDS and stationary phases and plated in medium supplemented with canavanine, was assessed. Neither the wild type nor *ncr1* Δ cells formed canavanine-resistant colonies, at both growth stages tested (not shown), indicating that *ncr1* Δ mutant cells do not exhibit genome instability.

CHAPTER 5. Conclusions and future perspectives

NPC1 is an integral membrane protein of LE/Lys, involved in intracellular lipid trafficking through the endocytic pathway. Specifically, it mediates cholesterol export from LE/Lys, promoting its utilization in the cell and delivery to other organelles or the plasma membrane (3, 15). Autosomal recessive inheritance of loss-of-function mutations in the NPC1 protein causes NPC1 disease, which is an LSD characterized by progressive accumulation of cholesterol and sphingolipids in LE/Lys (7). The clinical profile of this disorder is remarkably diverse, but neurodegeneration, failure of visceral organs and subsequent premature death are the primary consequences (3). The *S. cerevisiae* model of NPC1 originates from deletion of Ncr1 – the functional orthologue of the NPC1 protein, residing in vacuolar membranes –, and has been used to study the molecular aetiology and pathogenesis of NPC1 disease due to conservation of such mechanisms and easy genetic manipulation (36, 37, 39). Moreover, yeast lacking Ncr1 (*ncr1Δ* cells) exhibit multiple phenotypes of NPC1-deficient mammalian cells, including mitochondrial fragmentation, decreased respiration and premature death (41). In analogy to ceramide build-up in NPC1-deficient cells (43), Vilaça *et al.* (44) reported phytoceramide accumulation in *ncr1Δ* yeast. Constituting the catalytic core of the CAPP complex, the Ser/Thr phosphatase Sit4 is activated by ceramide species and regulates multiple biological processes, including cell cycle progression, mitochondrial function and longevity (80). Consistently, its implication in mitochondrial dysfunction and decreased CLS of *ncr1Δ* cells was described (44). Besides forming the CAPP complex, Sit4 can interact with Tap42 to regulate nitrogen utilization in yeast through NCR, upregulating Gln3 activation (91).

Gln3 is a transcriptional activator of the NCR pathway, which promotes the utilization of preferable nitrogen sources (e.g., Glu and Gln) and inhibits the utilization and uptake of poor nitrogen sources (e.g., proline) (84). Among other functions, Gln3 upregulates the expression of Gdh1, which catalyses amination of α-KG to Glu during growth, and the expression of GS, which converts Glu to Gln (92). Previous studies showed that Gln3 is hyperactivated in *ncr1Δ* yeast in a Sit4-dependent manner (44). Hence, we hypothesized that Gdh1 and Gln1 expression was increased in *ncr1Δ* cells, upregulating Glu and Gln synthesis. TORC1 is a conserved master regulator of cell growth and nutrient availability sensor, known to decrease mitochondrial respiration, autophagy and longevity (70, 71, 118). In both mammals and yeast, TORC1 is activated by amino acids, with Gln and leucine being the best described potent activators of this complex in the latter (60, 63) Therefore, we further speculated that increased Glu, but especially Gln, synthesis could upregulate TORC1 activation in the yeast model of NPC1, negatively regulating mitochondrial function, autophagy and longevity.

Our results indicate that, in fact, TORC1 activity in *ncr1Δ* cells is downregulated, in both exponential and PDS growth phases (Figure 7). Thus, Gln3 hyperactivation does not cause TORC1 upregulation in yeast lacking Ncr1. Plus, *GLN3* deletion in *ncr1Δ* cells did not

ameliorate mitochondrial dysfunction (Figure 10) and promoted only a slight increase of CLS (Figure 9). In agreement with the observation that TORC1 is downregulated in this yeast model of NPC1, Xu *et al.* (53) reported decreased TORC1 activity in *NPC1*-knockdown human endothelial cells. However, it should be noted that other reports implicate TORC1 upregulation in NPC1 disease pathology, so the degree of TORC1 activity could be tissue- or cell type-dependent (54). Our data is not sufficient to conclude if decreased activation of TORC1 in *ncr1Δ* cells has a detrimental effect, so further studies should be performed to understand how processes downstream of TORC1, such as protein synthesis, are affected in these cells.

Autophagy is an intracellular catabolic pathway for degradation of cytosolic components (biomolecules and organelles) via substrate engulfment by autophagosomes, which subsequently fuse with lysosomes/vacuoles for substrate breakdown by residing hydrolases (97). As an adaptive response to adverse conditions, autophagy is upregulated under nutrient starvation, increasing the turnover of macromolecules into their building blocks, which can exit the lysosome/vacuole through permeases for their reutilization (56, 113). Moreover, it provides a clearance mechanism for oxidized molecules, toxic proteins and damaged organelles (e.g., mitochondria), preventing their accumulation in the cell, which is important for cell death delay (101). Hence, autophagy downregulation decreases lifespan, whereas its upregulation extends longevity in multiple organisms (58, 126). Autophagy is negatively regulated by TORC1, which prevents assembly of the Atg1 kinase complex and, therefore, autophagy initiation, in yeast (120).

Multiple studies have shown that autophagic flux is blocked in NPC1-deficient cells, including neurons, and that this contributes to NPC1 pathology (26, 27). Specifically, autophagosome turnover seems to be compromised, which has been suggested to result from impaired fusion with endosomes (28). In agreement, we observed that autophagic flux is compromised in *ncr1Δ* cells (Figure 8), even though TORC1 activity was decreased throughout growth. This suggests that autophagic defects in these cells are not caused by TORC1 dysregulation. Interestingly, expression of Atg8 was significantly decreased in *ncr1Δ* cells (7.5-fold) (Figure 8 – C). This alteration may contribute to autophagic flux blockage, as Atg8 is required for phagophore expansion and sealing and, therefore, autophagosome formation (107, 168). Of note, *GLN3* deletion in *ncr1Δ* cells did not restore autophagic flux nor Atg8 levels (Figure 8), even though Gln3 has been proposed to transcriptionally repress *ATG8* (167). Additional studies are necessary to clarify the mechanism behind autophagic flux impairment in this yeast model of NPC1. Nonetheless, we suggest that impairment of autophagy progression in *ncr1Δ* yeast may contribute to accumulation of aged mitochondria and, thus, the previously reported decreased respiratory capacity and mitochondrial fragmentation in this mutant (44). Indeed, increased autophagy induction was shown to ameliorate mitochondrial dysfunction in NPC1-

deficient cells (54). Of note, autophagic flux impairment in *ncr1Δ* cells may derive from inadequate vacuolar acidification (40) and a consequent decrease in proteolysis (116).

Glu and Gln play particularly important roles in amino acid metabolism because they provide all the nitrogen necessary for yeast biosynthetic processes (92). As a precursor of Glu and Gln, among other amino acids, α-KG also impacts amino acid metabolism. Likewise, execution of autophagy at adequate levels is fundamental for maintenance of amino acid homeostasis, especially under nitrogen limitation, when delivery of amino acids to the cytosol and protein synthesis rely on autophagy upregulation (113). The facts that Gln3 is upregulated, TORC1 activity is decreased and that autophagic flux is blocked in *ncr1Δ* yeast prompted us to characterize amino acid homeostasis in this mutant. In agreement with the observation that TORC1 activity is not upregulated in *ncr1Δ* cells, an intracellular amino acid analysis revealed that Gln levels were not significantly increased (Figure 15). Likewise, leucine levels were not affected by *NCR1* deletion. In contrast, the intracellular Glu content was significantly increased during both late exponential and PDS phases (Figure 15). We also observed that α-KG levels were reduced in late exponential phase (Figure 11), suggesting that Glu synthesis from α-KG is upregulated in *ncr1Δ* cells, potentially through Gln3-mediated increased transcription of *GDH1*. Other significant alterations in amino acid levels of *ncr1Δ* cells included increased levels of phenylalanine during exponential growth and of asparagine, aspartate, isoleucine and methionine/valine, during PDS phase (Figure 15). Hence, the amino acid content of *ncr1Δ* cells seems to be increased throughout growth, in relation to the wild type's. This may result from upregulation of amino acid synthesis from α-KG and Glu, or from decreased amino acid utilization for protein synthesis, due to TORC1 downregulation. Of note, alterations in amino acid metabolism and their levels have also been reported in NPC1 murine cerebellum and liver (133, 134).

Since yeast vacuoles are the lysosome-equivalent compartment for autophagic degradation in yeast and are involved in amino acid storage, regulating amino acid availability in the cytosolic pool (117), we also evaluated the amino acid content of vacuoles isolated from *ncr1Δ* cells. Our results reveal abnormal accumulation of threonine in *ncr1Δ* vacuoles, as well as a tendency for increased Glu, aspartate, serine, Gln, arginine, glycine, methionine/valine and lysine vacuolar levels, in relation to the wild type (Figure 18). We hypothesize that dysregulation of amino acid transporters or amino acid biosynthesis pathways may contribute to amino acid homeostasis alteration in *ncr1Δ* cells. Indeed, ongoing studies in our laboratory aiming to characterize changes in the vacuolar proteome revealed alterations in the phosphorylation state of specific vacuolar transporters.

Recent studies identified α-KG as a metabolite with anti-aging properties. Treatment of various organisms with α-KG was shown to extend longevity (138-140) and, in yeast, growth medium

supplementation with α-KG increases CLS, in association with increased oxidative stress resistance, mitochondrial respiration and also amino acid and protein synthesis (146, 170). In *C. elegans* and *D. melanogaster*, α-KG was suggested to enhance longevity through inhibition of TORC1 signalling and consequent upregulation of autophagy. Importantly, increasing Glu concentration in growth medium was also reported to enhance yeast longevity, promoting oxidative stress resistance and cell biomass increase (132). In this study, we showed that supplementation with α-KG, Glu and Gln increased the CLS of the wild type strain (1.4-1.6-fold) (Figure 12). However, the effects of supplementation with α-KG or Glu were remarkably superior in *ncr1Δ* cells, causing a 2.4-fold and 3-fold increase in CLS, whereas Gln supplementation promoted a 1.5-fold increase in CLS, as in wild type cells (Figure 12). Arginine supplementation also increased CLS in wild type cells but not in *ncr1Δ* cells (not shown), suggesting that Glu and Gln do not increase longevity simply due to augmented nitrogen supply. Interestingly, CLS extension promoted by α-KG, Glu or Gln supplementation was accompanied by attenuation of culture acidification (Table 3), which is observed in yeast cultures under calorie restriction, an intervention known to delay aging in various eukaryotes. Since α-KG was demonstrated to enhance longevity through TORC1 downregulation in *C. elegans* (140) and Glu and Gln can modulate TORC1 activity in yeast (63), we searched for a relation between the CLS-extending effect of these supplements in *ncr1Δ* cells and effects on TORC1 activity. The supplementation of α-KG induced a 2-fold reduction of TORC1 activation in *ncr1Δ* cells, whereas Glu induced a 2.3-fold increase (Figure 13), so it is not clear how modulation of TORC1 can impact the longevity of *ncr1Δ* cells. Like Glu, Gln exhibited a tendency to increase TORC1 activation (Figure 13). Although the three supplements promoted autophagy upregulation in the wild type strain, they did not restore the autophagic flux of yeast lacking Ncr1 (Figure 14), indicating that TORC1 modulation in these cells does not ameliorate autophagic defects and that the aging-delaying effect of these supplements is independent of autophagy induction. Our results also suggest that the protective effect of α-KG supply is not associated with the improvement of mitochondrial respiration capacity (data not shown).

In wild type cells, α-KG supplementation led to alterations in the amino acid content, which included an increase of Glu levels during exponential growth and an overall tendency for augmented amino acid levels (Figures 16-17). Interestingly, these effects were suppressed in *ncr1Δ* cells. Plus, α-KG attenuated phenylalanine accumulation in *ncr1Δ* cells during exponential growth (Figure 16 – B) and tended to decrease aspartate accumulation in PDS phase (Figure 17 – B), which may be related to its CLS-extending effect. Analyses with more replicates will be performed for accurate characterization of amino acid homeostasis in *ncr1Δ* cells under non-supplemented and supplemented conditions.

In both yeast and mammals, α -KG is an obligatory cofactor of JmjC domain-containing demethylases and DNA-demethylating Tet enzymes (135). The former catalyse demethylation of histone lysine residues and alterations in their activity have been implicated in longevity regulation (135, 150, 152). Consistently, modulation of α -KG availability can affect demethylation of histone proteins and the aging process (181). In yeast, expression of histone H3 can be regulated by methylation of lysine residues and decreased levels of histones negatively affect longevity (150). In this study, we observed that histone H3 levels are significantly reduced in *ncr1* Δ cells (Figure 19), which may contribute to their shortened CLS. Supplementation with α -KG did not significantly affect H3 levels in these cells (Figure 19), indicating that regulation of H3 levels is not behind the CLS-extending effect of α -KG supplementation. Whether α -KG can modulate the CLS of *ncr1* Δ cells through regulation of the methylation state of H3 lysine residues remains to be determined.

In summary, our results demonstrate that hyperactivation of Gln3 does not mediate TORC1 upregulation, autophagy impairment or mitochondrial dysfunction in the yeast model of NPC1. However, these cells exhibit decreased α -KG levels and increased Glu levels, which is consistent with Gln3 hyperactivation, as well as altered amino acid homeostasis. Notably, α -KG, Glu and, to lower extent, Gln increased the CLS of *ncr1* Δ cells. Additionally, we report that these cells exhibit significantly reduced histone H3 levels, which may contribute to its premature ageing. Overall, this study and future research may provide new insights on the molecular aetiology and pathology of NPC1.

CHAPTER 6. References

1. De Duve C, Pressman BC, Gianetto R, Wattiaux R, Appelmans F. Tissue fractionation studies. 6. Intracellular distribution patterns of enzymes in rat-liver tissue. *Biochem J.* 1955;60(4):604-17.
2. Platt FM, d'Azzo A, Davidson BL, Neufeld EF, Tiffit CJ. Lysosomal storage diseases. *Nat Rev Dis Primers.* 2018;4(1):27.
3. Vanier MT. Niemann-Pick disease type C. *Orphanet J Rare Dis.* 2010;5(1):16.
4. Schuchman EH, Desnick RJ. Types A and B Niemann-Pick Disease. *Mol Genet Metab.* 2017;120(1-2):27-33.
5. Torres S, Balboa E, Zanlungo S, Enrich C, Garcia-Ruiz C, Fernandez-Checa JC. Lysosomal and Mitochondrial Liaisons in Niemann-Pick Disease. *Front Physiol.* 2017;8:982.
6. Wassif CA, Cross JL, Iben J, Sanchez-Pulido L, Cougnoux A, Platt FM, *et al.* High incidence of unrecognized visceral/neurological late-onset Niemann-Pick disease, type C1, predicted by analysis of massively parallel sequencing data sets. *Genet Med.* 2016;18(1):41-8.
7. Vanier MT. Complex lipid trafficking in Niemann-Pick disease type C. *J Inher Metab Dis.* 2015;38(1):187-99.
8. Xie C, Turley SD, Dietschy JM. Cholesterol accumulation in tissues of the Niemann-Pick type C mouse is determined by the rate of lipoprotein-cholesterol uptake through the coated-pit pathway in each organ. *Proc Natl Acad Sci USA.* 1999;96(21):11992-7.
9. Geberhiwot T, Moro A, Dardis A, Ramaswami U, Sirrs S, Marfa MP, *et al.* Consensus clinical management guidelines for Niemann-Pick disease type C. *Orphanet J Rare Dis.* 2018;13(1):50.
10. Naureckiene S, Sleat DE, Lackland H, Fensom A, Vanier MT, Wattiaux R, *et al.* Identification of *HE1* as the Second Gene of Niemann-Pick C Disease. *Science.* 2000;290(5500):2298-301.
11. Li X, Wang J, Coutavas E, Shi H, Hao Q, Blobel G. Structure of human Niemann-Pick C1 protein. *Proc Natl Acad Sci USA.* 2016;113(29):8212-7.
12. Vanier MT, Millat G. Structure and function of the NPC2 protein. *Biochim Biophys Acta.* 2004;1685(1-3):14-21.
13. Friedland N, Liou HL, Lobel P, Stock AM. Structure of a cholesterol-binding protein deficient in Niemann-Pick type C2 disease. *Proc Natl Acad Sci USA.* 2003;100(5):2512-7.
14. Xu S, Benoff B, Liou HL, Lobel P, Stock AM. Structural Basis of Sterol Binding by NPC2, a Lysosomal Protein Deficient in Niemann-Pick Type C2 Disease. *J Biol Chem.* 2007;282(32):23525-31.
15. Kwon HJ, Abi-Mosleh L, Wang ML, Deisenhofer J, Goldstein JL, Brown MS, *et al.* Structure of N-terminal Domain of NPC1 Reveals Distinct Subdomains for Binding and Transfer of Cholesterol. *Cell.* 2009;137(7):1213-24.

16. Li X, Saha P, Li J, Blobel G, Pfeffer SR. Clues to the mechanism of cholesterol transfer from the structure of NPC1 middle luminal domain bound to NPC2. *Proc Natl Acad Sci USA*. 2016;113(36):10079-84.
17. Millat G, Marçais C, Tomasetto C, Chikh K, Fensom AH, Harzer K, *et al*. Niemann-Pick C1 Disease: Correlations between NPC1 Mutations, Levels of NPC1 Protein, and Phenotypes Emphasize the Functional Significance of the Putative Sterol-Sensing Domain and of the Cysteine-Rich Luminal Loop. *Am J Hum Genet*. 2001;68(6):1373-85.
18. Runz H, Dolle D, Schlitter AM, Zschocke J. NPC-db, a Niemann-Pick Type C Disease Gene Variation Database. *Hum Mutat*. 2008;29(3):345-50.
19. Gelsthorpe ME, Baumann N, Millard E, Gale SE, Langmade SJ, Schaffer JE, *et al*. Niemann-Pick Type C1 I1061T Mutant Encodes a Functional Protein That Is Selected for Endoplasmic Reticulum-associated Degradation Due to Protein Misfolding. *J Biol Chem*. 2008;283(13):8229-36.
20. Shammas H, Kuech EM, Rizk S, Das AM, Naim HY. Different Niemann-Pick C1 Genotypes Generate Protein Phenotypes that Vary in their Intracellular Processing, Trafficking and Localization. *Sci Rep*. 2019;9(1):5292.
21. Lusa S, Blom TS, Eskelinen EL, Kuismanen E, Månsson JE, Simons K, *et al*. Depletion of rafts in late endocytic membranes is controlled by NPC1-dependent recycling of cholesterol to the plasma membrane. *J Cell Sci*. 2001;114(Pt 10):1893-900.
22. Abi-Mosleh L, Infante RE, Radhakrishnan A, Goldstein JL, Brown MS. Cyclodextrin overcomes deficient lysosome-to-endoplasmic reticulum transport of cholesterol in Niemann-Pick type C cells. *Proc Natl Acad Sci USA*. 2009;106(46):19316-21.
23. Subramanian K, Hutt DM, Scott SM, Gupta V, Mao S, Balch WE. Correction of Niemann-Pick type C1 trafficking and activity with the histone deacetylase inhibitor valproic acid. *J Biol Chem*. 2020;295(23):8017-35.
24. Higashi Y, Murayama S, Pentchev PG, Suzuki K. Cerebellar degeneration in the Niemann-Pick type C mouse. *Acta Neuropathol*. 1993;85(2):175-84.
25. Karten B, Vance DE, Campenot RB, Vance JE. Cholesterol accumulates in cell bodies, but is decreased in distal axons, of Niemann-Pick C1-deficient neurons. *J Neurochem*. 2002;83(5):1154-63.
26. Ordonez MP, Roberts EA, Kidwell CU, Yuan SH, Plaisted WC, Goldstein LS. Disruption and therapeutic rescue of autophagy in a human neuronal model of Niemann Pick type C1. *Hum Mol Genet*. 2012;21(12):2651-62.
27. Maetzel D, Sarkar S, Wang H, Abi-Mosleh L, Xu P, Cheng AW, *et al*. Genetic and Chemical Correction of Cholesterol Accumulation and Impaired Autophagy in Hepatic and Neural Cells

Derived from Niemann-Pick Type C Patient-Specific iPS Cells. *Stem Cell Rep.* 2014;2(6):866-80.

28. Sarkar S, Carroll B, Buganim Y, Maetzel D, Ng AH, Cassady JP, *et al.* Impaired Autophagy in the Lipid-Storage Disorder Niemann-Pick Type C1 Disease. *Cell Rep.* 2013;5(5):1302-15.

29. Elrick MJ, Yu T, Chung C, Lieberman AP. Impaired proteolysis underlies autophagic dysfunction in Niemann-Pick type C disease. *Hum Mol Genet.* 2012;21(22):4876-87.

30. Yu W, Gong JS, Ko M, Garver WS, Yanagisawa K, Michikawa M. Altered cholesterol metabolism in Niemann-Pick type C1 mouse brains affects mitochondrial function. *J Biol Chem.* 2005;280(12):11731-9.

31. Wos M, Szczepanowska J, Pikula S, Tytki-Szymanska A, Zablocki K, Bandorowicz-Pikula J. Mitochondrial dysfunction in fibroblasts derived from patients with Niemann-Pick type C disease. *Arch Biochem Biophys.* 2016;593:50-9.

32. Kann O, Kovács R. Mitochondria and neuronal activity. *Am J Physiol Cell Physiol.* 2007;292(2):C641-57.

33. Platt FM, Neises GR, Dwek RA, Butters TD. *N*-Butyldeoxynojirimycin Is a Novel Inhibitor of Glycolipid Biosynthesis. *J Biol Chem.* 1994;269(11):8362-5.

34. Lachmann RH, te Vrugte D, Lloyd-Evans E, Reinkensmeier G, Sillence DJ, Fernandez-Guillen L, *et al.* Treatment with miglustat reverses the lipid-trafficking defect in Niemann-Pick disease type C. *Neurobiol Dis.* 2004;16(3):654-8.

35. Patterson MC, Mengel E, Vanier MT, Moneuse P, Rosenberg D, Pineda M. Treatment outcomes following continuous miglustat therapy in patients with Niemann-Pick disease Type C: a final report of the NPC Registry. *Orphanet J Rare Dis.* 2020;15(1):104.

36. Oliveira AV, Vilaça R, Santos CN, Costa V, Menezes R. Exploring the power of yeast to model aging and age-related neurodegenerative disorders. *Biogerontology.* 2017;18(1):3-34.

37. Berger AC, Hanson PK, Nichols JW, Corbett AH. A Yeast Model System for Functional Analysis of the Niemann–Pick Type C Protein 1 Homolog, Ncr1p. *Traffic.* 2005;6(10):907-17.

38. Winkler MBL, Kidmose RT, Szomek M, Thaysen K, Rawson S, Muench SP, *et al.* Structural Insight into Eukaryotic Sterol Transport through Niemann-Pick Type C Proteins. *Cell.* 2019;179(2):485-97 e18.

39. Malathi K, Higaki K, Tinkelenberg AH, Balderes DA, Almanzar-Paramio D, Wilcox LJ, *et al.* Mutagenesis of the putative sterol-sensing domain of yeast Niemann Pick C-related protein reveals a primordial role in subcellular sphingolipid distribution. *J Cell Biol.* 2004;164(4):547-56.

40. Brett CL, Kallay L, Hua Z, Green R, Chyou A, Zhang Y, *et al.* Genome-Wide Analysis Reveals the Vacuolar pH-Stat of *Saccharomyces cerevisiae*. *PLoS One.* 2011;6(3):e17619.

41. Vilaça R, Silva E, Nadais A, Teixeira V, Matmati N, Gaifem J, *et al.* Sphingolipid signalling mediates mitochondrial dysfunctions and reduced chronological lifespan in the yeast model of Niemann-Pick type C1. *Mol Microbiol.* 2014;91(3):438-51.
42. Lloyd-Evans E, Morgan AJ, He X, Smith DA, Elliot-Smith E, Sillence DJ, *et al.* Niemann-Pick disease type C1 is a sphingosine storage disease that causes deregulation of lysosomal calcium. *Nat Med.* 2008;14(11):1247-55.
43. Tharkeshwar A, Trekker J, Vermeire W, Pauwels J, Sannerud R, Priestman DA, *et al.* A novel approach to analyze lysosomal dysfunctions through subcellular proteomics and lipidomics: the case of NPC1 deficiency. *Sci Rep.* 2017;7(1).
44. Vilaça R, Barros I, Matmati N, Silva E, Martins T, Teixeira V, *et al.* The ceramide activated protein phosphatase Sit4 impairs sphingolipid dynamics, mitochondrial function and lifespan in a yeast model of Niemann-Pick type C1. *Biochim Biophys Acta.* 2018;1864(1):79-88.
45. Condon KJ, Sabatini DM. Nutrient regulation of mTORC1 at a glance. *J Cell Sci.* 2019;132(21).
46. Heitman J, Movva NR, Hall MN. Targets for Cell Cycle Arrest by the Immunosuppressant Rapamycin in Yeast. *Science.* 1991;253(5022):905-9.
47. Sabatini DM, Erdjument-Bromage H, Lui M, Tempst P, Snyder SH. RAFT1: a mammalian protein that binds to FKBP12 in a rapamycin-dependent fashion and is homologous to yeast TORs. *Cell.* 1994;78(1):35-43.
48. Loewith R, Jacinto E, Wullschleger S, Lorberg A, Crespo JL, Bonenfant D, *et al.* Two TOR Complexes, Only One of which Is Rapamycin Sensitive, Have Distinct Roles in Cell Growth Control. *Mol Cell.* 2002;10(3):457-68.
49. Eltschinger S, Loewith R. TOR Complexes and the Maintenance of Cellular Homeostasis. *Trends Cell Biol.* 2016;26(2):148-59.
50. Gaubitz C, Oliveira TM, Prouteau M, Leitner A, Karuppasamy M, Konstantinidou G, *et al.* Molecular Basis of the Rapamycin Insensitivity of Target Of Rapamycin Complex 2. *Mol Cell.* 2015;58(6):977-88.
51. Zaragoza D, Ghavidel A, Heitman J, Schultz MC. Rapamycin Induces the G₀ Program of Transcriptional Repression in Yeast by Interfering with the TOR Signaling Pathway. *Mol Cell Biol.* 1998;18(8):4463-70.
52. Saxton RA, Sabatini DM. mTOR Signaling in Growth, Metabolism, and Disease. *Cell.* 2017;168(6):960-76.
53. Xu J, Dang Y, Ren YR, Liu JO. Cholesterol trafficking is required for mTOR activation in endothelial cells. *Proc Natl Acad Sci USA.* 2010;107(10):4764-9.

54. Davis OB, Shin HR, Lim CY, Wu EY, Kukurugya M, Maher CF, *et al.* NPC1-mTORC1 Signaling Couples Cholesterol Sensing to Organelle Homeostasis and Is a Targetable Pathway in Niemann-Pick Type C. *Dev Cell.* 2021;56(3):260-76.e7.
55. Teixeira V, Costa V. Unraveling the role of the Target of Rapamycin signaling in sphingolipid metabolism. *Prog Lipid Res.* 2016;61:109-33.
56. Broer S, Broer A. Amino acid homeostasis and signalling in mammalian cells and organisms. *Biochem J.* 2017;474(12):1935-63.
57. Aris JP, Fishwick LK, Marraffini ML, Seo AY, Leeuwenburgh C, Dunn WA, Jr. Amino Acid Homeostasis and Chronological Longevity in *Saccharomyces cerevisiae*. *Subcell Biochem.* 2012;57:161-86.
58. Alvers AL, Fishwick LK, Wood MS, Hu D, Chung HS, Dunn WA, Jr., *et al.* Autophagy and amino acid homeostasis are required for chronological longevity in *Saccharomyces cerevisiae*. *Aging Cell.* 2009;8(4):353-69.
59. Canfield C-A, Bradshaw PC. Amino acids in the regulation of aging and aging-related diseases. *Transl Med Aging.* 2019;3:70-89.
60. Binda M, Péli-Gulli MP, Bonfils G, Panchaud N, Urban J, Sturgill TW, *et al.* The Vam6 GEF Controls TORC1 by Activating the EGO Complex. *Mol Cell.* 2009;35(5):563-73.
61. Zoncu R, Bar-Peled L, Efeyan A, Wang S, Sancak Y, Sabatini DM. mTORC1 Senses Lysosomal Amino Acids Through an Inside-Out Mechanism That Requires the Vacuolar H⁺-ATPase. *Science.* 2011;334(6056):678-83.
62. Dechant R, Saad S, Ibáñez AJ, Peter M. Cytosolic pH Regulates Cell Growth through Distinct GTPases, Arf1 and Gtr1, to Promote Ras/PKA and TORC1 Activity. *Mol Cell.* 2014;55(3):409-21.
63. Stracka D, Jozefczuk S, Rudroff F, Sauer U, Hall MN. Nitrogen Source Activates TOR (Target of Rapamycin) Complex 1 via Glutamine and Independently of Gtr/Rag Proteins. *J Biol Chem.* 2014;289(36):25010-20.
64. Jewell JL, Kim YC, Russell RC, Yu FX, Park HW, Plouffe SW, *et al.* Differential regulation of mTORC1 by leucine and glutamine. *Science.* 2015;347(6218):194-8.
65. Tanigawa M, Maeda T. An In Vitro TORC1 Kinase Assay That Recapitulates the Gtr-Independent Glutamine-Responsive TORC1 Activation Mechanism on Yeast Vacuoles. *Mol Cell Biol.* 2017;37(14).
66. Mulleder M, Calvani E, Alam MT, Wang RK, Eckerstorfer F, Zelezniak A, *et al.* Functional Metabolomics Describes the Yeast Biosynthetic Regulome. *Cell.* 2016;167(2):553-65 e12.
67. Longo VD, Fabrizio P. Chronological aging in *Saccharomyces cerevisiae*. *Subcell Biochem.* 2012;57:101-21.

68. Braun RJ, Büttner S, Ring J, Kroemer G, Madeo F. Nervous yeast: modeling neurotoxic cell death. *Trends Biochem Sci.* 2010;35(3):135-44.
69. Harrison DE, Strong R, Sharp ZD, Nelson JF, Astle CM, Flurkey K, *et al.* Rapamycin fed late in life extends lifespan in genetically heterogeneous mice. *Nature.* 2009;460(7253):392-5.
70. Pan Y, Shadel GS. Extension of chronological life span by reduced TOR signaling requires down-regulation of Sch9p and involves increased mitochondrial OXPHOS complex density. *Aging.* 2009;1(1):131-45.
71. Bonawitz ND, Chatenay-Lapointe M, Pan Y, Shadel GS. Reduced TOR Signaling Extends Chronological Life Span via Increased Respiration and Upregulation of Mitochondrial Gene Expression. *Cell Metab.* 2007;5(4):265-77.
72. Urban J, Soulard A, Huber A, Lippman S, Mukhopadhyay D, Deloche O, *et al.* Sch9 Is a Major Target of TORC1 in *Saccharomyces cerevisiae*. *Mol Cell.* 2007;26(5):663-74.
73. Kaeberlein M, Powers RW, 3rd, Steffen KK, Westman EA, Hu D, Dang N, *et al.* Regulation of Yeast Replicative Life Span by TOR and Sch9 in Response to Nutrients. *Science.* 2005;310(5751):1193-6.
74. Wei M, Fabrizio P, Hu J, Ge H, Cheng C, Li L, *et al.* Life Span Extension by Calorie Restriction Depends on Rim15 and Transcription Factors Downstream of Ras/PKA, Tor, and Sch9. *PLoS Genet.* 2008;4(1):e13.
75. Sampaio-Marques B, Burhans WC, Ludovico P. Longevity pathways and maintenance of the proteome: the role of autophagy and mitophagy during yeast ageing. *Microb Cell.* 2014;1(4):118-27.
76. Alvers AL, Wood MS, Hu D, Kaywell AC, Dunn WA, Jr., Aris JP. Autophagy is required for extension of yeast chronological life span by rapamycin. *Autophagy.* 2009;5(6):847-9.
77. Bastians H, Ponstingl H. The novel human protein serine/threonine phosphatase 6 is a functional homologue of budding yeast Sit4p and fission yeast ppe1, which are involved in cell cycle regulation. *J Cell Sci.* 1996;109 (Pt 12):2865-74.
78. Garipler G, Mutlu N, Lack NA, Dunn CD. Deletion of conserved protein phosphatases reverses defects associated with mitochondrial DNA damage in *Saccharomyces cerevisiae*. *Proc Natl Acad Sci USA.* 2014;111(4):1473-8.
79. Nickels JT, Broach JR. A ceramide-activated protein phosphatase mediates ceramide-induced G1 arrest of *Saccharomyces cerevisiae*. *Genes Dev.* 1996;10(4):382-94.
80. Barbosa AD, Osório H, Sims KJ, Almeida T, Alves M, Bielawski J, *et al.* Role for Sit4p-dependent mitochondrial dysfunction in mediating the shortened chronological lifespan and oxidative stress sensitivity of Isc1p-deficient cells. *Mol Microbiol.* 2011;81(2):515-27.
81. Di Como CJ, Arndt KT. Nutrients, via the Tor proteins, stimulate the association of Tap42 with type 2A phosphatases. *Genes Dev.* 1996;10(15):1904-16.

82. Wang H, Wang X, Jiang Y. Interaction with Tap42 Is Required for the Essential Function of Sit4 and Type 2A Phosphatases. *Mol Biol Cell*. 2003;14(11):4342-51.
83. Beck T, Hall MN. The TOR signalling pathway controls nuclear localization of nutrient-regulated transcription factors. *Nature*. 1999;402(6762):689-92.
84. Hofman-Bang J. Nitrogen Catabolite Repression in *Saccharomyces cerevisiae*. *Mol Biotechnol*. 1999;12(1):35-73.
85. Crespo JL, Powers T, Fowler B, Hall MN. The TOR-controlled transcription activators GLN3, RTG1, and RTG3 are regulated in response to intracellular levels of glutamine. *Proc Natl Acad Sci USA*. 2002;99(10):6784-9.
86. Bertram PG, Choi JH, Carvalho J, Ai W, Zeng C, Chan TF, *et al*. Tripartite Regulation of Gln3p by TOR, Ure2p, and Phosphatases. *J Biol Chem*. 2000;275(46):35727-33.
87. Tate JJ, Cooper TG. Five Conditions Commonly Used to Down-regulate Tor Complex 1 Generate Different Physiological Situations Exhibiting Distinct Requirements and Outcomes. *J Biol Chem*. 2013;288(38):27243-62.
88. Blinder D, Coschigano PW, Magasanik B. Interaction of the GATA Factor Gln3p with the Nitrogen Regulator Ure2p in *Saccharomyces cerevisiae*. *J Bacteriol*. 1996;178(15):4734-6.
89. Hardwick JS, Kuruvilla FG, Tong JK, Shamji AF, Schreiber SL. Rapamycin-modulated transcription defines the subset of nutrient-sensitive signaling pathways directly controlled by the Tor proteins. *Proc Natl Acad Sci USA*. 1999;96(26):14866-70.
90. Yan G, Shen X, Jiang Y. Rapamycin activates Tap42-associated phosphatases by abrogating their association with Tor complex 1. *EMBO J*. 2006;25(15):3546-55.
91. Tate JJ, Tolley EA, Cooper TG. Sit4 and PP2A Dephosphorylate Nitrogen Catabolite Repression-Sensitive Gln3 When TorC1 Is Up- as Well as Downregulated. *Genetics*. 2019;212(4):1205-25.
92. Mara P, Fragiadakis GS, Gkountromichos F, Alexandraki D. The pleiotropic effects of the glutamate dehydrogenase (GDH) pathway in *Saccharomyces cerevisiae*. *Microb Cell Fact*. 2018;17(1):170.
93. DeLuna A, Avendaño A, Riego L, González A. NADP-Glutamate Dehydrogenase Isoenzymes of *Saccharomyces cerevisiae*. *J Biol Chem*. 2001;276(47):43775-83.
94. Lee YJ, Kim KJ, Kang HY, Kim HR, Maeng PJ. Involvement of GDH3-encoded NADP⁺-dependent Glutamate Dehydrogenase in Yeast Cell Resistance to Stress-induced Apoptosis in Stationary Phase Cells. *J Biol Chem*. 2012;287(53):44221-33.
95. Magasanik B, Kaiser CA. Nitrogen regulation in *Saccharomyces cerevisiae*. *Gene*. 2002;290(1-2):1-18.

96. Chen EJ, Kaiser CA. Amino acids regulate the intracellular trafficking of the general amino acid permease of *Saccharomyces cerevisiae*. Proc Natl Acad Sci USA. 2002;99(23):14837-42.
97. Klionsky DJ, Emr SD. Autophagy as a Regulated Pathway of Cellular Degradation. Science. 2000;290(5497):1717-21.
98. Mijaljica D, Prescott M, Devenish RJ. Microautophagy in mammalian cells: revisiting a 40-year-old conundrum. Autophagy. 2011;7(7):673-82.
99. Harding TM, Hefner-Gravink A, Thumm M, Klionsky DJ. Genetic and Phenotypic Overlap between Autophagy and the Cytoplasm to Vacuole Protein Targeting Pathway. J Biol Chem. 1996;271(30):17621-4.
100. Yang Z, Klionsky DJ. Eaten alive: a history of macroautophagy. Nat Cell Biol. 2010;12(9):814-22.
101. Kanki T, Klionsky DJ. Mitophagy in Yeast Occurs through a Selective Mechanism. J Biol Chem. 2008;283(47):32386-93.
102. Tsukada M, Ohsumi Y. Isolation and characterization of autophagy-defective mutants of *Saccharomyces cerevisiae*. FEBS Lett. 1993;333(1-2):169-74.
103. Klionsky DJ, Cregg JM, Dunn WA, Jr., Emr SD, Sakai Y, Sandoval IV, *et al.* A Unified Nomenclature for Yeast Autophagy-Related Genes. Dev Cell. 2003;5(4):539-45.
104. Nakatogawa H, Suzuki K, Kamada Y, Ohsumi Y. Dynamics and diversity in autophagy mechanisms: lessons from yeast. Nat Rev Mol Cell Biol. 2009;10(7):458-67.
105. Stephan JS, Yeh YY, Ramachandran V, Deminoff SJ, Herman PK. The Tor and PKA signaling pathways independently target the Atg1/Atg13 protein kinase complex to control autophagy. Proc Natl Acad Sci USA. 2009;106(40):17049-54.
106. Yeh YY, Shah KH, Herman PK. An Atg13 Protein-mediated Self-association of the Atg1 Protein Kinase Is Important for the Induction of Autophagy. J Biol Chem. 2011;286(33):28931-9.
107. Xie Z, Nair U, Klionsky DJ. Atg8 Controls Phagophore Expansion during Autophagosome Formation. Mol Biol Cell. 2008;19(8):3290-8.
108. Kirisako T, Ichimura Y, Okada H, Kabeya Y, Mizushima N, Yoshimori T, *et al.* The Reversible Modification Regulates the Membrane-Binding State of Apg8/Aut7 Essential for Autophagy and the Cytoplasm to Vacuole Targeting Pathway. J Cell Biol. 2000;151(2):263-76.
109. Ichimura Y, Kirisako T, Takao T, Satomi Y, Shimonishi Y, Ishihara N, *et al.* A ubiquitin-like system mediates protein lipidation. Nature. 2000;408(6811):488-92.
110. Nair U, Yen WL, Mari M, Cao Y, Xie Z, Baba M, *et al.* A role for Atg8-PE deconjugation in autophagosome biogenesis. Autophagy. 2012;8(5):780-93.

111. Torggler R, Papinski D, Kraft C. Assays to Monitor Autophagy in *Saccharomyces cerevisiae*. *Cells*. 2017;6(3).
112. Takeshige K, Baba M, Tsuboi S, Noda T, Ohsumi Y. Autophagy in Yeast Demonstrated with Proteinase-deficient Mutants and Conditions for its Induction. *J Cell Biol*. 1992;119(2):301-11.
113. Onodera J, Ohsumi Y. Autophagy Is Required for Maintenance of Amino Acid Levels and Protein Synthesis under Nitrogen Starvation. *J Biol Chem*. 2005;280(36):31582-6.
114. Li SC, Kane PM. The Yeast Lysosome-like Vacuole: Endpoint and Crossroads. *Biochim Biophys Acta*. 2009;1793(4):650-63.
115. Bianchi F, van't Klooster JS, Ruiz SJ, Poolman B. Regulation of Amino Acid Transport in *Saccharomyces cerevisiae*. *Microbiol Mol Biol Rev*. 2019;83(4).
116. Nakamura N, Matsuura A, Wada Y, Ohsumi Y. Acidification of Vacuoles Is Required for Autophagic Degradation in the Yeast, *Saccharomyces cerevisiae*. *J Biochem*. 1997;121(2):338-44.
117. Kawano-Kawada M, Kakinuma Y, Sekito T. Transport of Amino Acids across the Vacuolar Membrane of Yeast: Its Mechanism and Physiological Role. *Biol Pharm Bull*. 2018;41(10):1496-501.
118. Noda T, Ohsumi Y. Tor, a Phosphatidylinositol Kinase Homologue, Controls Autophagy in Yeast. *J Biol Chem*. 1998;273(7):3963-6.
119. Shin CS, Huh WK. Bidirectional regulation between TORC1 and autophagy in *Saccharomyces cerevisiae*. *Autophagy*. 2011;7(8):854-62.
120. Kamada Y, Yoshino K, Kondo C, Kawamata T, Oshiro N, Yonezawa K, *et al*. Tor Directly Controls the Atg1 Kinase Complex To Regulate Autophagy. *Mol Cell Biol*. 2010;30(4):1049-58.
121. Yeasmin AM, Waliullah TM, Kondo A, Kaneko A, Koike N, Ushimaru T. Orchestrated Action of PP2A Antagonizes Atg13 Phosphorylation and Promotes Autophagy after the Inactivation of TORC1. *PLoS One*. 2016;11(12):e0166636.
122. Inoue Y, Klionsky DJ. Regulation of macroautophagy in *Saccharomyces cerevisiae*. *Semin Cell Dev Biol*. 2010;21(7):664-70.
123. Zhang C, Cuervo AM. Restoration of chaperone-mediated autophagy in aging liver improves cellular maintenance and hepatic function. *Nature medicine*. 2008;14(9):959-65.
124. Wang JH, Ahn IS, Fischer TD, Byeon JI, Dunn WA, Jr., Behrns KE, *et al*. Autophagy Suppresses Age-Dependent Ischemia and Reperfusion Injury in Livers of Mice. *Gastroenterology*. 2011;141(6):2188-99.e6.

125. Aris JP, Alvers AL, Ferraiuolo RA, Fishwick LK, Hanvivatpong A, Hu D, *et al.* Autophagy and leucine promote chronological longevity and respiration proficiency during calorie restriction in yeast. *Exp Gerontol.* 2013;48(10):1107-19.
126. Pyo JO, Yoo SM, Ahn HH, Nah J, Hong SH, Kam TI, *et al.* Overexpression of Atg5 in mice activates autophagy and extends lifespan. *Nat Commun.* 2013;4:2300.
127. Sampaio-Marques B, Felgueiras C, Silva A, Rodrigues F, Ludovico P. Yeast chronological lifespan and proteotoxic stress: is autophagy good or bad? *Biochem Soc Trans.* 2011;39(5):1466-70.
128. Powers RW, 3rd, Kaeberlein M, Caldwell SD, Kennedy BK, Fields S. Extension of chronological life span in yeast by decreased TOR pathway signaling. *Genes Dev.* 2006;20(2):174-84.
129. Gomes P, Sampaio-Marques B, Ludovico P, Rodrigues F, Leão C. Low auxotrophy-complementing amino acid concentrations reduce yeast chronological life span. *Mech Ageing Dev.* 2007;128(5-6):383-91.
130. Orentreich N, Matias JR, DeFelice A, Zimmerman JA. Low Methionine Ingestion by Rats Extends Life Span. *J Nutr.* 1993;123(2):269-74.
131. Plummer JD, Johnson JE. Extension of Cellular Lifespan by Methionine Restriction Involves Alterations in Central Carbon Metabolism and Is Mitophagy-Dependent. *Front Cell Dev Biol.* 2019;7:301.
132. Wu Z, Song L, Liu SQ, Huang D. Independent and Additive Effects of Glutamic Acid and Methionine on Yeast Longevity. *PLoS One.* 2013;8(11):e79319.
133. Kennedy BE, Hundert AS, Goguen D, Weaver IC, Karten B. Presymptomatic Alterations in Amino Acid Metabolism and DNA Methylation in the Cerebellum of a Murine Model of Niemann-Pick Type C Disease. *Am J Pathol.* 2016;186(6):1582-97.
134. Ruiz-Rodado V, Nicoli ER, Probert F, Smith DA, Morris L, Wassif CA, *et al.* ¹H NMR-Linked Metabolomics Analysis of Liver from a Mouse Model of NP-C1 Disease. *J Proteome Res.* 2016;15(10):3511-27.
135. Salminen A, Kauppinen A, Hiltunen M, Kaarniranta K. Krebs cycle intermediates regulate DNA and histone methylation: Epigenetic impact on the aging process. *Ageing Res Rev.* 2014;16:45-65.
136. Ljungdahl PO, Daignan-Fornier B. Regulation of Amino Acid, Nucleotide, and Phosphate Metabolism in *Saccharomyces cerevisiae*. *Genetics.* 2012;190(3):885-929.
137. Tsukada Y, Fang J, Erdjument-Bromage H, Warren ME, Borchers CH, Tempst P, *et al.* Histone demethylation by a family of JmjC domain-containing proteins. *Nature.* 2006;439(7078):811-6.

138. Shahmirzadi AA, Edgar D, Liao CY, Hsu YM, Lucanic M, Shahmirzadi AA, *et al.* Alpha-Ketoglutarate, an Endogenous Metabolite, Extends Lifespan and Compresses Morbidity in Aging Mice. *Cell Metab.* 2020;32(3):447-56.e6.
139. Su Y, Wang T, Wu N, Li D, Fan X, Xu Z, *et al.* Alpha-ketoglutarate extends *Drosophila* lifespan by inhibiting mTOR and activating AMPK. *Aging.* 2019;11(12):4183-97.
140. Chin RM, Fu X, Pai MY, Vergnes L, Hwang H, Deng G, *et al.* The metabolite alpha-ketoglutarate extends lifespan by inhibiting ATP synthase and TOR. *Nature.* 2014;510(7505):397-401.
141. Durán RV, Oppliger W, Robitaille AM, Heiserich L, Skendaj R, Gottlieb E, *et al.* Glutaminolysis Activates Rag-mTORC1 Signaling. *Mol Cell.* 2012;47(3):349-58.
142. Yao K, Yin Y, Li X, Xi P, Wang J, Lei J, *et al.* Alpha-ketoglutarate inhibits glutamine degradation and enhances protein synthesis in intestinal porcine epithelial cells. *Amino Acids.* 2012;42(6):2491-500.
143. Baracco EE, Castoldi F, Durand S, Enot DP, Tadic J, Kainz K, *et al.* α -Ketoglutarate inhibits autophagy. *Aging.* 2019;11(11):3418-31.
144. Miller SM, Magasanik B. Role of NAD-linked glutamate dehydrogenase in nitrogen metabolism in *Saccharomyces cerevisiae*. *J Bacteriol.* 1990;172(9):4927-35.
145. Burdyliuk N, Bayliak M. Effects of Long-Term Cultivation on Medium with Alpha-Ketoglutarate Supplementation on Metabolic Processes of *Saccharomyces cerevisiae*. *J Aging Res.* 2017;2017:8754879.
146. Bayliak MM, Hrynkiv OV, Knyhynytska RV, Lushchak VI. Alpha-ketoglutarate enhances freeze-thaw tolerance and prevents carbohydrate-induced cell death of the yeast *Saccharomyces cerevisiae*. *Arch Microbiol.* 2018;200(1):33-46.
147. Luger K, Mäder AW, Richmond RK, Sargent DF, Richmond TJ. Crystal structure of the nucleosome core particle at 2.8 Å resolution. *Nature.* 1997;389(6648):251-60.
148. Smith MM, Murray K. Yeast H3 and H4 histone messenger RNAs are transcribed from two non-allelic gene sets. *J Mol Biol.* 1983;169(3):641-61.
149. Choe J, Kolodrubetz D, Grunstein M. The two yeast histone H2A genes encode similar protein subtypes. *Proc Natl Acad Sci USA.* 1982;79(5):1484-7.
150. Mei Q, Xu C, Gogol M, Tang J, Chen W, Yu X, *et al.* Set1-catalyzed H3K4 trimethylation antagonizes the HIR/Asf1/Rtt106 repressor complex to promote histone gene expression and chronological life span. *Nucleic Acids Res.* 2019;47(7):3434-49.
151. Feser J, Truong D, Das C, Carson JJ, Kieft J, Harkness T, *et al.* Elevated Histone Expression Promotes Life Span Extension. *Mol Cell.* 2010;39(5):724-35.
152. Sen P, Dang W, Donahue G, Dai J, Dorsey J, Cao X, *et al.* H3K36 methylation promotes longevity by enhancing transcriptional fidelity. *Genes Dev.* 2015;29(13):1362-76.

153. Gietz RD, Schiestl RH. High-efficiency yeast transformation using the LiAc/SS carrier DNA/PEG method. *Nat Protoc.* 2007;2(1):31-4.
154. Mesquita A, Weinberger M, Silva A, Sampaio-Marques B, Almeida B, Leão C, *et al.* Caloric restriction or catalase inactivation extends yeast chronological lifespan by inducing H₂O₂ and superoxide dismutase activity. *Proc Natl Acad Sci USA.* 2010;107(34):15123-8.
155. Kushnirov VV. Rapid and reliable protein extraction from yeast. *Yeast.* 2000;16(9):857-60.
156. Zhang T, Lei J, Yang H, Xu K, Wang R, Zhang Z. An improved method for whole protein extraction from yeast *Saccharomyces cerevisiae*. *Yeast.* 2011;28(11):795-8.
157. Cools M, Rompf M, Mayer A, André B. Measuring the Activity of Plasma Membrane and Vacuolar Transporters in Yeast. *Methods Mol Biol.* 2019;2049:247-61.
158. Wiederhold E, Gandhi T, Permentier HP, Breitling R, Poolman B, Slotboom DJ. The Yeast Vacuolar Membrane Proteome. *Mol Cell Proteomics.* 2009;8(2):380-92.
159. McCombie G, Medina-Gomez G, Lelliott CJ, Vidal-Puig A, Griffin JL. Metabolomic and Lipidomic Analysis of the Heart of Peroxisome Proliferator-Activated Receptor-γ Coactivator 1-β Knock Out Mice on a High Fat Diet. *Metabolites.* 2012;2(2):366-81.
160. Madia F, Gattazzo C, Wei M, Fabrizio P, Burhans WC, Weinberger M, *et al.* Longevity mutation in *SCH9* prevents recombination errors and premature genomic instability in a Werner/Bloom model system. *J Cell Biol.* 2008;180(1):67-81.
161. Weinberger M, Feng L, Paul A, Smith DL, Jr., Hontz RD, Smith JS, *et al.* DNA Replication Stress Is a Determinant of Chronological Lifespan in Budding Yeast. *PLoS One.* 2007;2(8):e748.
162. González A, Shimobayashi M, Eisenberg T, Merle DA, Pendl T, Hall MN, *et al.* TORC1 Promotes Phosphorylation of Ribosomal Protein S6 via the AGC Kinase Ypk3 in *Saccharomyces cerevisiae*. *PLoS One.* 2015;10(3):e0120250.
163. Kuroda K, Hammer SK, Watanabe Y, Montano Lopez J, Fink GR, Stephanopoulos G, *et al.* Critical Roles of the Pentose Phosphate Pathway and *GLN3* in Isobutanol-Specific Tolerance in Yeast. *Cell Syst.* 2019;9(6):534-47 e5.
164. Yanagisawa H, Ishii T, Endo K, Kawakami E, Nagao K, Miyashita T, *et al.* L-leucine and SPNS1 coordinately ameliorate dysfunction of autophagy in mouse and human Niemann-Pick type C disease. *Sci Rep.* 2017;7(1):15944.
165. Castellano BM, Thelen AM, Moldavski O, Feltes M, van der Welle RE, Mydock-McGrane L, *et al.* Lysosomal Cholesterol Activates mTORC1 via an SLC38A9-Niemann Pick C1 Signaling Complex. *Science.* 2017;355(6331):1306-11.
166. Chan TF, Bertram PG, Ai W, Zheng XF. Regulation of APG14 Expression by the GATA-type Transcription Factor Gln3p. *J Biol Chem.* 2001;276(9):6463-7.

167. Bernard A, Jin M, Xu Z, Klionsky DJ. A large-scale analysis of autophagy-related gene expression identifies new regulators of autophagy. *Autophagy*. 2015;11(11):2114-22.
168. Lang T, Schaeffeler E, Bernreuther D, Bredschneider M, Wolf DH, Thumm M. Aut2p and Aut7p, two novel microtubule-associated proteins are essential for delivery of autophagic vesicles to the vacuole. *EMBO J*. 1998;17(13):3597-607.
169. Ordonez MP. Defective mitophagy in human Niemann-Pick Type C1 neurons is due to abnormal autophagy activation. *Autophagy*. 2012;8(7):1157-8.
170. Bayliak M, Burdyliuk N, Lushchak V. Growth on Alpha-Ketoglutarate Increases Oxidative Stress Resistance in the Yeast *Saccharomyces cerevisiae*. *Int J Microbiol*. 2017;2017:5792192.
171. Burtner CR, Murakami CJ, Kennedy BK, Kaeberlein M. A molecular mechanism of chronological aging in yeast. *Cell Cycle*. 2009;8(8):1256-70.
172. Ludovico P, Sousa MJ, Silva MT, Leão CL, Côrte-Real M. *Saccharomyces cerevisiae* commits to a programmed cell death process in response to acetic acid. *Microbiology*. 2001;147(Pt 9):2409-15.
173. Brauer MJ, Yuan J, Bennett BD, Lu W, Kimball E, Botstein D, *et al*. Conservation of the metabolomic response to starvation across two divergent microbes. *Proc Natl Acad Sci USA*. 2006;103(51):19302-7.
174. Kaminsky YG, Kosenko EA, Kondrashova MN. Metabolites of citric acid cycle, carbohydrate and phosphorus metabolism, and related reactions, redox and phosphorylating states of hepatic tissue, liver mitochondria and cytosol of the pigeon, under normal feeding and natural nocturnal fasting conditions. *Comp Biochem Physiol B*. 1982;73(4):957-63.
175. Yang Z, Huang J, Geng J, Nair U, Klionsky DJ. Atg22 Recycles Amino Acids to Link the Degradative and Recycling Functions of Autophagy. *Mol Biol Cell*. 2006;17(12):5094-104.
176. van 't Klooster JS, Cheng TY, Sikkema HR, Jeucken A, Moody DB, Poolman B. Membrane Lipid Requirements of the Lysine Transporter Lyp1 from *Saccharomyces cerevisiae*. *J Mol Biol*. 2020;432(14):4023-31.
177. D'Arcangelo G, Grossi D, De Chiara G, de Stefano MC, Cortese G, Citro G, *et al*. Glutamatergic neurotransmission in a mouse model of Niemann-Pick type C disease. *Brain Res*. 2011;1396:11-9.
178. Hoffman JM, Soltow QA, Li S, Sidik A, Jones DP, Promislow DE. Effects of age, sex, and genotype on high-sensitivity metabolomic profiles in the fruit fly, *Drosophila melanogaster*. *Aging Cell*. 2014;13(4):596-604.
179. Edwards C, Canfield J, Copes N, Brito A, Rehan M, Lipps D, *et al*. Mechanisms of amino acid-mediated lifespan extension in *Caenorhabditis elegans*. *BMC Genet*. 2015;16(1):8.

180. Cools M, Lissoir S, Bodo E, Ulloa-Calzonzin J, DeLuna A, Georis I, *et al.* Nitrogen coordinated import and export of arginine across the yeast vacuolar membrane. *PLoS Genet.* 2020;16(8):e1008966.
181. Wang Y, Deng P, Liu Y, Wu Y, Chen Y, Guo Y, *et al.* Alpha-ketoglutarate ameliorates age-related osteoporosis via regulating histone methylations. *Nat Commun.* 2020;11(1):5596.